Roles of HtrA1 and HtrA3 in the development of mouse placenta

By

Md. Zobaer Hasan

Research Supervisor

Professor Masashi Kawaichi

A thesis submitted in partial fulfillment for the degree of Doctor of Philosophy

Acknowledgements

First of all I would like to thank Professor Masashi Kawaichi for his constant support and supervision during my PhD. Thanks for giving me the chance to work in this laboratory and for all the trust you had in me. I would like to thanks Dr. Chio Oka, for her continuous supervision and patience with me and taught me all the necessary techniques in molecular biology. I would like to express my sincere thankfulness and gratitude to Professor Kenji Kohno and Professor Sadao Shiosaka for their constructive comments and suggestions for my research. I would also like to thank Dr. Yasumasa Ishida and Dr. Eishou Matsuda for their helpful suggestions.

I am thankful to all the members in the 'Kawaichi Lab' for creating a very nice working atmosphere, for all the discussions and the nice time we had. Specially, I would like to thank 'Supanji' for guiding me as an elder brother during my earlier year at this lab. I want to thank 'Tomomi Kotoku' for the great friendship and extraordinary support for the social life in Japan. I would also like to thank Muthi Ikawati Syafa for the discussion about research and specially her lovely angel 'Syafa' for energizing me always with his playfulness.

Furthermore I would like to thank all the members I came into contact at the 'Kawaichi Lab'. You were such fantastic collegues! I can hardly imagine finding something like this again. Specially, I want to thank Tomonori Nishi for all his support and patience during my early settling down in Japan. You became never tired of discussing all my questions again and again.

I want to thank my parents, my wife and my sister for bearing me with all their love and affection and keep patience and belief in me. Without them, it could have been impossible to carry on and cope up with the incidents in life. You showed me what is important and how to keep the right balance.

Most importantly, I would like to thank MEXT for financial support to pursue my doctoral degree and introducing a supreme cultural heritage, here in Japan.

List of Publications

Lab name (Supervisor)	Gene Function in Animals (Professor Masashi Kawaichi)		
Name (surname) (given name)	Hasan Md. Zobaer	Date	(2014/10/28)

First-author publication(s) from your doctoral research
(Title, authors, year of issue, name of the journal, volume, page)

1) Abnormal development of mouse placenta in the absence of HtrA1. Md. Zobaer Hasan, Muthi Ikawati Syafa, Jiraporn Tocharus, Masashi Kawaichi and Chio Oka. Developmental Biology. DOI: 10.1016/j.ydbio.2014.10.015 (2014).

Other co-authored publication(s) during your doctoral research
(Title, authors, year of issue, name of the journal, volume, page)

1) HtrA1 is induced by oxidative stress and enhances cell senescence through p38 MAPK pathway. Supanji, Mari Shimomachi, Md. Zobaer Hasan, Masashi Kawaichi and Chio Oka. Experimental Eye Research 112, P 79-92 (2013).

Summary

The HtrA (High Temperature Requirement Factor) family of secretory serine proteases has been found in different species ranging from bacteria to human and takes part in cells' protection against stress conditions. Four HtrA members have been identified in mammals. Among them HtrA1 and HtrA3 have similar domain architecture. HtrA1 and 3 digest various extracellular matrix proteins and inhibit TGF- β signaling with their protease activity. Both these genes have abundant expression in placenta and implicated in placental development.The placenta implants the conceptus into the uterine wall, protects the fetus from the maternal immune response, and changes the maternal vasculature to ensure maternal blood delivery to the implantation site to promote nutrient exchange, and secretes hormones pregnancy to adapt the changes in pregnancy. I was particularly interested in the role of HtrA1 and HtrA3 in placentation as deregulation of these two genes reported in human preeclampsia, a disorder in pregnancy associated with hypertension and proteinuria with intra uterine growth restriction. Our lab developed HtrA1 KO, HtrA3 KO and HtrA1/3 double KO mice. In this thesis, I have examined placentas from these KO mice on different gestational stages using various histochemical staining methods and in situ hybridization of trophoblast differentiation markers to understand the function of HtrA1 and HtrA3 in placentation.

Firstly, I examined the possible outcomes of abnormal placentation. The body weight of embryos on E12.5 and 14.5 and newborn pups produced by mating of homozygous HtrA1 or HtrA3 knockout mice is lower than that of the progeny of wild type mice and the difference persisted for 1-2 months after birth, suggesting abnormalities in placentation.

To analyze the roles of HtrAs in placenta, I first examined the expression patterns of HtrA1 and 3. In situ hybridization shows that HtrA1 is expressed by the deciduas capsularis and outer ectoplacental cone-derived trophoblasts mostly around E7.5-8.5 and the HtrA1 expression gradually diminishes by E10.5, whereas HtrA3 is expressed mainly by the deciduas basalis cells around E 9.5 and the expression decreases by E12.5.

Then I examined placental sections histochemically. The HtrA1 -/-, HtrA3 -/- and HtrA1/3 -/- mice have shorter labyrinth and fewer spongiotrophoblasts in the junctional zone compare to wild type mice on E10.5. The shorter labyrinth is caused by decrease in the area of fetal blood vessels. IsolectinB4 staining which specifically stains fetal blood vessels shows that branching of blood vessels is severely reduced in E 14.5 knockout placentas.

Large islands of glycogen-positive trophoblasts, which originate from spongiotrophoblastprecursors are present in the labyrinth of E14.5 knockout mice, but not in wild type mice. This cell type normally invades into the maternal decidua by E14.5 but it remains in the labyrinth of knockout placentas. I also found some void or vacuole-like structures in the junctional zone of E14.5 HtrA1 -/-, HtrA3 -/- and HtrA1/3 -/- placentas, whereas those spaces are filled with spongiotrophoblasts in wild type mice. As these data show that various types of trophoblasts are affected in the knockout placentas, I next examine the subtype specification of trophoblasts by in situ hybridization using sub-type specific probes. I use placentas from E9.5-E12.5, since at these stages HtrA1 and HtrA3 are expressed and various trophoblast differentiation occurs as well. In HtrA1-/- placentas, spiral artery remodeling related trophoblasts are reduced along with other trophoblasts originated from the outer ectoplacental cone where HtrA1 is expressed. On the other hand inner ectoplacental cone derived trophoblasts are increased in the KO placentas, probably due to a compensatory effect of the defective differentiation of trophoblast from the outer ectoplacental cone.

Trophoblast proliferatation, differentiation and invasion are critically regulated by various growth factors, their binding proteins, adhesion molecules, and extracellular matrix proteins produced by the decidua and trophoblast itself. TGF-β is among the growth factors involved in placental development, and inhibition of TGF-β has been reported to promote trophoblast differentiation. Since HtrA1 and HtrA3 are known to inhibit TGF-β, I examine the activation level of TGF- β signaling. Phosphorylated Smad 2/3 is increased in E10.5 placentas.

All these data indicate HtrA1 and 3 play an important, if not essential roles in regulation of sub-type differentiation of trophoblasts by inhibiting TGF-β.

Table of Contents

1. Introduction

The HtrA (High Temperature Requirement factor A) family of serine proteases has been found in a wide range of species from bacteria, plants to humans. The key feature of the members of this family is the combination of a protease catalytic domain with one or more C-terminal PDZ domains, which are known to interact with hydrophobic C-termini of proteins (Clausen et al. 2002) (Fig I-1). They are trimers in their active forms. Each family member has unique N-terminal domains, such as a secretion signal, an organelle localization signal, a transmembrane domain, or other functional domains like an insulin-like growth factor-binding domain (IGFBP) or a protease inhibitor domain (Kim and Kim 2005). Each member therefore, has a unique sub- or extracellular localization and distinct physiological functions, although a common feature of family members seems to be a role of stress responsive genes.

Mammals have four HtrA members. Human HtrA1 has been linked with the pathogenesis of various diseases, such as CARASIL, age-related macular degeneration, osteoarthritis, Alzheimer's disease, cancers and preeclampsia. HtrA3 was first identified as a pregnancy related serine protease, because the expression of HtrA3 drastically upregulated during the development of mouse placenta. Dysregulation of HtrA1 and HtrA3 has been linked with development of preeclampsia.

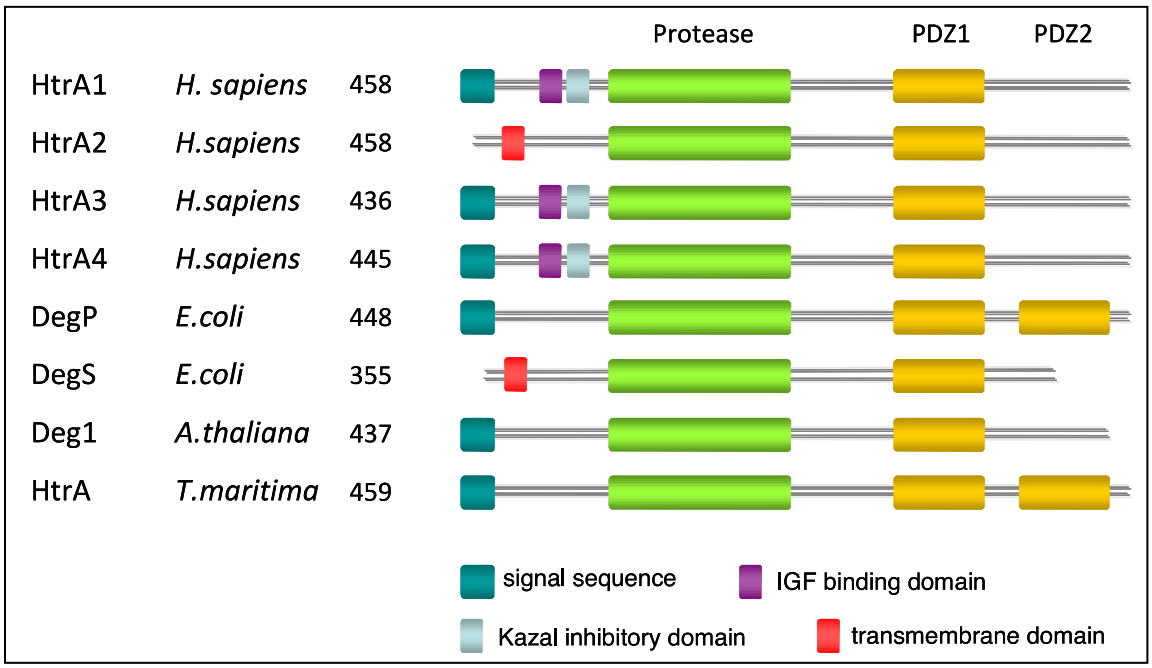

Figure I-1. Domain organization of HtrA family members. IGFBP, insulin growth factor; Protease, trypsin-likeserine protease domain; PDZ, Postsynaptic density, Disc large, ZonulaOcludens domain.Numbers show amino acid residues of proteins. Adopted from Clausen et al., 2002.

1-1 Bacterial HtrA proteins

HtrA was first identified in *E. coli* by two phenotypes of null mutations. Mutants either showed an increased sensitivity to high temperature (HtrA) or failed to digest denatured proteins in the periplasm (Deg) (Lipinska et al., 1989). *E. coli* has three HtrA proteins; DegP, DegQ and DegS; all localize in the periplasm.

DegP promotes survival of *E.coli* at temperature above 42°C. DegP is activated by the interaction of its PDZ domains with hydrophobic segments of heat-denatured proteins, and cleaves these denatured proteins to reduce their toxic effects (Kolmar et al. 1996). DegP has also a chaperone activity (Spiess et al. 1999). It recognizes and binds to nascent proteins secreted through the inner membrane and enhances the folding of the proteins. Temperature shifts activities of DegP; the chaperone activity is dominant at low temperatures (~28°C), while the protease activity is dominant at high temperatures (~42°C) (Spiess et al. 1999).

DegQ has similar substrate specificity as DegP (Kolmar et al. 1996). Overexpression of DegQ can complement the phenotypes of DegP null mutants (Waller et al. 1996). Hence, it is a functional substitute for DegP in *E. coli* (Waller et al. 1996).

DegS differs from DegP and DegQ in substrate specificity, localization and functions. DegS is an inner membrane protein with its protease and PDZ domains localized in the periplasm. The PDZ domains of DegS bind heat-denatured outer membrane porin and activate the protease activity. Activated DegS cleaves an inner membrane protein RseA, which binds and inactivates a stress response sigma factor σ^E in the cytoplasm. σ^E is released upon degradation of RseA and initiates transcription of stress response genes (Alba BM et al., 2002, Hasselblatt et al. 2007).

Expression of bacterial HtrA genes is induced by stress stimuli such as heat, reactive oxygen, and exposure to ethanol, or osmotic shock. Bacterial HtrAs are, therefore, stress responsive genes.

1-2 Mammalian HtrA proteins

Mammals have HtrA proteins, HtrA1–4. Those can be categorized into two groups according to their domain structure. HtrA2 possesses a mitochondrial localization signal and a transmembrane domain and localizes in the mitochondrial membrane with its protease domain protruding into the intermembrane space. In contrast, the N-termini of HtrA1, 3 and 4 contain secretion signal sequences, insulin-like growth factor binding protein (IGFBP) and Kazal type protease inhibitor domains (Fig I-2). The latter two domains involve in protein-protein interactions. HtrA1, 2 and 3 have been well characterized, but expression of HtrA4 seems very low or restricted to specific organs, and information on HtrA4 is limited.

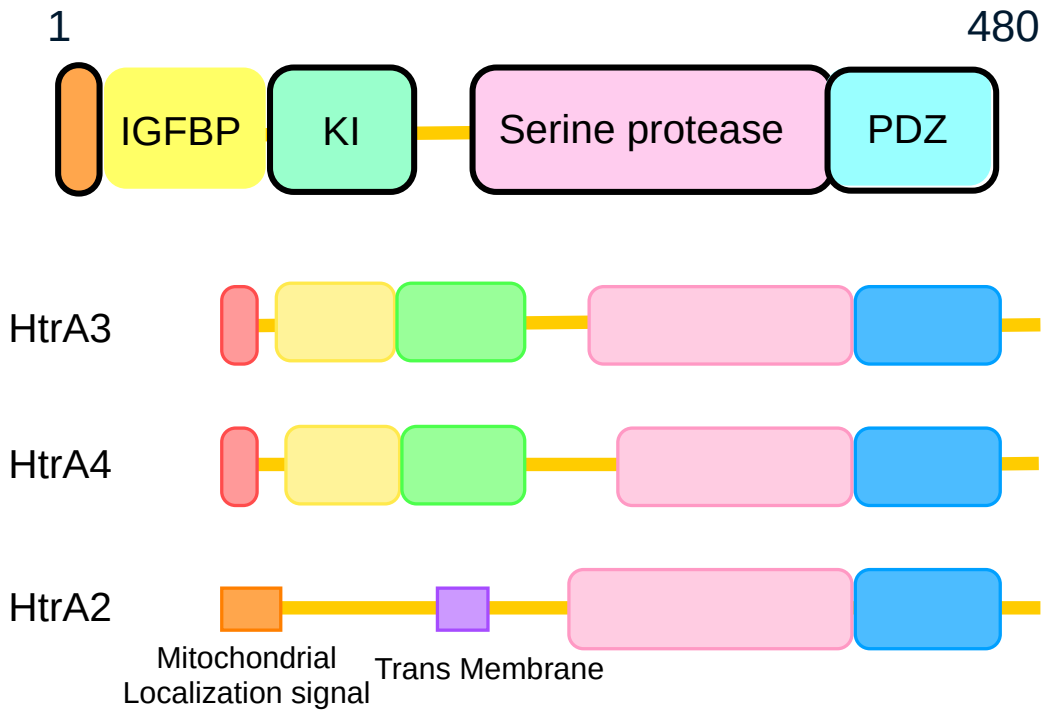

Figure I-2. Structure of mammalian HtrA family proteins. IGFBP= Insulin like growth factor binding protein, KI= Kazal type protease inhibitor.

1-2-1 HtrA2 and diseases

HtrA2 knockout mice or homozygous mice of naturally-occurring loss-of-function mutation of HtrA2 (Mnd2, motor neuron degeneration 2) display severe neurological symptoms similar to Parkinson's disease and die around one month after birth (Vande Walle L et al, 2008). Those mice fail to gain weight, and their organs such as the heart, thymus and spleen are strikingly small (Martins L. M., 2004). Mitochondria of affected tissues are severely degenerated. Miss sense mutations of human HtrA2 are linked with familiar Parkinson's disease in Belgium and Germany (Strauss et al. 2005; Bogaerts et al., 2008). These findings, together with the analogy with bacterial DegP, suggest that HtrA2 plays essential roles in the protein unfolding response in mitochondria either by digesting or re-folding denatured proteins.

Upon apoptotic stimulations, HtrA2 is secreted into the cytoplasm from mitochondria, and induces apoptosis in caspase-dependent as well as independent manners (Suzuki et al., 2001). HtrA2 has been reported to bind to presenilin-2 or cleave APP, thus implicated in pathogenesis of Alzheimer´s disease (Gupta et al. 2004, Park et al. 2006).

1-2-2 HtrA1 and diseases

HtrA1 is secreted out of cells. It digests extracellular matrix proteins. Identified substrates include proteoglycans, such as decorin and biglycan (Tsuchiya et al.), glycoproteins such as fibronectin and fibromodulin (S Grau et al., 2006), elastine and fibulin 5 (Jones et al., 2011, Vierkotten et al., 2011).

HtrA1 suppresses TGF-β signaling in a protease activity dependent manner, probably by degrading extracellular proteoglycans, which bind and concentrate TGF-β family cytokines in the close vicinity of cells (Oka et al, 2004).

HtrA1 was initially identified as a protein downregulated in SV40 transformed fibroblasts (Zumbrunn and Trueb 1996). Expression of HtrA1 is also decreased in melanomas, ovarian cancer and lung cancer (Baldi et al., 2002, Chien et al., 2004, Esposito et al., 2006). Overexpression of HtrA1 inhibits tumor cell growth, proliferation and migration (Baldi et al., 2002). HtrA1 is, therefore, thought to be a tumor suppressor gene.

HtrA1 is increased in joint cartilage of osteoarthritis patients (Hu et al., 1998). In arthritis model mice, HtrA1 expression is induced in terminally differentiated chondrocytes, which are destined to death and degrade surrounding cartilage matrix to induce ossification (Tsuchiya et al, 2005). Probably HtrA1 aggravates arthritis by degrading cartilage matrix and inducing terminal differentiation of chondrocyte by inhibiting TGF-β signaling.

Loss of function mutations of the human *HTRA1* gene causes CARASIL (Cerebral Autosomal Recessive Arteriopathy with Subcortical Infarcts and

Leukoencephalopathy) (Hara et al. 2009). Cerebral arteries of CARASIL patients show arteriosclerosis with intimal thickening, heavy deposition of collagen and proteoglycans, and with loss of vascular smooth muscle cells. Loss of HtrA1 activity may lead to accumulation of extracellular matrix proteins, and enhances TGF-β signaling which further induces extracellular protein production.

SNPs in the promoter region of human *HTRA1* gene are a major genetic risk factor for age-related macular degeneration (AMD) (Dewan et al. 2006, Yang et al. 2006). High-risk SNPs increase the expression of HtrA1. AMD is characterized by deposition of exracellular materials called drusen between the retinal pigment epithelium (RPE) and its basement membrane (Bruch's membrane) in the central region of the retina (the macula). At a late stage of AMD, blood vessels invade into the affected retinal region from the underlying choroid layer, which causes irreversible vision loss. Based on the finding from the transgenic mice overexpressing HtrA1 in RPE, it has been suggested that overexpressed HtrA1 digests either elastin or fibulin 5, resulting in destruction of elastic fibers which are the main constituent of Bruch's membrane and elastic laminae of blood vessels. (Vierkotten et al., 2011, Jones et al., 2011). These damages in the Bruch's membrane and blood vessel walls result in degeneration of RPE and responsive neoangiogenesis, both of which characterize AMD. Another risk factor of AMD is oxidative stress. The retina and RPE are subject to constant oxidative damages mainly due to excessive exposure to light. In accordance with bacterial *HtrA*s as stress response genes, human *HTRA1* expression is induced by oxidative stress along with cell senescence in RPE (Supanji et al, 2013)

1-2-3 HtrA3 and HtrA4

The HtrA3 protein shows 59% identity and 84% similarity to HtrA1 with the same domain structure (Fig I-2), and is expected to have the same biochemical activities. The expression profiles of HtrA1 and HtrA3are very similar (Tocharus et al. 2004), but frequently show complimentary expression patterns within a tissue; both are expressed

most highly in the placenta, but HtrA is mainly expressed in the decidua capsularis and HtrA3 in the decidua basalis (see below).

HtrA4 seems to be expressed in limited tissues, as very few are listed in the EST database. Recently HtrA4 is reported to play roles in placenta development: HtrA4 is expressed in the placenta and upregulated in pregnancy associated hypertension (preeclampsia) (Inagaki A et al., 2012). It is also reported that HtrA4 regulates trophoblasts invasion (Wang LJ et al., 2012).

1-3 HtrAs in pregnancy

HtrA1 and HtrA3 are most abundantly expressed in placenta. In human, HtrA1 and HtrA3 are upregulated in the placenta during the third and first trimester of pregnancy, respectively (Nie et al., 2003, De Luca et al., 2004).

In mouse, HtrA1 and HtrA3 are not expressed in non-pregnant uterus. HtrA1 mRNA is first detected in the implantation site on E7.5. HtrA1 expression increases drastically until E 9.5-E10.5, then decreased rapidly afterwards. The HtrA1 protein is

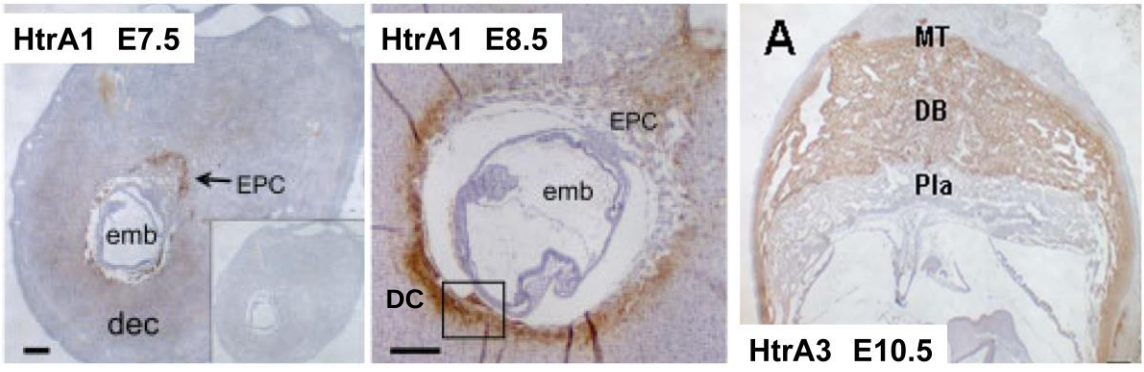

Figure I-3. Expression pattern of HtrA1 on E 7.5 and 8.5 (left two pictures) and HtrA3 on E10.5 (right) in the placenta.EPC, ectoplacental cone; emb, embryo; dec, decidua; DB, decidua basalis; Pla, fetal placenta; DC, decidua capsularis; MT, uterine endometrium. Adopted from Nie et al., 2005 and Nie et al., 2006.

localized in the fetal trophoblast layer (ectoplacental cone) immediately adjacent to the decidua basalis and in the maternal decidua capsularis (Fig I-3 Left) (G Nie et al., 2005).

The HtrA3 mRNA becomes detectable on E3.5 at the implantation site, increases up to E10.5, then decrease gradually. In contrast to HtrA1, HtrA3 is expressed almost exclusively in maternal decidua, and not in fetal trophoblasts. The HtrA3 protein is localized mainly in the decidua basalis (Fig I-3 Right) (Nie et al., 2006).

The blood levels of HtrA1 and HtrA3 (and HtrA4 as described above) are elevated in pregnant women who subsequently develop preeclampsia (Ajayi F et al., 2008, Li Y et al., 2011).

Preeclampsia is abnormal conditions in pregnancy and clinically diagnosed as the onset of acute hypertension and maternal organ dysfunction in women without history of hypertension (Brown et al., 2000). Besides hypertension, proteinuria, edema and platelet aggregation are the hallmarks of preeclampsia. Preeclampsia is one of the most potentially mortal factors in pregnancy and accounts for 15-20 % of pregnancy related mortalities. It does not only affect mother but also affect the fetus. The most dangerous thing is that preeclampsia is not diagnosed until the late pregnancy, as it is not a simple disease but rather a disorder with multiple symptoms.

The HtrA1 and HtrA3 expression is increased, along with their blood levels, in placentas of preeclampsia patients. The HtrA1 level is sometimes decreased in human preeclamptic placenta with intrauterine growth restriction of the fetus (Lorenzi T et al., 2009). Roles of HtrAs in the etiology of preeclampsia, therefore, have to be elucidated in more detail.

1-4 Development and functions of the mouse placenta

The placenta is the first organ that develops during early embryogenesis and plays important role to achieve successful pregnancy. The mouse placenta serves similar functions as the human placenta and gross anatomy is quite similar. Accordingly, it is considered as a good model to understand human placental development and disease.

1-4-1 Structure of mature mouse placenta

The placenta plays a wide variety of critical roles during pregnancy for both survival and growth of the fetus and well-being of the mother. The placenta implants the conceptus into the uterine wall, protects the fetus from the maternal immune system, modulates the maternal vasculature to deliver adequate blood supply to the implantation site, brings fetal and maternal blood in close contact to promote nutrient and oxygen exchange and waste disposal, and secretes hormones for pregnancy maintenance and adaptation. The mouse placenta matures after E10.5. A mature mouse placenta has three distinctive compartments (Fig I-4), the most distal to the fetus is known as the maternal decidua, the intermediate one is the junctional zone and the closest to the fetus is the labyrinth.

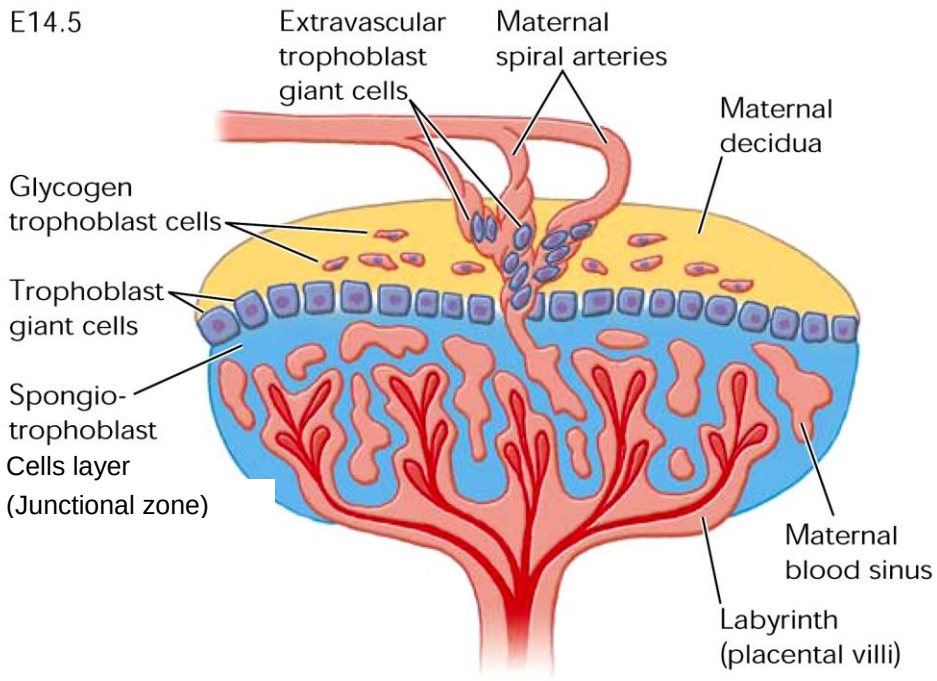

Figure I-4. A schematic structure of a mature (E14.5) mouse placenta. Adopted from Watson and Cross, 2005

Maternal decidua consists of stromal cells required for the response to progesterone, spiral arteries that carry maternal blood to the implantation site, and the maternal spiral artery related trophoblast cells that remodel these spiral arteries to increase blood flow, uterine natural killer (NK) cells (maternally derived lymphocytes involved in remodeling of maternal spiral arteries), and glycogen trophoblast cells (GlyT) derived from the fetal part that interstitially invade the decidua (Adamson et al., 2002). Spiral arteries, which are characteristic to the placenta ensure abundant blood flow to the fetal placenta during pregnancy, and at term, quickly constrict to avoid bleeding when the placenta detaches after the delivery of fetus.

The junctional zone is separated from the decidua by a layer of trophoblast giant cells (TGC), and mainly composed of two types of trophoblasts, spongiotrophoblasts (SpT) and glycogen trophoblasts (GlyT). The junctional zone provides the structural support to the labyrinth and also prevents the fetus from immature invasion of blood vessels. Maternal blood "bleeds' into canals in the junctional zone. The maternal blood canal is lined with canal-associated trophoblast giant cells.

Just beneath the junctional zone, distal to the decidual layer is the labyrinth layer, where fetal blood vessels and maternal blood spaces come in close contact to each other. These two blood vessels in the labyrinth are separated by a trilaminar arrangement of trophoblast cells, which is composed of a single layer of mononuclear subtype of TGC and two layers of multi -nucleated syncytiotrophoblasts formed by cell fusion (Fig I-5).

1-4-2 Development of mouse placenta

Mouse placental development starts in the blastocyst at E 3.5 (Fig I-5). The trophoectoderm is first specified from the inner cell mass (ICM). Around E 4.5, differentiation into different types of trophoblasts begins. Trophoectoderm cells in contact with inner cell mass (polar trophoectoderm) differentiate into the extraembryonic ectoderm and ectoplacental cone (Fig I-5). The mural trophoectoderm (distal to ICM) differentiates to form primary TGC by a process called endoreduplication and facilitates the process of implantation. At E7.5, the extraembryonic ectoderm gives rise to the chorion, a layer that surrounds the embryo. The chorion subsequently forms the

trophoblasts in the labyrinth. The ectoplacental cone will give rise to thejunctional zone.

The allantois grows from the embryo at around E 8.5 and attaches to the chorion. This is known as chorioallantoic attachment. The chorion then starts to fold to form villi and makes spaces where fetal blood vessels grow from the allantois. The villi form a network of blood vessels and together with the trophoblasts in the chorion give rise to the labyrinth. At E 9.5, Spongiotrophobalsts (SpT) and secondary TGC are formed between the decidua and labyrinth, which expand the labyrinth.

Around E10.5, trophoblasts of the chorion differentiate into multinucleated syncytiotrophoblasts and mononuclear syncytiotrophoblasts. Around E 12.5 glycogen trophoblasts start to differentiate in the junctional zone from the spongiotrophoblasts. The fetal vascular network and these trophoblasts form the branched villi of the labyrinth continue to develop and progress towardthe maternal decidua. Sinusoids filled with maternal blood and fetal blood vessels mingle together in the labyrinth and exchange nutrients, oxygen and waste products.

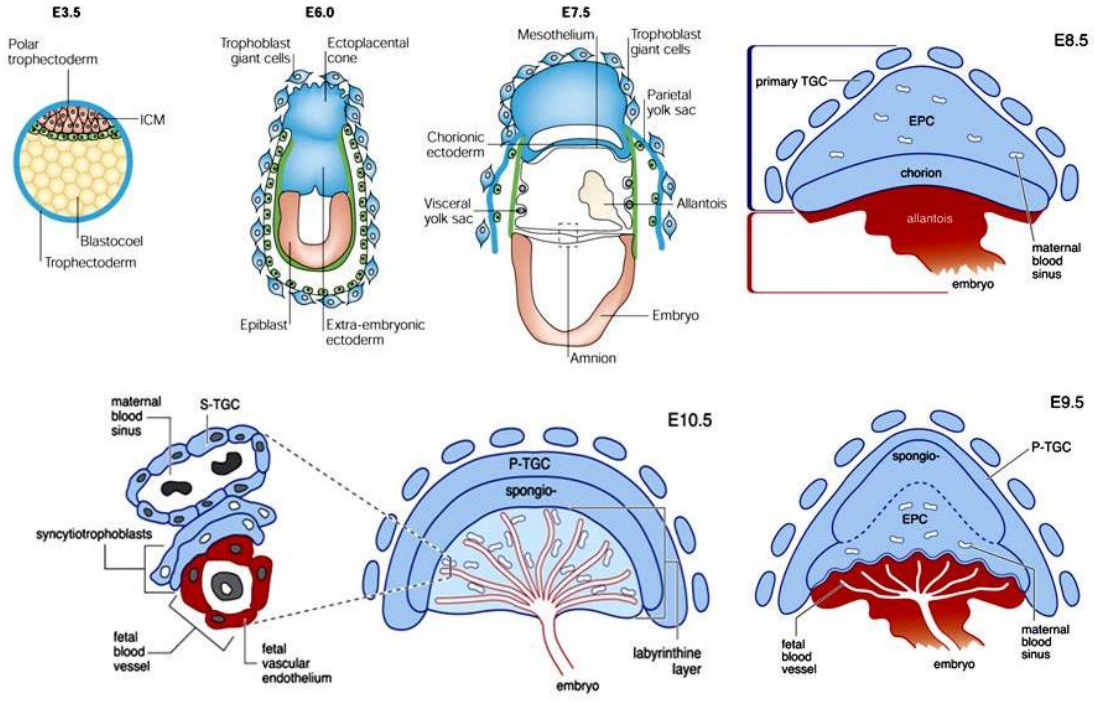

Figure I-5. Sequential events during mouse placenta development. TGC, trophoblastgiant cells; EPC, ectoplacental cone; P-TGC, parietal TGC; S-TGC, sinusoidal TGC; spongio-, spongiotrophoblasts layer or junctional zone. Adopted from Rossant and Cross, 2005, and Sally L. Dunwoodie, 2009.

1-4-3 Development of trophoblasts

The placenta exerts its various roles through the differentiated trophoblast cells in the placenta. They are major components of the fetal placenta and have distinct functions.

Trophoblast giant cells (TGC) are the first differentiated cell types specified around E 6.5 during placental development. Embryonic stem cells produce FGF4 and TGF- β to maintain the pluripotency of trophoblast stem cells and suppress the formation of TGC (Rossant and Ofer., 1977, Tanaka et al., 1998). Withdrawal of FGF 4 and TGF-β triggers TGC differentiation.

TGC are large polyploid mononuclear cells that are the result of endoreduplication – a process whereby TGC undergo several rounds of DNA replication without subsequent mitoses. TGC are invasive and phagocytic in nature, enabling them to perform their role in implantation. They are endocrine in character, too, releasing various paracrine factors important for promoting pregnancy. TGC are thought to play essential role in decidualization, a process which changes endometrial cells into decidual stromal cells, as they produce progesterone or other signals that regulate decidual cell differentiation. In mice, four subtypes of TGC with distinct functions have been identified at different stages of gestation and in different locations within the placenta (Simmons et al., 2007; Simmons et al., 2008b). They are; parietal TGC (P-TGC) formed around E 9.5, line the implantation site and are in direct contact with the decidua; spiral artery-associated TGC (SpA-TGC) formed around E 9.5 and regulate maternal spiral artery remodeling and blood flow into placenta; maternal blood canal-associated TGC (C-TGC)that arises around E 9.5 and regulate maternal vasculature and physiology; sinusoidal TGC (S-TGC) formed around E 11.5 within the sinusoidal blood spaces in the labyrinth(Fig I-6).

All subtypes of TGC share the common characteristics that they are large, have polyploid (usually single) nuclei, and are secretory in nature with their content of the Golgi and endoplasmic reticulum increasing during differentiation (Bevilacqua and Abrahamsohn, 1988). One important feature of TGC is that they are post mitotic and can exert their functions without risk of forming tumors (Hemberger, 2008). This is very important because they are invasive in nature and can promote angiogenesis locally.

Each subtype of TGC expresses different genes of the prolactin family and can be identified by the expression of these genes. For example, P-TGCs express Pl-I, Pl-II and Pl-f; SpA-TGCs express only Pl-f; C-TGCs express Pl-II and Pl-f; S-TGCs express Pl-II. TGC are originated from either Tpbpa positive or Tpbpa negative cell lineage. Pl-II and Pl-f expressing cells usually derived from both Tpbpa positive and negative cell precursors.

The junctional zone of the mouse placenta consists of SpT and GlyT cells. SpT maintain structural integrity of the placenta. On the basis of marker expression, SpT and GlyT originate from the ectoplacental cone and express Tpbpa (Fig I-6). Their differentiation seems to be complementary: several genes have opposite effects on the development of these two cell types. For example, deletion of Mash2, SOCS3, or PPAR leads to increase in TGC and loss of SpT (Guillemot et al., 1994, Tanaka et al., 1997, Takahashi Y et al., 2003, Wang H et al., 2007).

In the labyrinth, maternal blood is separated from the fetal blood vessels by three types of trophoblast cells; those are consist of S-TGCs and two types of syncytiotrophoblasts (SynT-I and II) (Fig I-4). S-TGC, SynT-I and SynT-II are dissimilar in form and function from each other; S-TGCs are largely secretory mononuclear polyploidtrophoblast cells (Simmons and Cross, 2005, Simmons et al., 2007), while SynT-I and SynT-II cells are multinuclear diploid cells that transport nutrients and produce hormones, as well as mediating evasion from the maternal immune system (Dupressoir et al., 2009). Cell lineages of trophoblasts and markers that discriminate each trophoblast are summarized in Fig I-6.

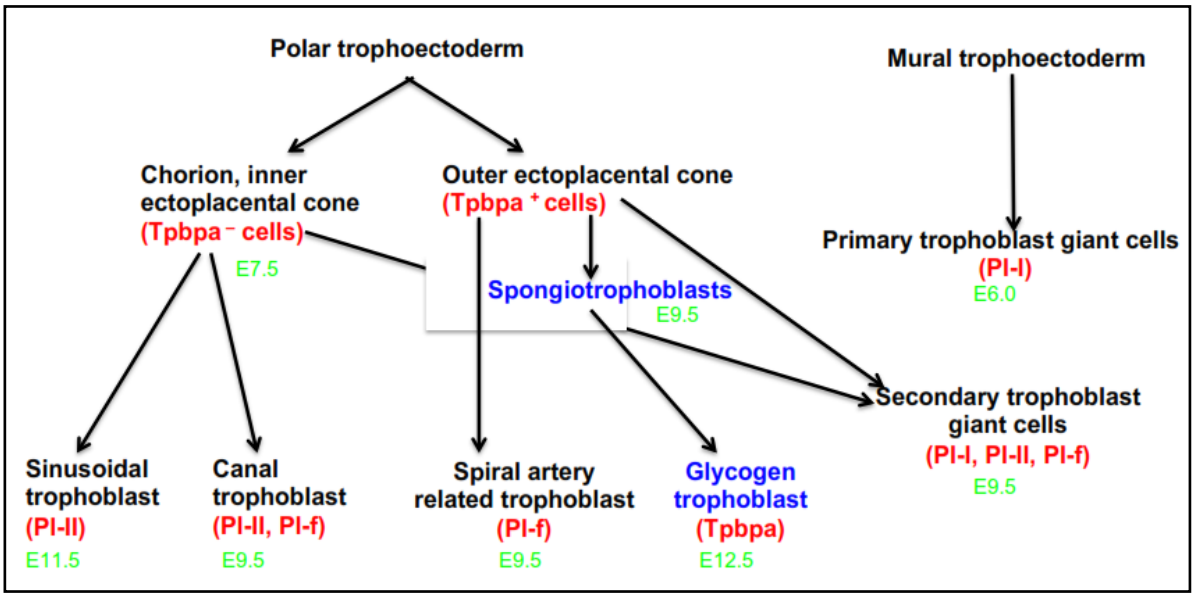

Figure I-6: Development of different subtypes of trophoblasts. Pl-I is the marker for P-TGC; Pl-II is the marker for P-TGC, C-TGC and S-TGC; Pl-f is the marker for P-TGC, C-TGC and SpA-TGC; Tpbpa is the marker for SpT and GlyT.Embryonic day shown in red indicates the time when each trophoblast appears. Adopted from D.Simmons et al., 2007.

1-5 Etiology of preeclampsia

Preeclampsia is a multi-factorial disease; both maternal and fetal factors contribute to the etiology of preeclampsia. Common feature is inadequate development and/or functions of the placenta (Redman et al., 2005, Wang et al., 2009). Genetic factors and multiple pregnancy are among the most frequent causes of preeclampsia.

Defective invasion of trophoblasts leads to preeclampsia (Hung et al., 2002, GS Whitley and JE Cartwright., 2010). During normal placentation, SpA-TGCs invade the maternal decidua, associate with maternal arteries and induce remodeling into spiral arteries. The remodeling dilates the arteries and makes them less sensitive to vasoconstriction, and thereby increases the maternal blood flow into the fetal placenta about 10-fold, the increase in blood flow is essential for the growing needs of fetus. Inadequate remodeling results in under perfusion which causes hypoxia, thrombosis, and chronic inflammation in the fetal placenta. Hypoxic conditions stimulate trophoblast proliferation and block the differentiation into invasive trophoblasts (Zhou et al., 1997),

contributing to a vicious cycle that aggravates preeclampsia. Defects in spiral artery remodeling also results in an uneven blood flow to the fetal placenta and induce an ischemic-reperfusion insult due to local fluctuation in oxygen concentration, causing oxidative stress (Hung et al., 2002).

Invasion of SpA-TGC requires up-regulation of protease activities such as MMP-2 and MMP-9 to degrade ECM, and inhibited by Interferon-γ and TGF-β. Therefore perturbation of these factors can also induce preeclampsia (Knofler., 2010).

1-6 Purpose of this study

Since the placenta expresses *HtrA1* and *HtrA3* most highly among all organs in mouse and human and their expression is dysregulated in preeclampsia, these secreted serine proteases should have important functions in both normal development and pathological conditions of the placenta. In this study, I try to understand the function of *HtrA1* and *HtrA3* in mouse placentation by taking advantage of *HtrA1*, *HtrA3*, and *HtrA1*/*HtrA3* gene knockout mice, which are produced in our laboratory. In particular, *HtrA3* knockout mouse and *HtrA1/HtrA3* double knockout mouse are available only in our laboratory.

1-7 Abbreviations

Here in this thesis, I refer to wild type moue as *HtrA*+/+; homozygous *HtrA1* single gene knockout mouse as $HtrA1^{-/-}$; homozygous *HtrA3* single gene knockout mouse as $HtrA3^{-/-}$, and *HtrA1/HtrA3* double gene knockout mouse as $HtrA1/3^{-/-}$.

Other abbreviations used to refer to various types of trophoblasts and the placental structures are;

EPC, ectoplacental cone

ICM, inner cell mass

GlyT, glycogen trophoblastcells

NK, natural killer cells

TGC, trophoblast giant cells

P-TGC, parietal TGC

S-TGC, sinusoidal TGC

SpA-TGC, spiral artery-associated TGC

C-TGC, maternal blood canal-associated TGC

SpT, Spongiotrophobalsts

SynT, syncytiotrophoblasts

2. Materials and Methods

2-1 Mice

HtrA1 and *HtrA*3gene knockout mice were generated by the conventional homologous recombination method using RF8 ES cells. The details of the targeting vector for disruption of the *HtrA1*gene and the preliminary characterization of *HtrA1* gene knockout mice were described previously (Tsuchiya et al., 2005, Jones et al., 2011). *HtrA1* knockout mice were maintained either as a mixed 129/Sv and C56BL/6 background or as a Balb/C background after more than 10 generations of backcrossing. To generate *HtrA3* knockout mice, a targeting vector was designed to remove 5'-end 424 bases from exon 1 of the *HtrA3* gene (see Figure M-1). The absence of the *HtrA3* transcript in homozygous *HtrA3* knockout mice was confirmed by northern blot of total RNA prepared from the placenta. *HtrA3* knockout mice were maintained as a mixed 129/Sv and C56BL/6 background. All animal experiments were approved by the Animal Welfare Committee of Nara Institute of Science and Technology. Noon on the day when the vaginal plug was detected was set as embryonic day 0.5 (E0.5).

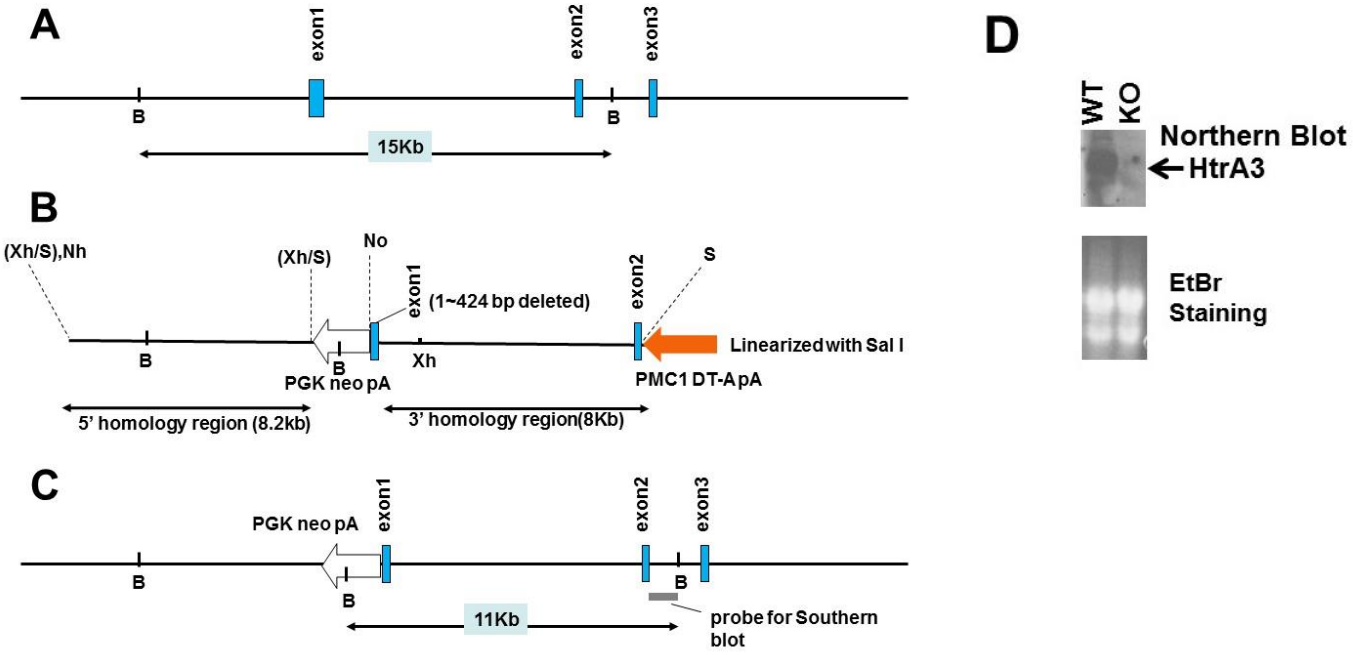

Figure M-1. Gene targeting of mouse *HtrA3*. A) Genome structure of the exon1-exon3 region of mouse HtrA3 gene. **B)** Structure of the targeting vector. **C)** Structure of targeted *HtrA3* gene. The 5'-end of *HtrA3* exon1 (1-424 bp) was deleted. **D)** Northern blot of mRNA prepared from wild type and homozygous *HtrA3* knockout mice. B, *BamHI* site; S, *Sal* I site; Xh, *Xho* I site; No, *Not* I site. Open arrow shows a PGK-neo-PolyA cassette. Orange arrow shows a PMC-diphtheria toxin (DT-A)-PolyA cassette.

2-2 Genotyping

Genotypes of the mice were determined by polymerase chain reaction (PCR). Genomic DNA was isolated from tails of 1month old mice. The cut tail was lysed in 500μL tail DNA lysis solution containing 50 mM Tris-HCl (pH 7.6), 100 mM EDTA, 100mM NaCl, 1 % SDS and Proteinase K (0.2 mg / mL) at 55°C overnight. One □l of RnaseA (10 mg/ml) was added and incubated at 37°C for 1 h. The lysate was then extracted with equal volume of phenol: chloroform solution by rotating for 30 min followed by centrifugation for 5 min at 15,000 RPM at room temperature. After centrifugation, an equal volume of isopropanol was added to the water phase and DNA precipitate was collected by centrifugation for 5 min. The precipitate was rinsed with 70% ethanol and then air dried at room temperature for 15 min. The rinsed DNA was dissolved in 100μl of water. PCR was run for 35 cycles (95℃ for 0.5 min for denaturation; 55℃ for 0.5 min for annealing; 72℃ for 1 min for extension), followed by extension at 72℃ for 5 min.

For HtrA1 genotyping the targeted allele was identified with the following primers–

Forward primer- 5'- AATGGGCTGACCGCTTCCTCGTGCTT-3'

Reverse primer- 5'- TGTGCACGCCGTCGTACTGT-3'.

The wild type allele was identified with the following primers-

Forward primer- 5'- CACTACGCATTGCAGCCCCTC-3'

Reverse primer- 5'- CGTACCACGCTCCTGTCTTT-3'

For HtrA3 genotyping the targeted allele was identified with the following primers-

Forward primer- 5'-GCACACGTCGGCATAAGTAT-3'

Reverse primer- 5'- GGGGAACTTCCTGACTAGGG-3'

The wild type allele was identified with the following primers

Forward primer- 5'- ACTGTCTTGGCCTTTAAGCG-3'

Reverse primer-5'- GCACACGTCGGCATAAGTAT-3'

PCR products were separated by electrophoresis with1.0-1.5% agarose gels in 1x TAE buffer. Gels were then stained with ethidium bromide for 15-20 min and DNA was visualized under UV light.

2-3 Tissue preparation

Placentas were harvested from timed mating at E9.5, 10.5, 12.5, 14.5 and 16.5. The noon of the day when vaginal plague was detected was designated as E 0.5. Mice were killed by overdose of pentobarbital and fixed with 4 % paraformaldehyde in phosphate-buffered saline (PFA/PBS). Tissues were fixed overnight in 4% in PFA/PBS and then rinsed in PBS twice. For paraffin embedding, tissues were dehydrated through a graded ethanol series and embedded in paraffin wax. Five μm sections were cut from paraffin block at room temperature. For frozen histological sections, after fixation with 4% PFA/PBS, tissues were incubated in 30% sucrose in PBS overnights. When the

tissues sank completely into the sucrose solution, they were embedded in OCT compound (Sakura) at room temperature and frozen with liquid nitrogen. OCT blocks were then stored at -80℃ until use and 10-12 μm sections were cut at -20℃ using cryostat (Microm).

2-4 Histology

Hematoxylin and eosin staining was performed for histological evaluation. Paraffin sections were de-waxed in xylene for 15 min and then rehydrated in and graded ethanol series (100%, 90%, 80% and 70%) and washed twice with distilled water for 5 min each. Samples were stained in Mayer's Hematoxylin (Wako) for 10 min and washed in running tap water for 10 min. Then the sections were stained with eosin for 2 min, followed by washing with distilled water for 10 sec and dehydration with 80%, 90%, and 100% ethanol. The sections were then cleared in xylene before mounting with Soft Mount Solution (Wako). For periodic acid schiff (PAS) staining, placental sections were dewaxed and rehydrated and then incubated with 0.5% periodic acid for 5 min at room temperature. Subsequently, the slides were rinsed with distilled water and then immersed in Schiff's reagent (Wako) (0.5% pararosaniline chloride, 0.15M HCl, 0.425% $K_2S_2O_5$) for 15 min at room temperature. The sections were then rinsed with tap water to develop the color. The sections were counterstained with Haematoxylin (Mayer) for 2 min, dehydrated and then mounted with Soft Mount Solution. For isolectin B4 staining, sections were immersed in boiled citrate buffer (pH6.0) for antigen retrieval. After slowly cooled down to room temperature for 1-2 h, the sections were incubated with 0.3% H_2O_2 in methanol for 30 min. Then the sections were treated with 200 μl of Block Ace at room temperature for 30 min. Isolectin antibody (biotin-labeled, Vector laboratories) diluted 100 fold and was applied over the sections and incubate at 4°C over-night. The sections were then washed with TPBS (0.05% of tween 20 in 1X PBS) 3 times for 5 min each. They were then incubated with horseradish peroxidase-conjugated streptavidin (1/100, KPL) for 1 h at room temperature and then subjected to DAB development.

2-5 In situ hybridization on tissue sections

The HtrA1 (Oka et al., 2004) probe and HtrA3 (Tocharus et al., 2004) probe have been described previously. Tpbpa probe (Camey et al., 1993) was a kind gift from Dr. James Cross. Pl-I, Pl-II and Pl-f probes were from Dr. David Simmons and have been described previously (Simmons et al., 2007)

E.coli harboring a plasmid containing probe cDNA was cultured in 100 ml of LB broth containing 100 µg/mL of ampicillin overnight at 37°C with shaking. The cells were harvested by centrifugation, and plasmid DNA was extracted using the QIAGEN Plasmid Maxi Kit according to the manufacturer's instructions Plasmid DNA was linearized by an appropriate restriction enzymes and subject to in vitro transcription. One µg of linearized DNA was incubated with 10X buffer, 10X labeling mix, RNase inhibitor and RNA polymerase (T3 or T7) for 2 hs at 37°C. After treating with1 µl of RNase free DNase (Promega) for 20 min at 37°C, 1 mM EDTA was added to stop the DNase reaction. Product RNA was precipitated with ethanol and dissolved in RNase-free water.

Paraffin sections were rehydrated in an ethanol series (100%, 90%, 80% and 70%) and distilled water. Sections were then fixed with 4% paraformaldehyde in PBS and then treated with proteinase K buffer (1 µg/ml proteinase K, in 0.1 M Tris-HCl and 0.1 M EDTA (pH 8.0)) for 30 min at 37°C. The sections were washed with PBS for 3 min at room temperature. Subsequently, the sections were incubated at room temperature in 0.1 M triethanolamine (TEA) for 2 min, thenin 0.25% (v/v) acetic anhydride in 0.1 M TEA buffer (pH8.0) for 10 min and finally with 0.2N HCl/PBS for 5 min.The sections were washed with PBS. RNA probe prepared in 5X SSC and 50% formamide was applied over the washed sections. The sections were covered with Parafilms and incubated at 55 °C overnight in a moisture chamber. After overnight incubation sections were briefly washed in 5X SSC and then washed with 2X SSC for 20 min at 55°C twice, followed by washing twice with 0.2X SSC for 20 min each at 55 °C. Samples were washed with TBS for 5 min at room temperature and blocked with 0.5% blocking reagent along with 20% goat serum in TBS for 1 h. Anti digoxigenin antibody diluted 1/1000 fold with 0.5% Blocking Reagents and 20% goat serum in TBS was applied over the sections,

and the sections were incubated overnight at 4 °C. The sections were washed and then incubated with NBT/BCIP for 6-12 h to detect signals.

2-6 Histomorphometry and Statistical Analysis

For quantitative analysis of the blood spaces in the labyrinth, paraffin sections of E10.5placentas were stained with hematoxylin and eosin. For each conceptus at E10.5, three different sections of the placenta were analyzed. The maternal blood spaces were identified by the presence of non-nucleated maternal red blood cells and fetal blood spaces were identified by the presence of nucleated dark purple color cells. The area of blood spaces were measured using NIS Elements software (Nikon). Statistical significance was calculated by Graphpad software by using ‘unpaired student’s t-test’ method. For other quantitative analysis, total length measurement, spongiotrophoblasts area, glycogen trophoblast area, three different sections per placenta at 100 μm intervals from the central region near the site of umbilical cord attachment were analyzed.

2-7 Blood pressure measurement

Blood pressure was measured in conscious mice using the tail cuff method as described previously (Oron-Herman et al., 2008). Mice were inserted in a chamber provided by the company (Softron Co, Japan) and body temperature was maintained at 37 ℃ during the measurement. The average of 5 consecutive readings was recorded.

2-8 Western blotting

Placenta tissues were obtained from the E10.5 HtrA +/+ and HtrA1 -/-mice. The placentas were homogenized in RIPA lysis buffer (50 mM Tris-HCl at pH 8.0, 150 mM NaCl, 1% NP-40, 0.5% sodium deoxycholate, 0.1% sodium dodecyl sulfate (SDS)) with

1 mM PMSF, and 10 μg/ml protease inhibitor cocktail. The homogenates were centrifuged at 15,000 RPM for 20 min at 4^{o}C. The supernatant were removed and analyzed by Western blot. Western blot was performed by standard methods using an antibody against phosphorylated Smad2 (pSmad2) (Santa Cruz). Briefly, a SDS-polyacrylamide (12.5%) gel was used for electrophoresis, and 20 μl each of placenta extracts was applied to a well of the gel. Electrophoresis was carried out at 100 volt. After running, proteins were transferred from the gel to PVDF membrane using a wet transfer tank. The membrane was then blocked in 4% skim milk in Tris-buffered saline containing 0.05% tween 20 (TBS-T) for 1 h. The blocked membrane was incubated with anti-pSmad2 antibody (1/2000 diluted with TBS-T containing 4% skim milk) overnight at 4^{o}C. The membrane was then washed with TBS-T three times each for 10 min. The washed membrane was incubated with a horse radish peroxidase conjugated anti-mouse IgG (1/20000diluted, GE Health Care) for 1 h at room temperature. The membrane was washed again with TBS-T three times each for 10 min. Then, peroxidase activity was detected by ECL^{Plus} (GE Health Care) and visualized by exposing on X-ray film (Fujifilm FLA500).

3. Results

3-1 Deletion of HtrA1 and HtrA3 results in intra uterine growth retardation

HtrA1$^{-/-}$, *HtrA3*$^{-/-}$ and *HtrA1/3*$^{-/-}$ mice are viable and fertile, but they are slightly smaller than wild type mice in the first several weeks after birth. Parents of homozygous *HtrA1*$^{-/-}$, *HtrA3*$^{-/-}$ or *HtrA1/3*$^{-/-}$ mice were mated and the body weight of the progenies was examined every week after birth (Fig. 1). The *HtrA1*$^{-/-}$ mice have the Balb/C genetic background. *HtrA3*$^{-/-}$ and *HtrA1/3*$^{-/-}$ mice have the 129/B6 background. Accordingly, Balb/C or 129/B9 wild type mice were used for comparison with *HtrA1*$^{-/-}$ or *HtrA3*$^{-/-}$ and *HtrA1/3* $^{-/-}$ mice, respectively.

Body weight of *HtrA1*$^{-/-}$ newborn pups was significantly lighter than that of wild type Balb/C mice until the third week, but the difference in body weight became insignificant in the fourth week (Fig. 1A). *HtrA3*$^{-/-}$ mice were also lighter than the wild type 129/B6 mice. The significant difference persisted only for two weeks in case of *HtrA3*$^{-/-}$ mice and then disappeared in the third week (Fig. 1B). *HtrA1/3*$^{-/-}$ pups were even lighter than *HtrA3*$^{-/-}$ mice. It took four weeks for the *HtrA1/3*$^{-/-}$ pups to catch up with the body weight of wild type mice (Fig. 1C). These differences in body weight in the early life suggest that the deficiency in *HtrA1* and *HtrA3* have detrimental effects on placental or embryonic development.

Next I examined the weight of embryos of these knockout mice. In order to make the comparison among the three KO mice possible, we used *HtrA1*$^{-/-}$ mice with genetic background of 129/B6 in this experiment and all the following experiments. Pregnant mice were sacrificed on the gestational day 14.5 (E14.5). Embryos and placentas were separately weighed. The embryos of all three types of KO mice were significantly lighter than wild type (*HtrA*+/+) embryos (Fig. 2A). The placentas of KO mice were also lighter than the wild type placentas (Fig. 2B).

A.

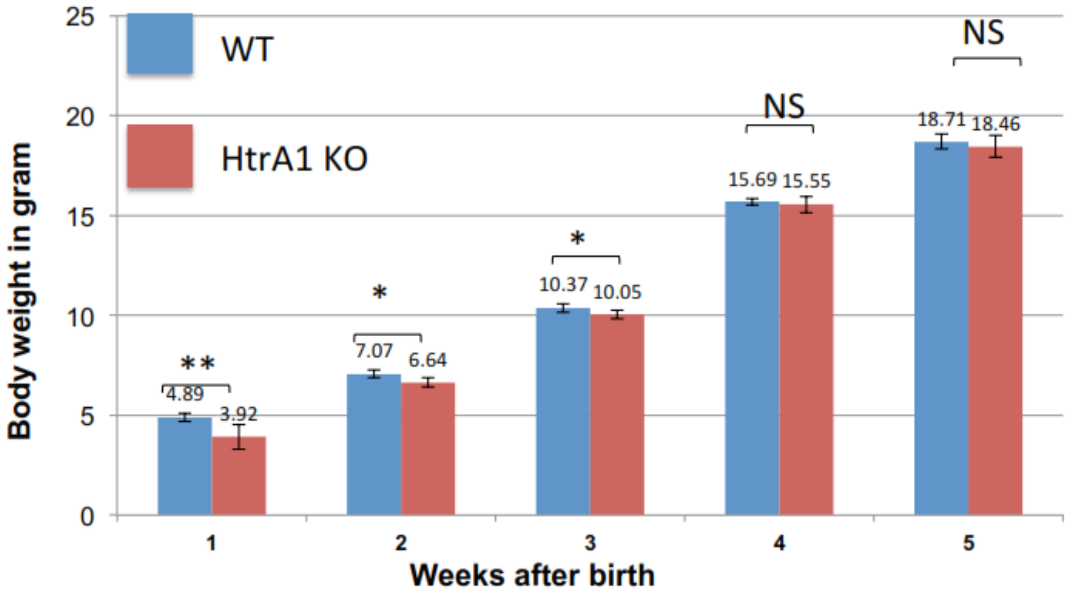
WT
HtrA1 KO
Body weight in gram
Weeks after birth
0
5
10
15
20
25
1
2
3
4
5
**
*
*
NS
NS
4.89
3.92
7.07
6.64
10.37
10.05
15.69
15.55
18.71
18.46

B.

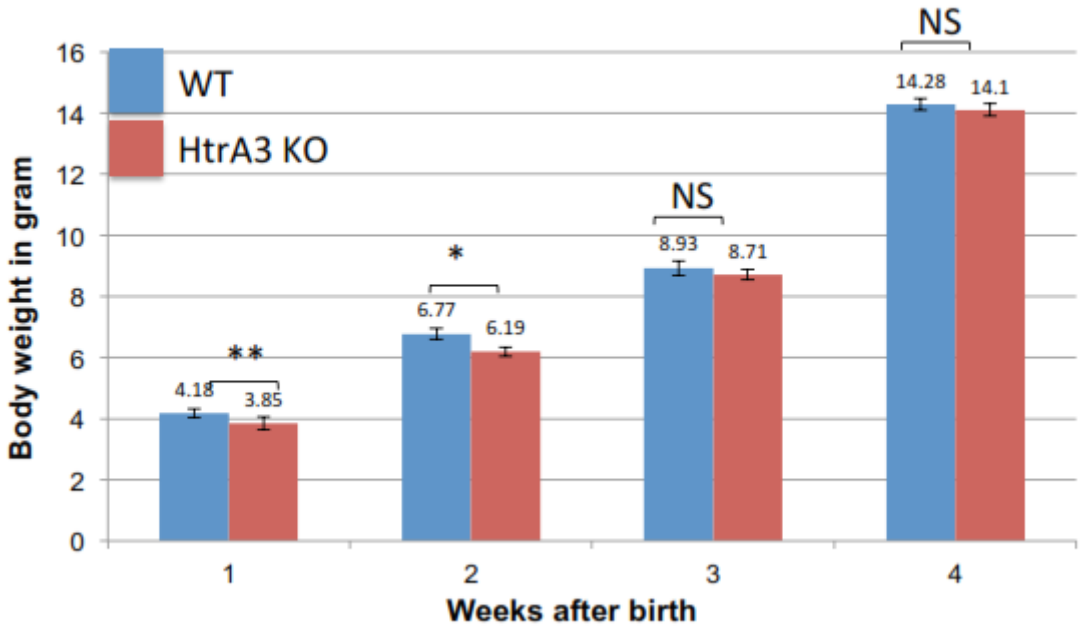
WT
HtrA3 KO
Body weight in gram
Weeks after birth
0
2
4
6
8
10
12
14
16
1
2
3
4
**
*
NS
NS
4.18
3.85
6.77
6.19
8.93
8.71
14.28
14.1

C.

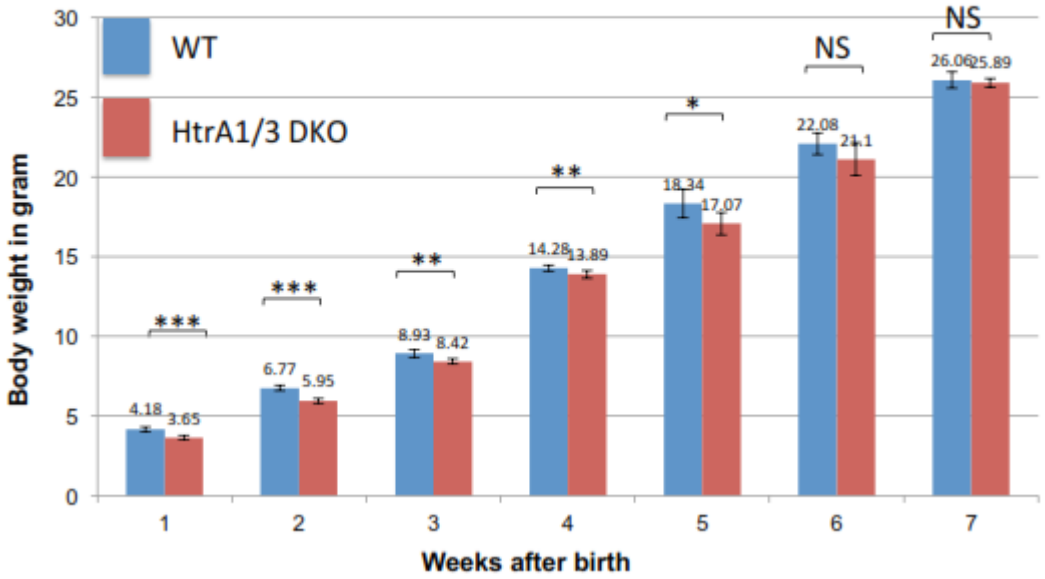

Figure 1. Low body weight of pups born from mating of *HtrA1*$^{-/-}$, *HtrA3*$^{-/-}$ and *HtrA1/3*$^{-/-}$ parents. A) Comparison of body weight of *HtrA*+/+ (N=8) and *HtrA1*$^{-/-}$ (N=7) pups from Balb/C genetic background after birth. **B)** Comparison of body weight of *HtrA*+/+ (N=10) and *HtrA3*$^{-/-}$ (N=8) mice pups from 129/B6 genetic background after birth. **C)** Comparison of body weight of *HtrA*+/+ (N=10) and *HtrA1/3*$^{-/-}$ pups (N=10) from129/B6 genetic background after their birth. P value was calculated by Student's T test. *= P<0.05, **= P<0.005 and ***= P< 0.0005. N shows the number pups used for the analysis.

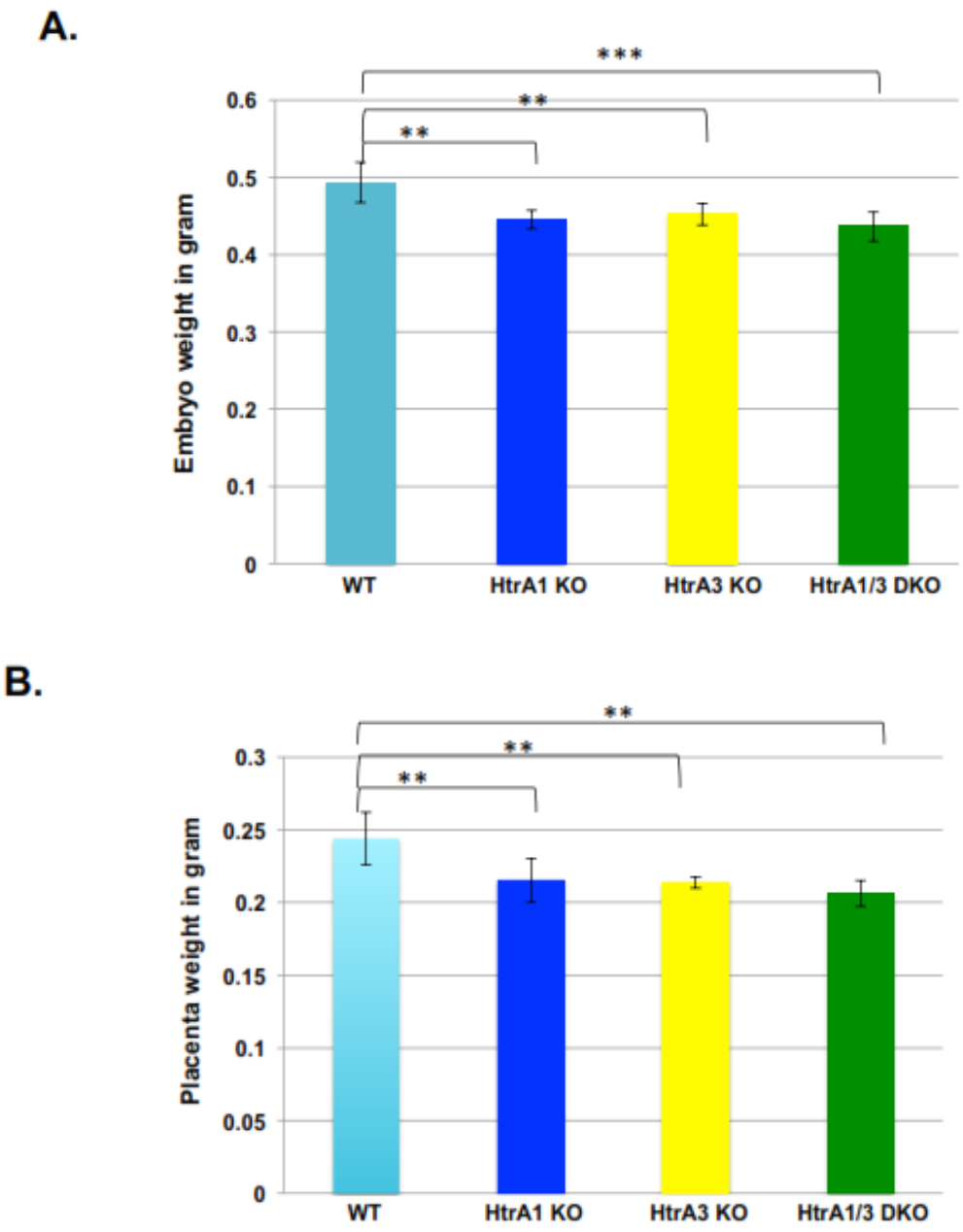

Figure 2. Decrease in weight of the placenta and embryos of *HtrA* KO mice at E14.5. **A)** Embryos were harvested from *HtrA*+/+ (N=8), *HtrA1*$^{-/-}$ (N=7), *HtrA3*$^{-/-}$ (N=7) and *HtrA1/3*$^{-/-}$ (N=8) mice at E14.5 and weight was measured immediately. **B)** Weight of placentas. All mice used in this experiment are from 129/B6 genetic background. P value was calculated by Student's T test. *= P<0.05, **= P<0.005 and ***= P< 0.0005. N shows the number pups used for the analysis.

3-2 The placental development is defective in *HtrA1* and *HtrA3* deficient mice at E10.5

I suspected that the defects in placenta caused smaller embryos and pups of *HtrA1*$^{-/-}$, *HtrA3*$^{-/-}$ or *HtrA1/3*$^{-/-}$ mice. Accordingly, I examined placenta sections. Paraffin sections of placentas were stained with HE (Fig. 3A). Total length of the placenta (maternal decidua+ fetal placenta) was shorter for all three types of homozygous KO mice as compared with the wild type (Fig 3B). Since the size of the maternal decidua of the KO mice and wild type mice did not differ, I focused on the fetal part of placenta and measured the area of the labyrinth and the junctional zone (Fig. 3C and D). Quantitative analysis revealed that the labyrinth (Fig. 3C) and the junctional zone (Fig 3D) are smaller in *HtrA1*$^{-/-}$, *HtrA3*$^{-/-}$ or *HtrA1/3*$^{-/-}$ placentas than the wild type placentas. In the labyrinth, fetal blood vessels are in close contact with maternal blood. The fetal blood vessels and maternal blood sinusoids can be separated based on the histology of blood cells; fetal blood cells are nucleated and stained dark blue with HE, while maternal blood cells are enucleated and stained red. The total area of fetal blood vessel cavity and that of maternal sinusoid cavity were measured (Fig. 4B and C). The maternal sinusoid area was decreased in the labyrinth of *HtrA1*$^{-/-}$, *HtrA3*$^{-/-}$ and *HtrA1/3*$^{-/-}$ placenta at E10.5 (Fig. 4B). Similarly, the area of fetal blood cavity was also reduced in these KO mice placentas as compared with the wild type placenta (Fig. 4C).

A

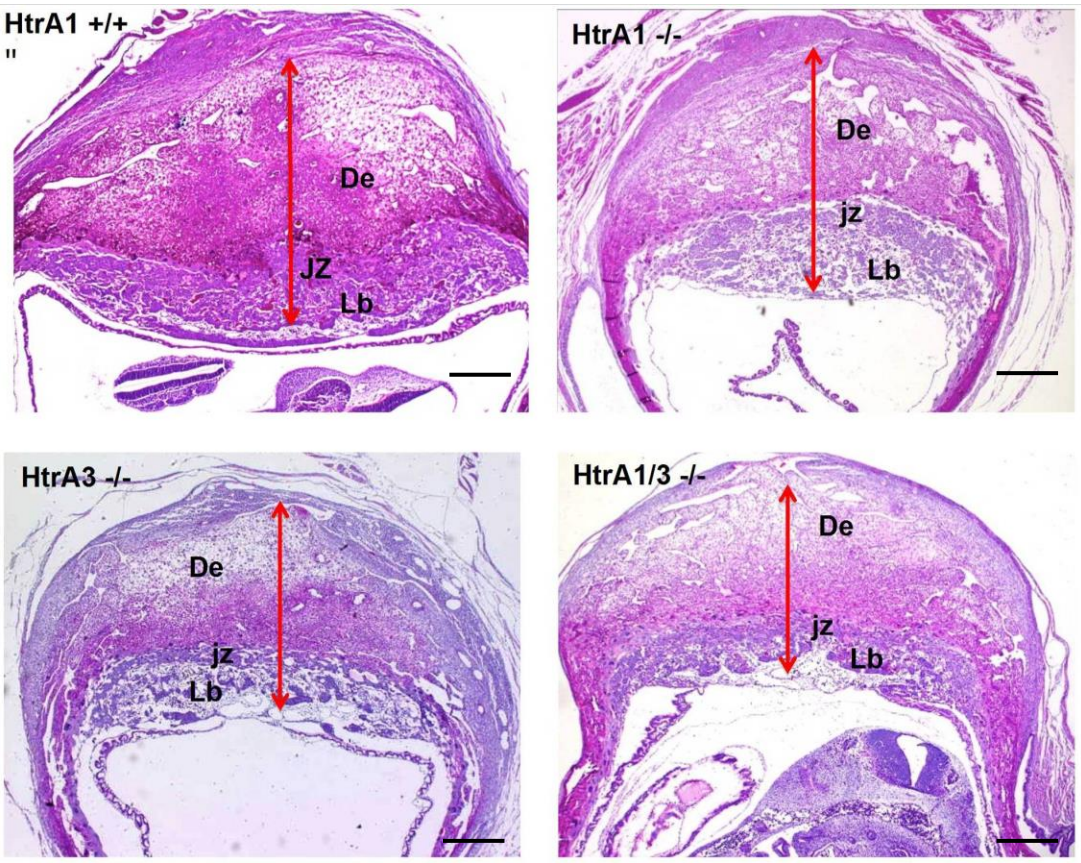
HtrA1 +/+
"
De
JZ
Lb
HtrA1 -/-
De
jz
Lb
HtrA3 -/-
De
jz
Lb
HtrA1/3 -/-
De
jz
Lb

B

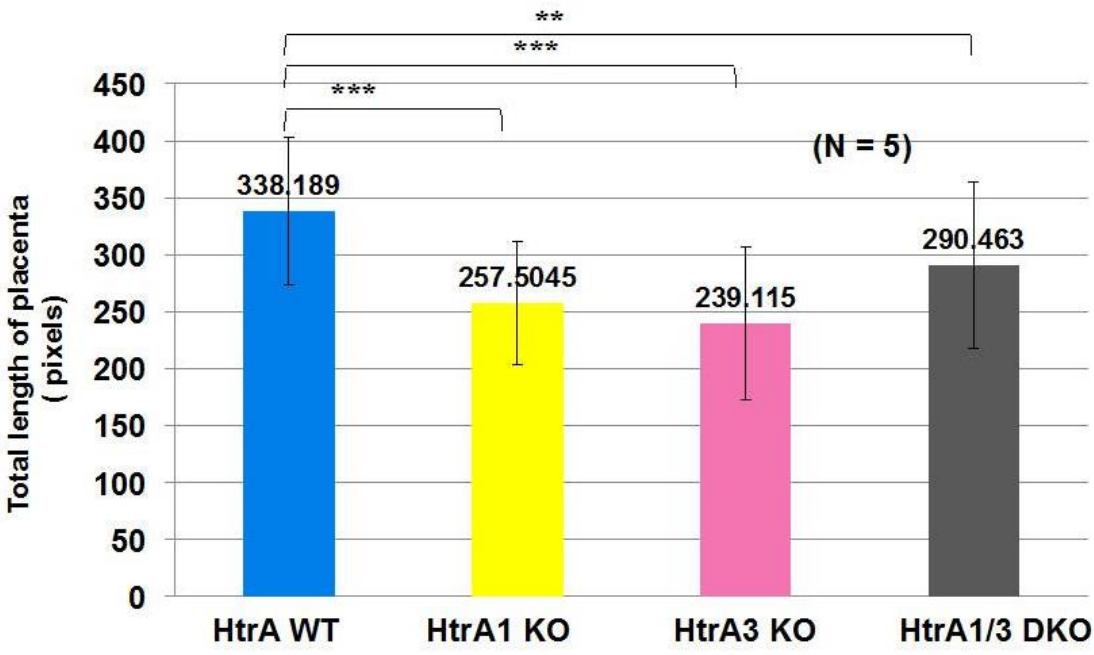
**
***
***
(N = 5)
338.189
257.5045
239.115
290.463
Total length of placenta (pixels)
450
400
350
300
250
200
150
100
50
0
HtrA WT
HtrA1 KO
HtrA3 KO
HtrA1/3 DKO

C

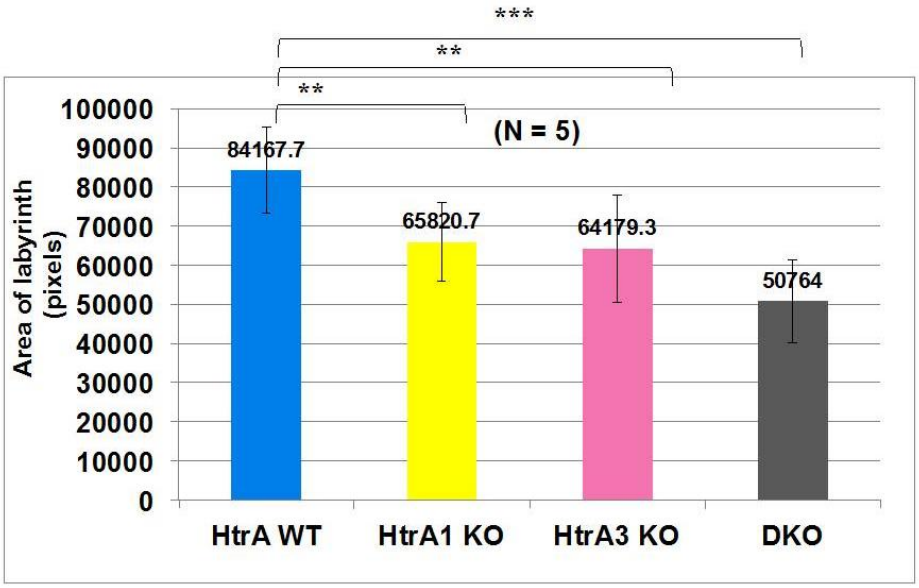

D

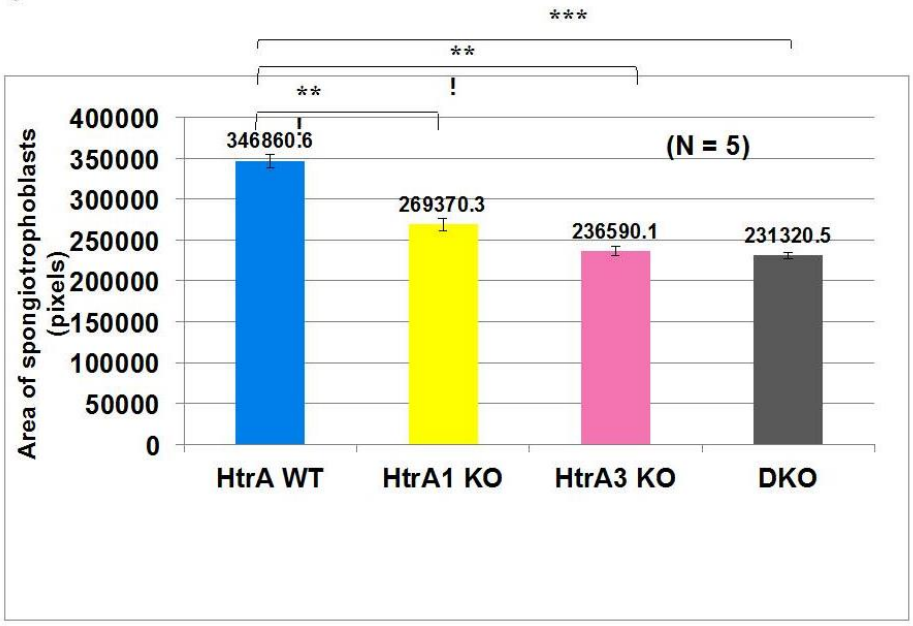

Figure 3. Placenta was smaller due to smaller labyrinth and junctional zone in *HtrA* KO mice at E10.5. **A)** *HtrA*+/+, *HtrA1*$^{-/-}$, *HtrA3*$^{-/-}$ and *HtrA1/3*$^{-/-}$ placentas were harvested at E10.5 and stained with HE. **B)** Total length of the placenta (maternal decidua plus fetal placenta) was measured (marked with red line in figure A). **C)** Area of the labyrinth. **D)** Area of the junctional zone (spongiotrophoblasts layer). P value was calculated by Student's T test. *= P<0.05, **= P<0.005 and ***= P< 0.0005. N shows the number of placentas used for quantification. Three different sections from each placenta were used for the analysis. Scale bars = 500 µm.

A

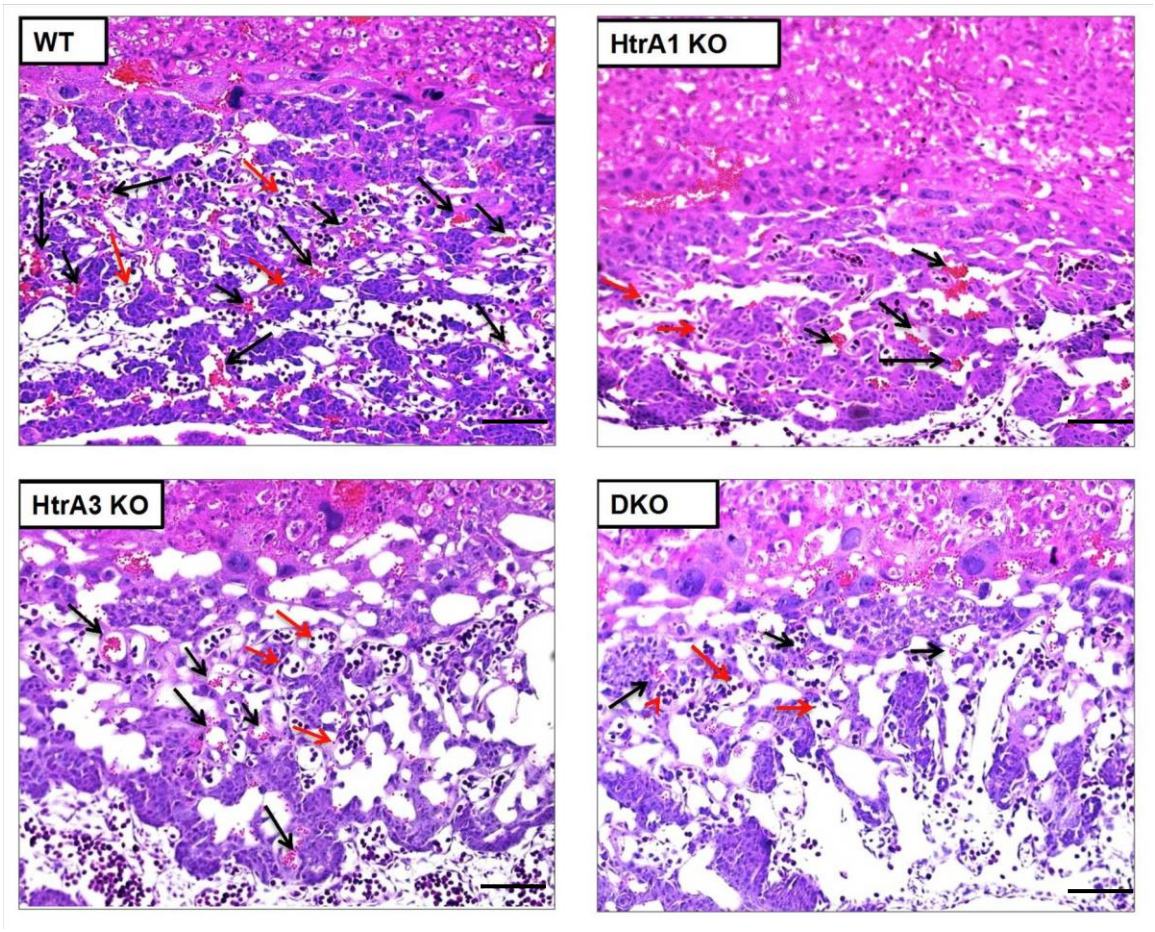
WT
HtrA1 KO
HtrA3 KO
DKO

B.

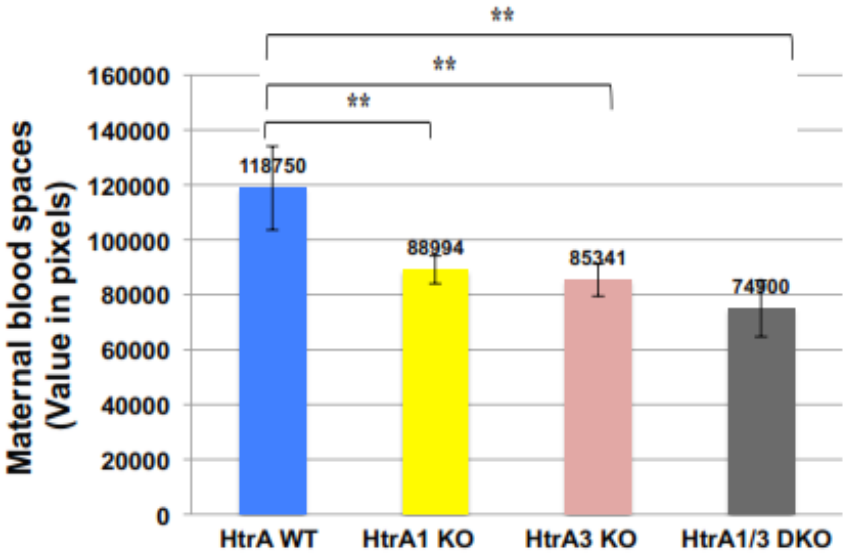
**
**
**
Maternal blood spaces (Value in pixels)
160000
140000
120000
100000
80000
60000
40000
20000
0
118750
88994
85341
74900
HtrA WT
HtrA1 KO
HtrA3 KO
HtrA1/3 DKO

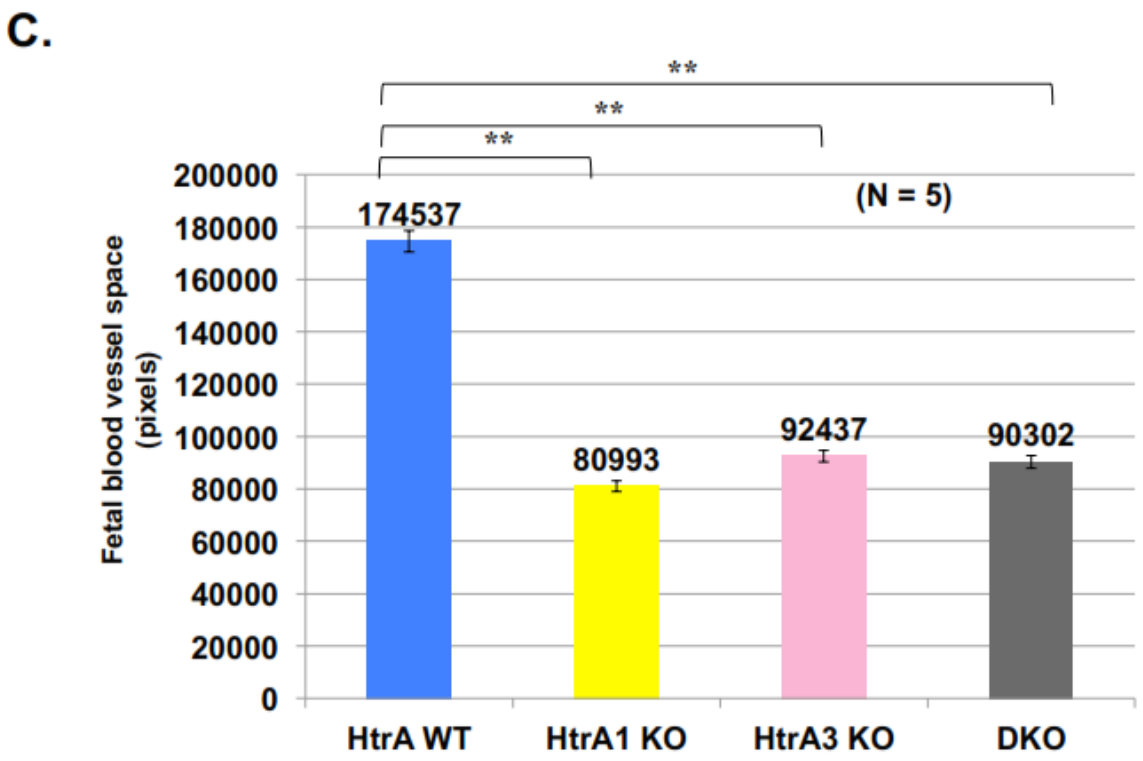

Figure 4. Area of maternal and fetal blood spaces in the labyrinth was decreased in *HtrA* KO mice at E10.5. **A)** HE staining showing the fetal part (labyrinth plus junctional zone) of the placenta and the maternal blood spaces (marked with black arrow) and fetal blood spaces (marked with red arrow) in the labyrinth. **B)** Maternal blood spaces in the labyrinth of *HtrA1* $^{-/-}$, *HtrA3* $^{-/-}$ and *HtrA1/3*$^{-/-}$ placenta at E10.5. **C)** Fetal blood spaces in *HtrA1*$^{-/-}$, *HtrA3*$^{-/-}$ and *HtrA1/3*$^{-/-}$ placenta. P value was calculated by Student's T test. *= P<0.05, **= P<0.005 and ***= P< 0.0005. N shows the number of placentas used for quantification. Three different sections from each placenta were used for the analysis. Scale bars = 500 µm.

3-3 Placental defects persist on E14.5 in *HtrA1* and *HtrA3* deficient mice

Placentas were removed from *HtrA1*$^{-/-}$, *HtrA3*$^{-/-}$ and *HtrA1/3*$^{-/-}$ mice at E 14.5. Paraffin sections of the placentas were stained with PAS (periodic acid-Schiff) (Fig. 5A). Reduction in total placenta length was observed in *HtrA1*$^{-/-}$, *HtrA3*$^{-/-}$ and *HtrA1/3*$^{-/-}$ placenta (Fig. 5B). The labyrinth was significantly smaller in *HtrA1*$^{-/-}$, *HtrA3*$^{-/-}$ and *HtrA1/3*$^{-/-}$ placentas as compared with the wild type placentas (Fig. 5C). Next, placentas were stained with isolectin B4, which specifically stains fetal blood vessels. The fetal vessels of the wild type placenta looked elongated with long straight segments, and ran parallel to each other toward the decidua (Fig. 6A), while those of *HtrA1*$^{-/-}$ (Fig. 6B), HtrA3$^{-/-}$ (Fig. 6C) and *HtrA1/3*$^{-/-}$ (Fig. 6D) placentas branched more, and were more randomly aligned. These abnormal structures of the fetal blood vessels were most prominent in *HtrA1/3*$^{-/-}$ mice (Fig. 6D).

PAS stains glycogen trophoblasts (GlyT) in the junctional zone. Some islands like structures were present in the labyrinth (Fig. 6A), and those were aggregates of PAS positive trophoblasts (Fig. 7A). The PAS positive islands in the labyrinth were larger and more abundant in *HtrA1*$^{-/-}$, *HtrA3*$^{-/-}$ and *HtrA1/3*$^{-/-}$ placentas than in the wild type placentas (Fig 7A). The total are of the PAS positive islands in the labyrinth were measured (Fig. 7B), and the result showed that the placentas of *HtrA1/3*$^{-/-}$ mice had the most PAS positive cells in the labyrinth.

PAS positive GlyT usually reside in the junctional zone and some invade the maternal decidua. In normal placenta, a small number of GlyT are left behind in the labyrinth, because of delayed migration of some trophoblasts toward the maternal decidua. Increase in PAS positive cells in the labyrinth indicated defective trophoblast migration in these KO mice. I, therefore, examined the cellular components of the junctional zone, which is mainly composed of spongiotrophoblasts (SpT) and GlyT. SpT, which are the main cell type in the junctional zone, are not stained with PAS and appear grey in the cytoplasm with large nuclei, while GlyT are stained magenta with

small and dense nuclei and vacuoles in the cytoplasm (Fig. 8A). SpT were decreased in all three types of knockout placentas (Fig. 8B). GlyT in the junctional zone were also decreased in knockout placentas as compared with the wild type (Fig. 8C). The decrease in both SpT and GlyT could result in the reduction of the thickness of the junctional zone.

SpT and GlyT in the junctional zone are derived from the ectoplacental cone-derived precursor cells. The above-mentioned data suggested that differentiation of the precursor cells and/or the migration of GlyT were defective in the KO mice. All the phenotypes displayed by the KO placentas disappeared by E 16.5 (Fig 9).

A

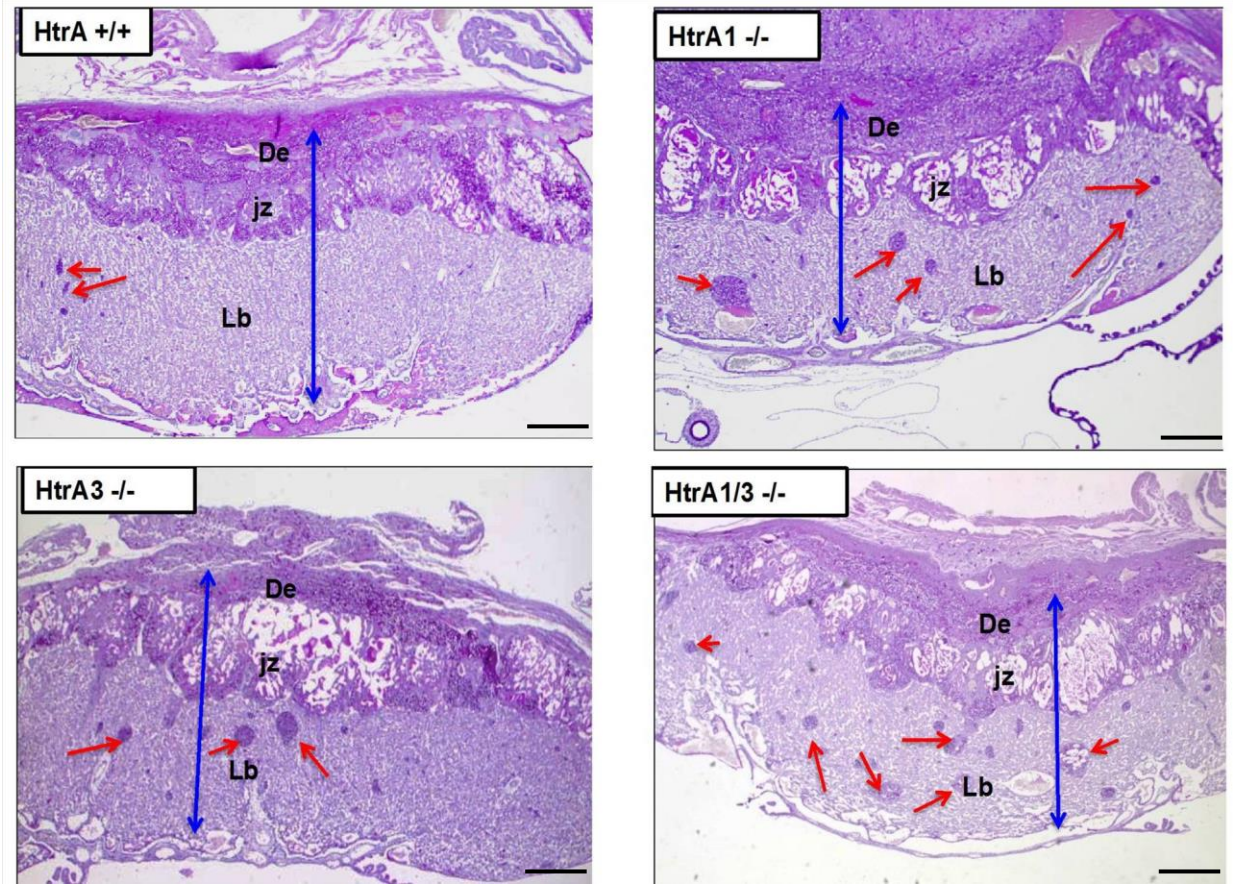
HtrA +/+
De
jz
Lb
HtrA1 -/-
De
jz
Lb
HtrA3 -/-
De
jz
Lb
HtrA1/3 -/-
De
jz
Lb

B

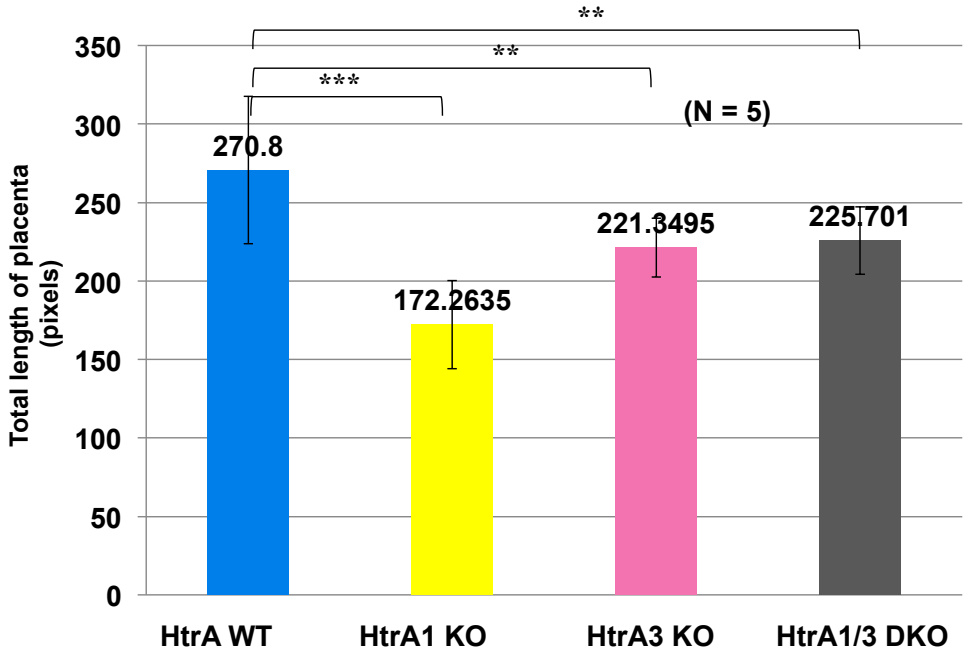
**
**
***
(N = 5)
Total length of placenta (pixels)
350
300
250
200
150
100
50
0
270.8
172.2635
221.3495
225.701
HtrA WT
HtrA1 KO
HtrA3 KO
HtrA1/3 DKO

C

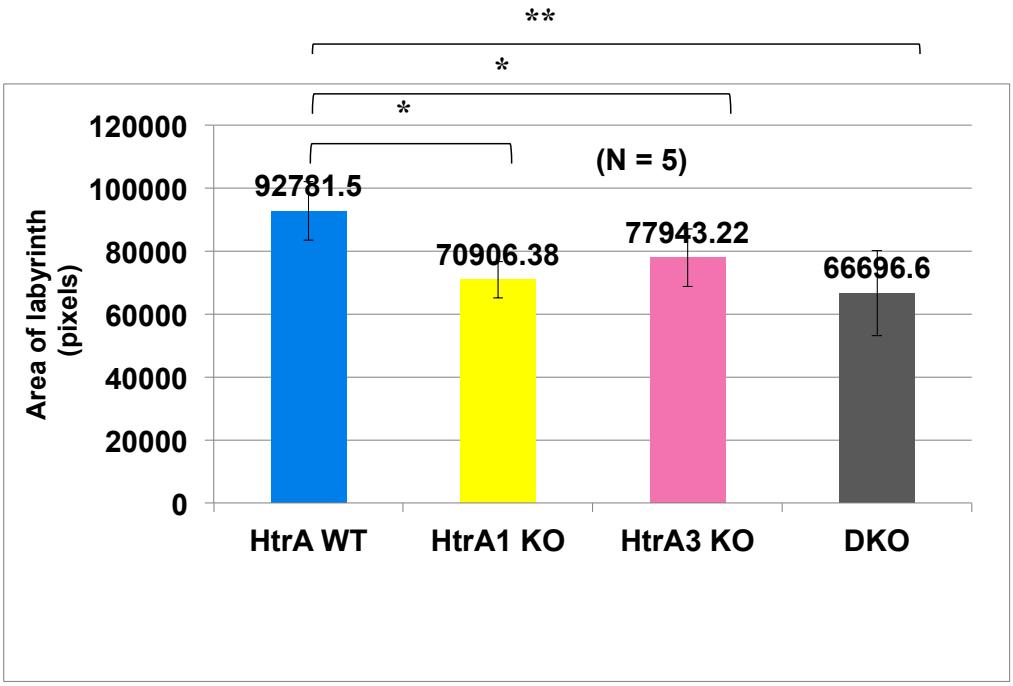

Figure 5. Placenta and labyrinth were smaller in *HtrA* KO mice at E14.5. A) *HtrA*+/+, *HtrA1* $^{-/-}$, *HtrA3*$^{-/-}$ and *HtrA1/3*$^{-/-}$ placentas were harvested and stained with PAS reagent. Red arrows show PAS positive glycogen cell islets in the labyrinth and blue lines show the total length of placenta. **B)** Total placental length (maternal decidua+ fetal placenta). **C)** Are of the labyrinth. P value was calculated by Student's T test. *= P<0.05, **= P<0.005 and ***= P< 0.0005. N shows the number of placentas used for quantification. Three different sections from each placenta were used for the analysis. Scale bars = 500 µm.

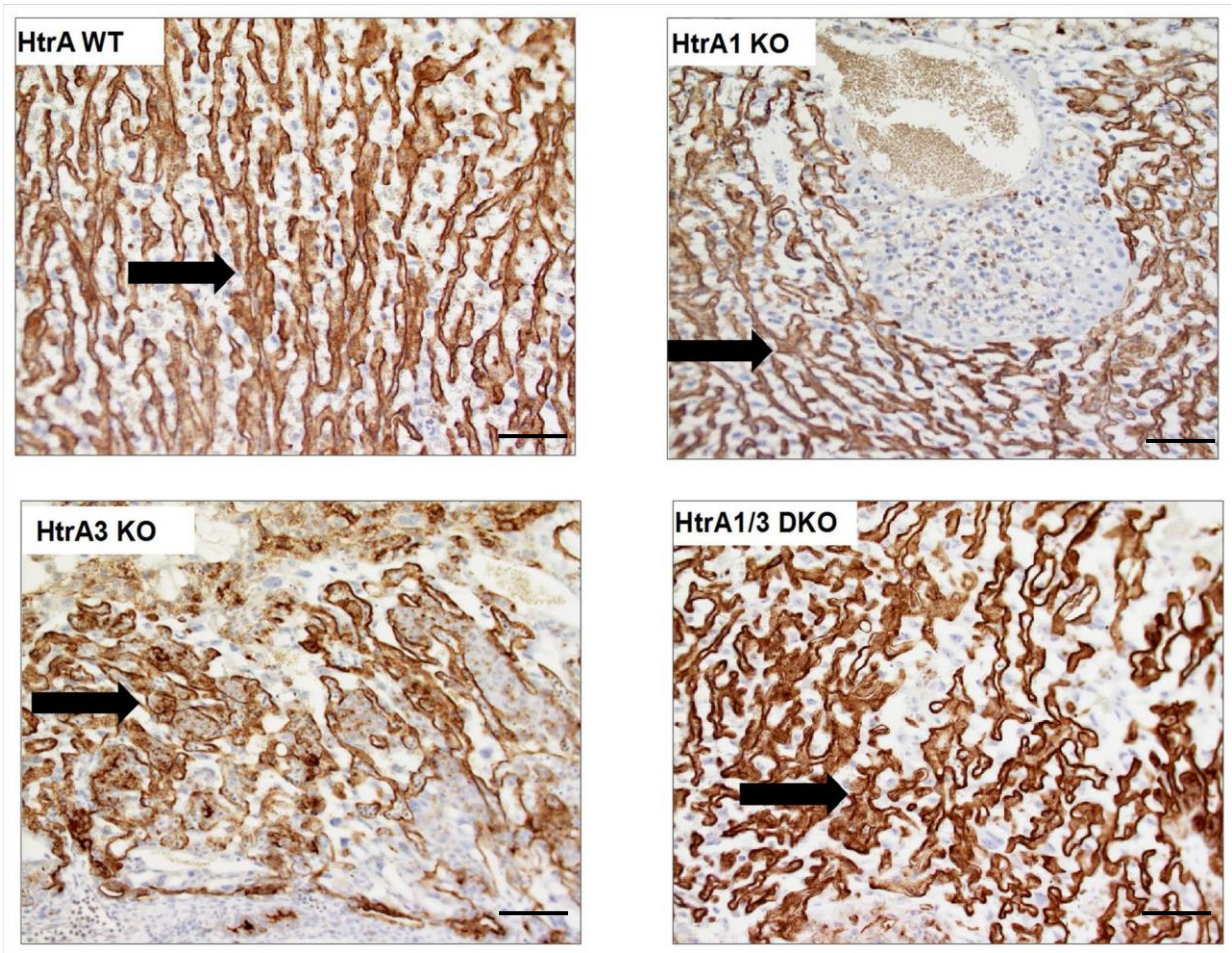

Figure 6. Branching angiogenesis was decreased in *HtrA1*$^{-/-}$, *HtrA3*$^{-/-}$ and *HtrA1/3*$^{-/-}$ mouse placentas at E14.5. Sections from *HtrA* +/+, *HtrA1*$^{-/-}$, *HtrA3*$^{-/-}$ and *HtrA1/3*$^{-/-}$ placentas at E14.5 were immunostained with anit-isolectin B4 antibody, which specifically stained fetal blood vessels. Fetal blood vessels are stained brown. Branching of vessels is pointed with black arrows. Scale bars = 500 µm.

A

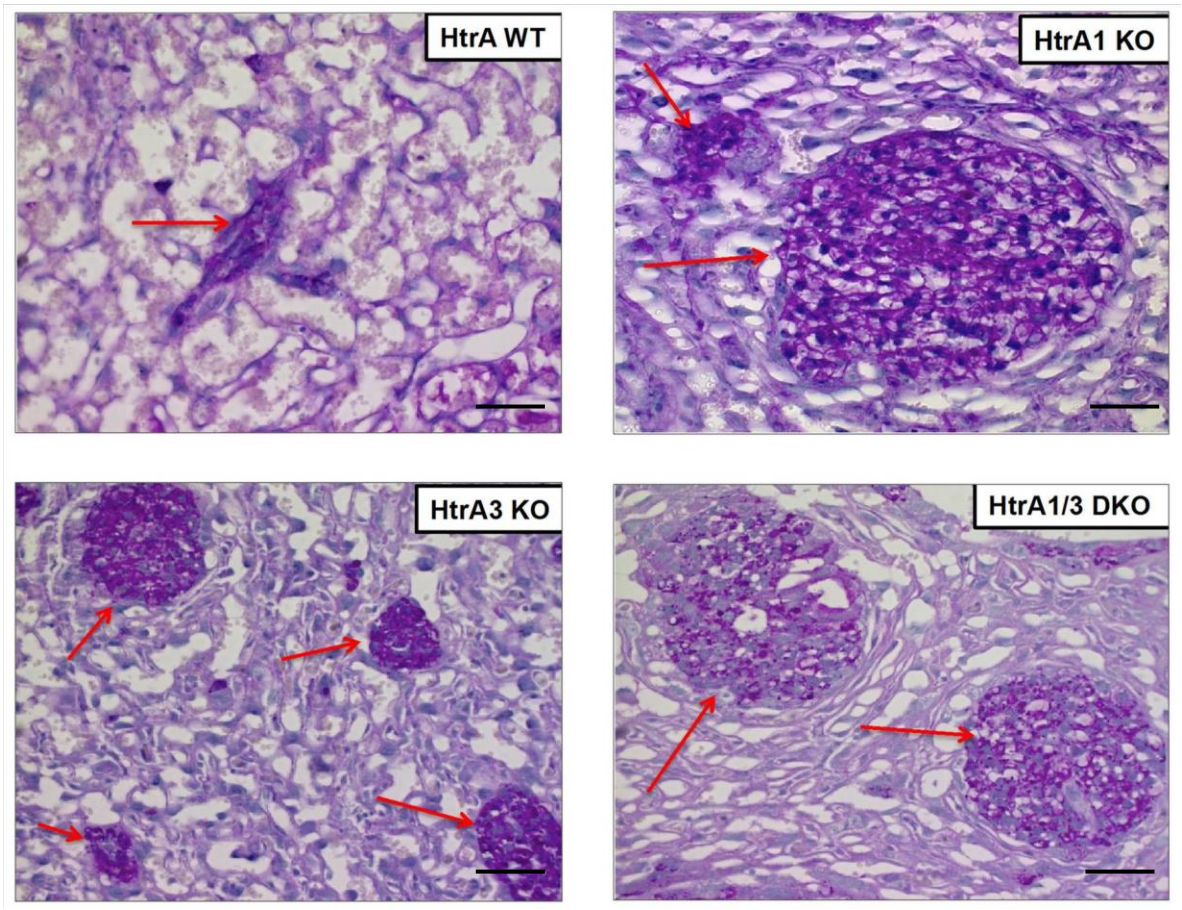
HtrA WT
HtrA1 KO
HtrA3 KO
HtrA1/3 DKO

B

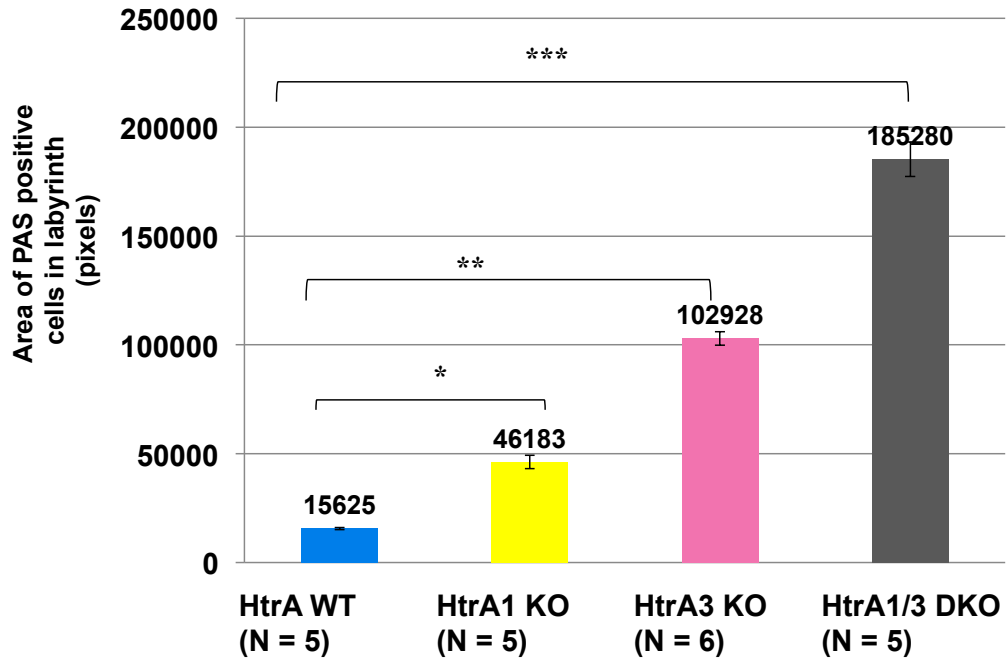
Area of PAS positive cells in labyrinth (pixels)
250000
200000
150000
100000
50000
0
***
**
*
185280
102928
46183
15625
HtrA WT (N = 5)
HtrA1 KO (N = 5)
HtrA3 KO (N = 6)
HtrA1/3 DKO (N = 5)

Figure 7. Large PAS-positive cell clusters remained in the labyrinth of *HtrA1*$^{-/-}$, *HtrA3*$^{-/-}$ and *HtrA1/3*$^{-/-}$ mouse placentas at E14.5. Sections of E14.5 placentas were stained with PAS. **A)** PAS positive structures (marked with red arrows) present in the labyrinth of *HtrA*+/+, *HtrA1*$^{-/-}$, *HtrA3*$^{-/-}$ and *HtrA1/3*$^{-/-}$ placenta. **B)** Area of PAS positive cells in the labyrinth. P value was calculated by Student's T test. *= P<0.05, **= P<0.005 and ***= P< 0.0005. N shows the number of placentas used for quantification. Three different sections from each placenta were used for the analysis. Scale bars = 500 μm.

A

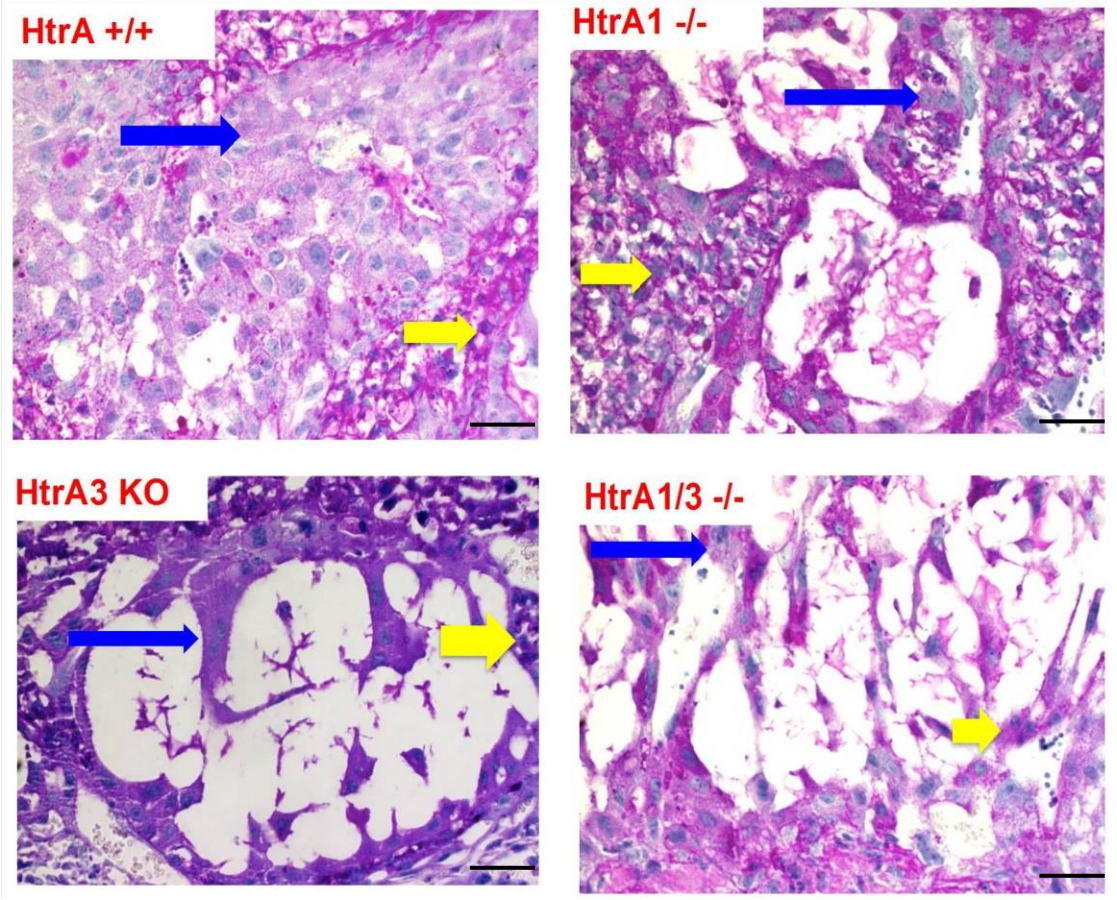
HtrA +/+
HtrA1 -/-
HtrA3 KO
HtrA1/3 -/-

B

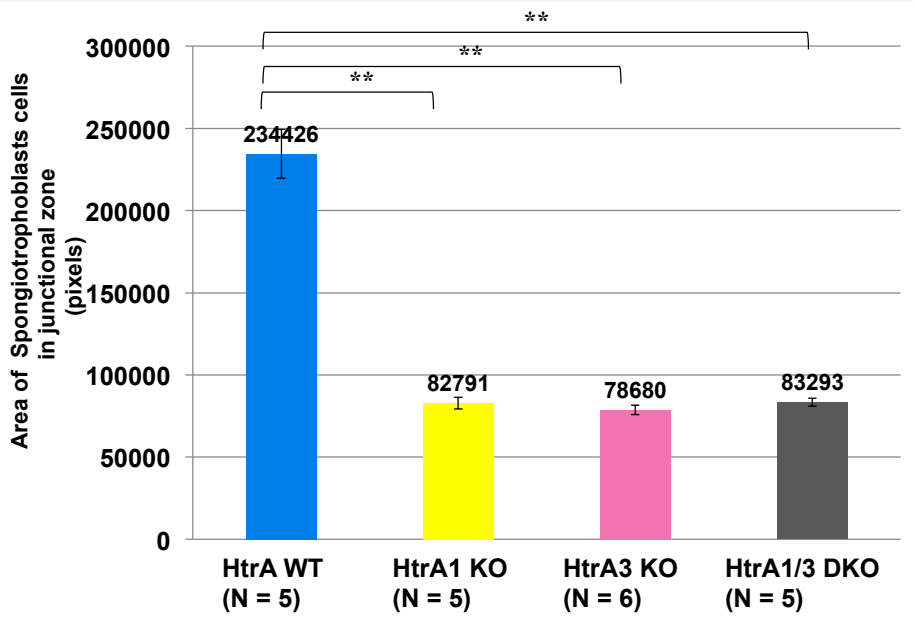
Area of Spongiotrophoblasts cells in junctional zone (pixels)
300000
250000
200000
150000
100000
50000
0
**
**
**
234426
82791
78680
83293
HtrA WT (N = 5)
HtrA1 KO (N = 5)
HtrA3 KO (N = 6)
HtrA1/3 DKO (N = 5)

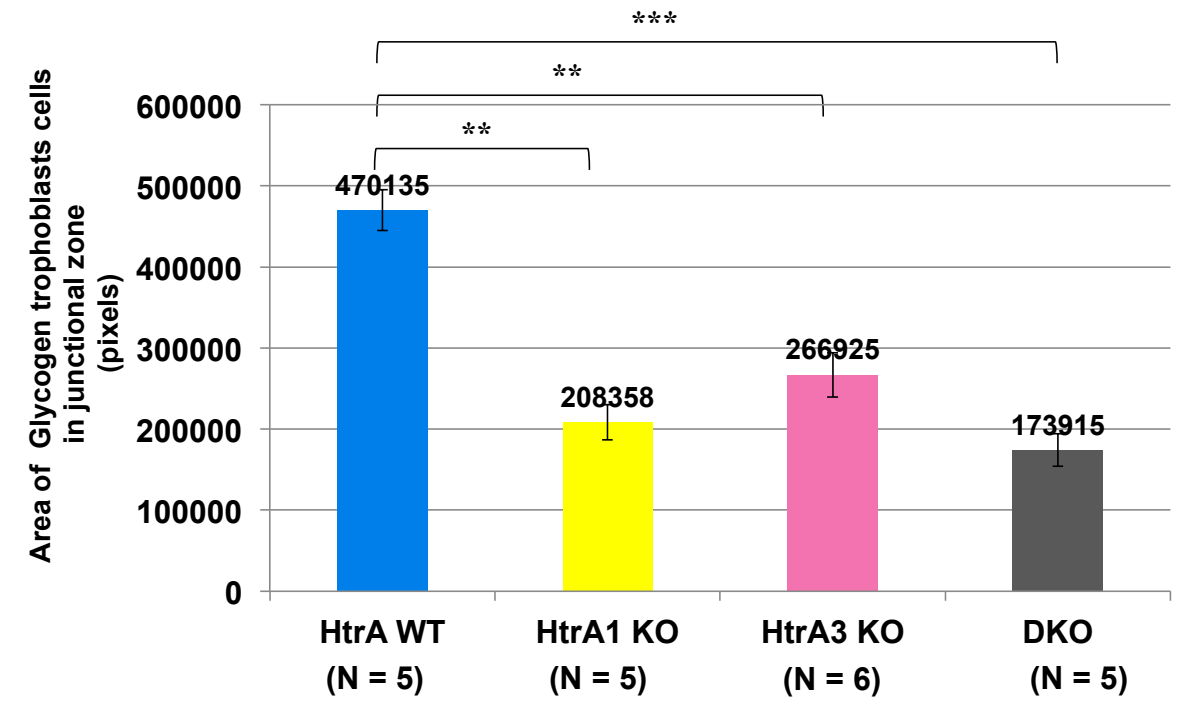

Figure 8. Spongiotrophoblasts and glycogen trophoblasts were reduced in the junctional zone in *HtrA1*$^{-/-}$, *HtrA3*$^{-/-}$ and *HtrA1/3*$^{-/-}$ mouse placentas at E 14.5. A) Presence of SpT (marked with blue arrows) and GlyT (marked with yellow arrows) in *HtrA*+/+, *HtrA1*$^{-/-}$, *HtrA3*$^{-/-}$ and *HtrA1/3*$^{-/-}$ mouse placentas at E14.5. **B)** Area occupied by SpT in the junctional zone. **C)** Area occupied by GlyT in the junctional zone. P value was calculated by Student's T test. *= P<0.05, **= P<0.005 and ***= P< 0.0005. N shows the number of placentas used for quantification. Three different sections from each placenta were used for the analysis. Scale bars = 500 µm.

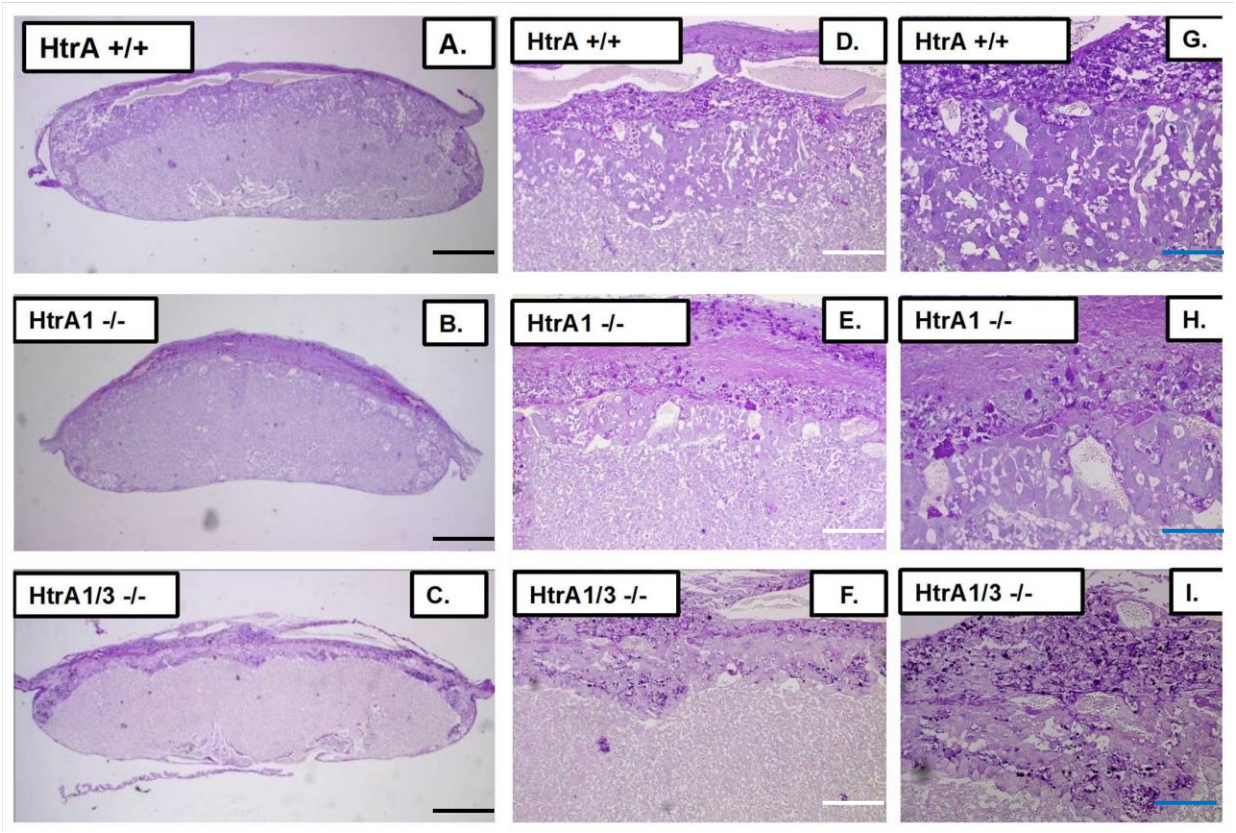

Figure 9. E16.5 placentas of *HtrA1*$^{-/-}$ and *HtrA1/3*$^{-/-}$ mice show normal histology. Sections from *HtrA*+/+, *HtrA1*$^{-/-}$, and *HtrA1/3*$^{-/-}$ placentas at E16.5 were stained with PAS. No differences were observed among *HtrA*$^{+/+}$ **(A)**, *HtrA1*$^{-/-}$ **(B)** and *HtrA1/3*$^{-/-}$ placentas **(C)**. **(D)** and **(G)** are magnified images of the junctional zone in the section depicted in (A); **(E)** and **(H)** are those in (B); **(F)** and **(I)** are those in (C). Black scale bars=1000 μm. White scale bars= 100 μm. Blue scale bars= 50 μm

3-4 Expression of *HtrA1* and *HtrA3* in the placenta

The expression of HtrA1 and HtrA3 has been analyzed mostly by immunostaining. Since these proteins are secretory, in situ hybridization is necessary to identify the cells expressing *HtrA1* and *HtrA3*.

In situ hybridization revealed that at E7.5, *HtrA1* mRNA was expressed by the cells in the decidua capsularis most strongly, and weakly by trophoblasts in the outer layer of the ectoplacental cone (Fig. 10 A, B), whereas *HtrA3* mRNA was not expressed at this stage (Fig. 10 C, D). At E8.5, HtrA3 started to express very faintly and diffusely in the maternal decidua both in the decidua basalis and decidua capsularis (Fig. 10 G, H). At this stage, expression of *HtrA1* continued in the outer ectoplacental cone and the decidua capsularis (Fig. 10 E, F). At E 9.5 and E 10.5, *HtrA1* expression became faint in the ectoplacental cone and restricted to a thin layer of cells in the outer ectoplacental cone (Fig. 11 A, B, C, G, H, and I). *HtrA1* expression in the decidua capsularis also decreased on E10.5 but still very strong compared to the expression in the ectoplacental cone (Fig. 11 G, H and I). *HtrA3* showed strong expression on E9.5 in the decidua basalis that borders on the ectoplacental cone (Fig. 11 D, E and F) and continued to show strong expression at E10.5 (Fig. 10 J, K and L). Along with decidual stromal cells, some cells around the maternal artery in the decidua expressed HtrA3 (Fig. 11 L, O and P). A few cells around the maternal artery in the decidua also expressed *HtrA1* (Fig 11 M and N)

In order to clearly identify cells that express *HtrA1* and *HtrA3*, I carried out in situ hybridization using various probes specific to trophoblast cell lineages (Fig. 12). In situ hybridization of E9.5 placenta with the *Tpbpa* probe, which is an ectoplacental cone marker in this stage, confirmed that *HtrA1* was expressed by trophoblast lineage cells in the outer layer of the ectoplacental cone (Fig. 12 A and F, also see Fig. 12 G and L). On the other hand, *HtrA3* was expressed by decidual cells outside the ectoplacental cone (Fig. 12 D and F, also see Fig. 12 G and L). The *HtrA1* expressing cells (see Fig. 12 G) were also positive for other trophoblast cell lineage markers, like *Pl-I* (Fig.12 H), *Pl-II* (Fig.12 I), and *Pl-f* (Fig.12 K). On the other hand, the *HtrA3* expressing cells (Fig.12 J) were completely negative for those trophoblast markers.

Trophoblast giant cells (TGC) demarcate the border between fetal and maternal tissues. TGC is the first trophoblast cell lineage differentiated around E6.5 from the mural trophoectoderm. TGC express *Pl-I* (Fig. 13). The *HtrA1* expressing cells in the capsule were negative for *Pl-I*, indicating that TGC do not express *HtrA1* (Fig. 13 D and F).

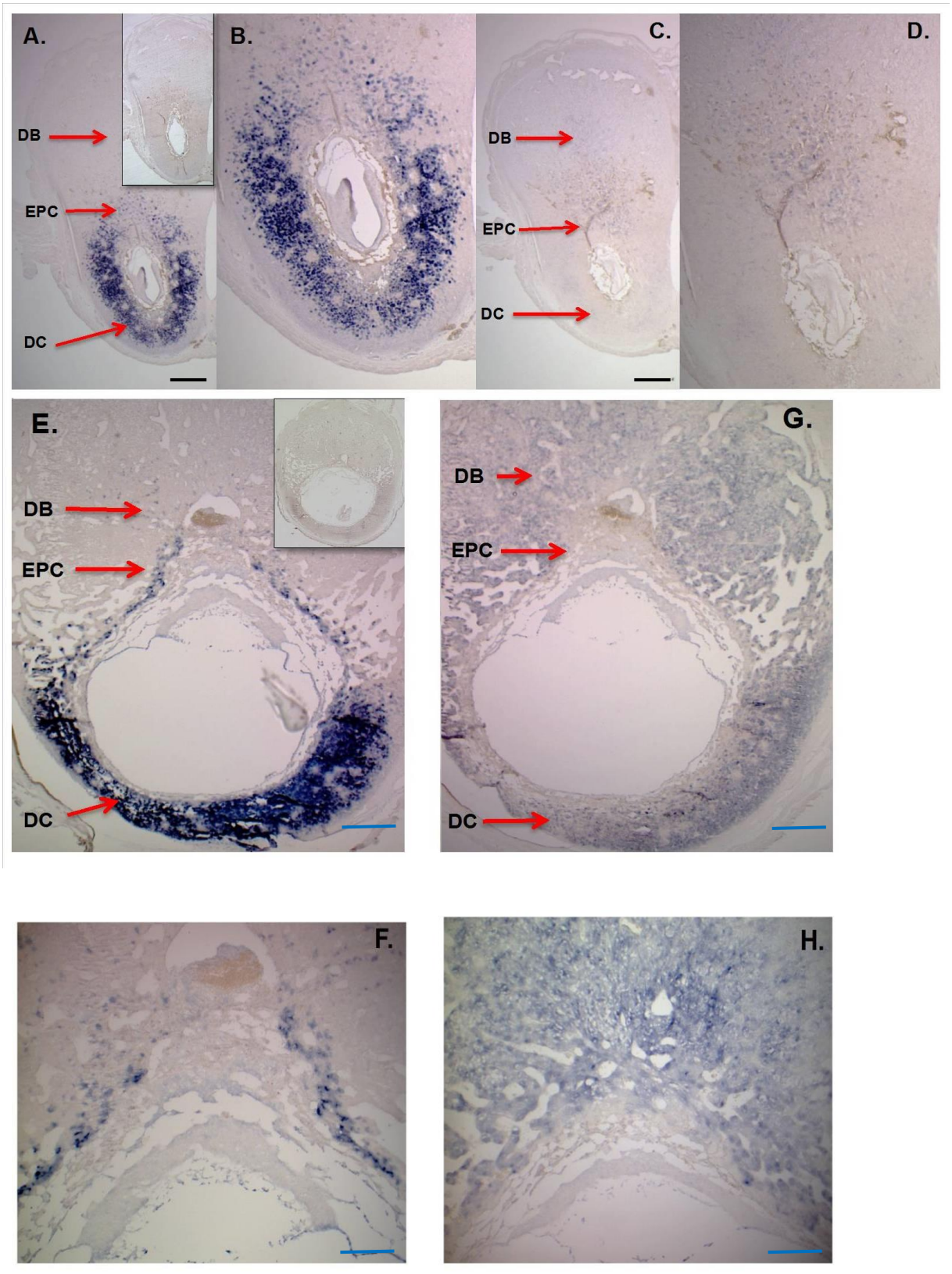
A.
DB
EPC
DC
B.
C.
DB
EPC
DC
D.
E.
DB
EPC
DC
G.
DB
EPC
DC
F.
H.

Figure 10. Expression of *HtrA1* and *HtrA3* at early stages of mouse placenta development. A) *HtrA1* expression in the placenta at E 7.5. **B)** Magnified image of (A) to show **HtrA1** expressing cells. **C)** *HtrA3* expression at E 7.5. **D)** Magnified image of (C) to show *HtrA3* expressing cells. **E) HtrA1** expression at E 8.5. **F)** Magnified image of EPC region from (E). **G)** *HtrA3* expression at E 8.5. **H)** Magnified image of DB region from (G). DB = Decidua Basalis, EPC = Ectoplacental Cone, DC = Decidua Capsularis. Insets in (A) and (E) show the results with sense control probes. Black scale bars=500 μm. White scale bars= 250 μm. Blue scale bars= 100 μm.

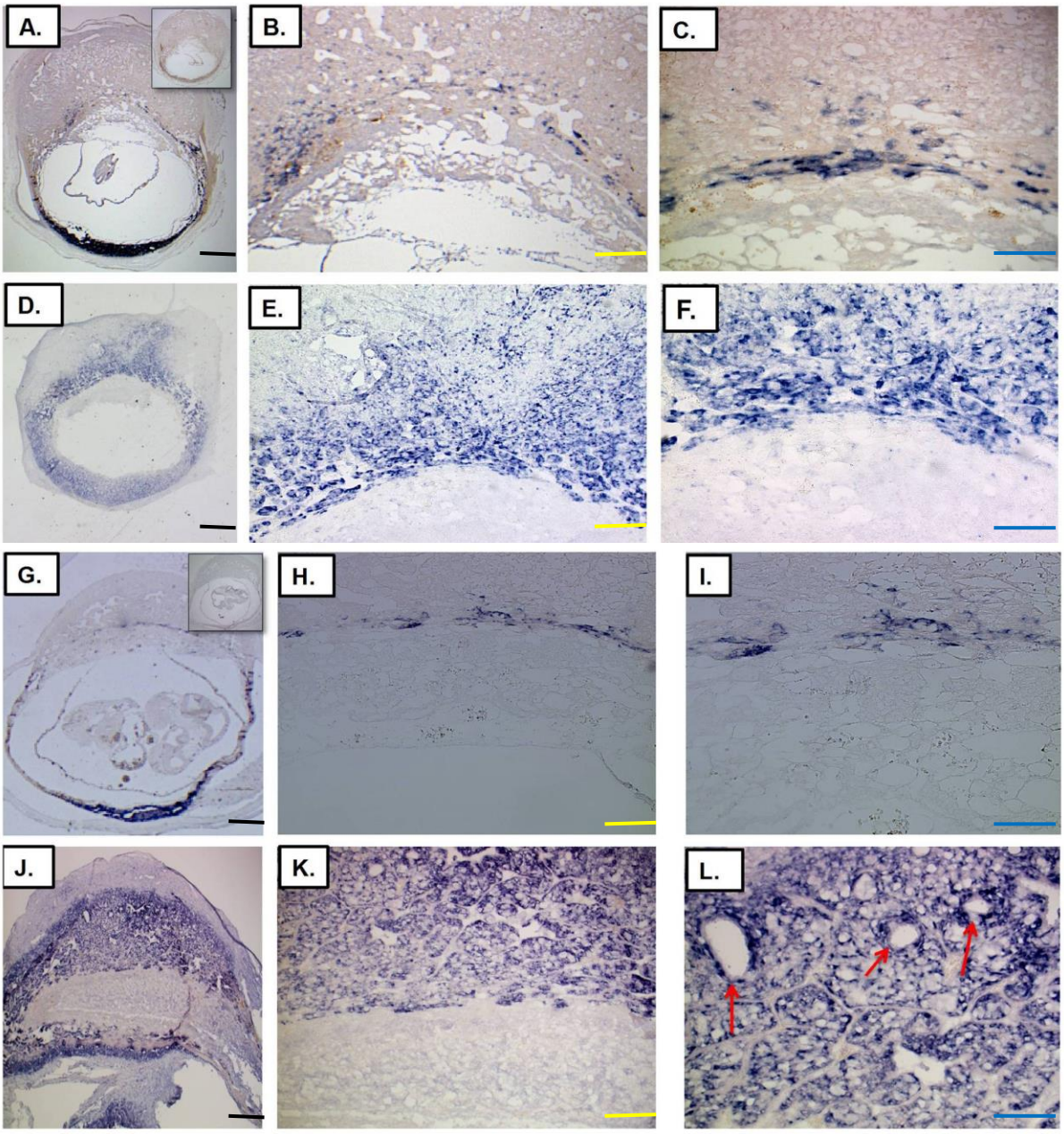
A.
B.
C.
D.
E.
F.
G.
H.
I.
J.
K.
L.

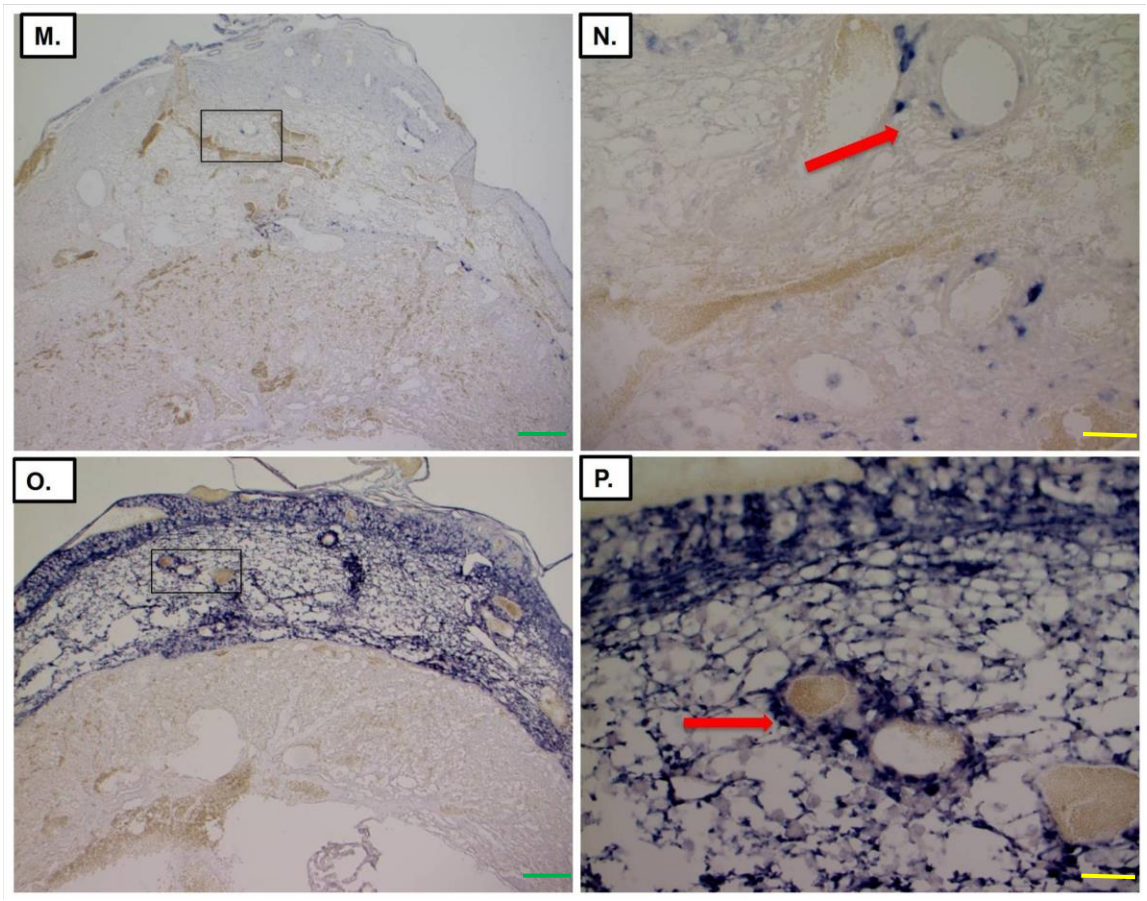

Figure 11. ***HtrA3*** **were strongly expressed, but** ***HtrA1*** **expression was diminished at E9.5 and E12.5. A) HtrA1** expression at E 9.5. **B)** , **C)** Magnified images from (A). **D)** *HtrA3* expression at E 9.5. **E)**, **F)** Magnified images from (D). **G)** Expression of *HtrA1* at E10.5. **H), I)** Magnified images from (G). **J)** Expression of *HtrA3* at E10.5. **K)**, **L)** Magnified images from (J). **M)** *HtrA1* expression at E12.5. **N)** Magnified area marked by a box in (M). **O)** *HtrA3* expression at E12.5. **P)** Magnified area marked by a box in (O) DB= Decidua Basalis, EPC= Ectoplacental Cone, DC= Decidua Capsularis. Insets of (A) and (G) are showing the sense probe result at E9.5 and E10.5 respectively. Black scale bars=500 μm. Green scale bars= 250 μm. Yellow scale bars= 100 μm. Blue scale bars= 50 μm.

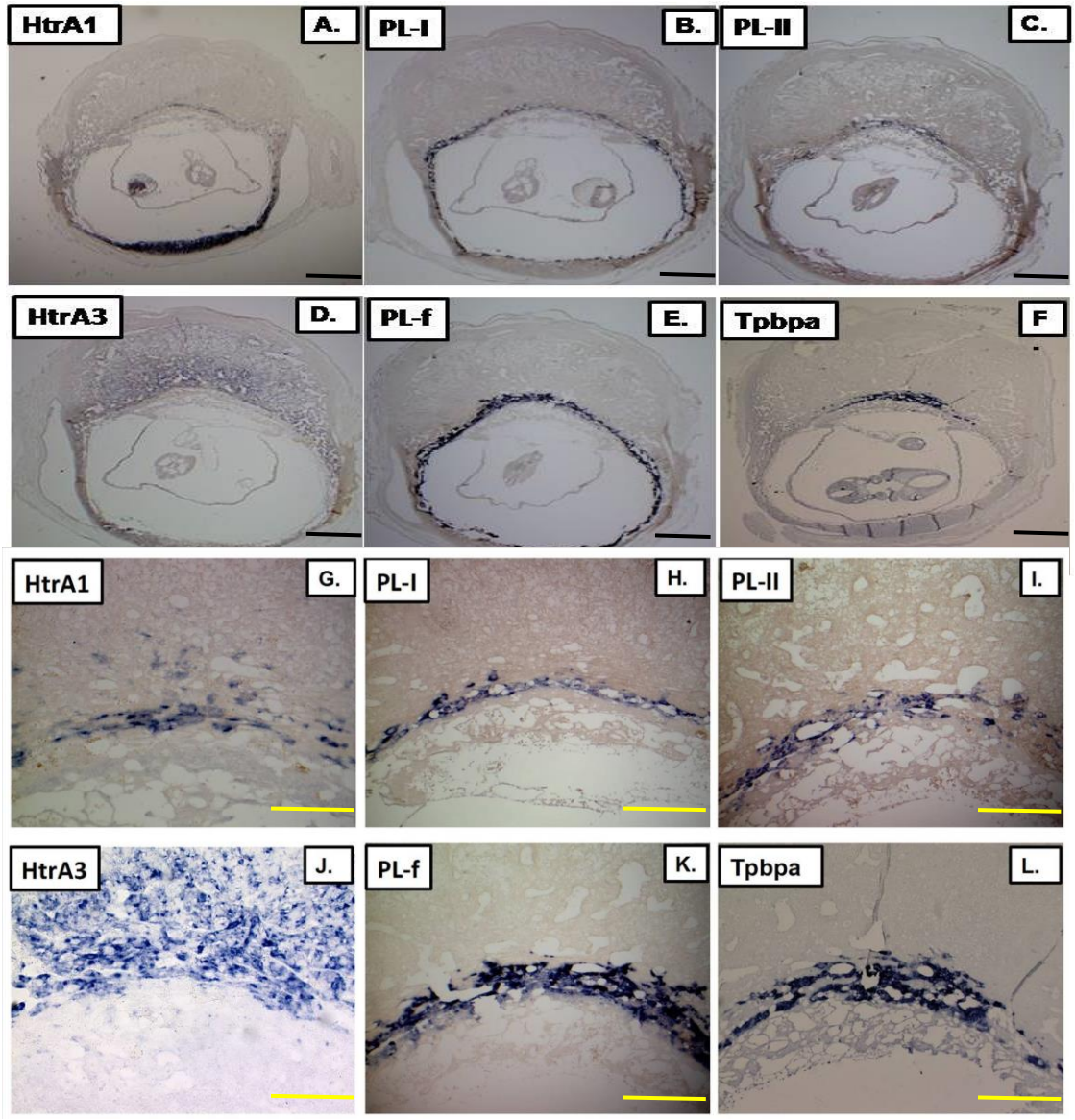

Figure 12. *HtrA1* was expressed by the trophoblasts residing in the outer ectoplacental cone at E9.5. E 9.5 placentas were analyzed by in situ hybridization using probes for *HtrA1* **(A)** and *HtrA3* **(D)**, along with other trophoblast markers, *Pl-I* **(B)**, *Pl-II* **(C)**, *Pl-f* **(E)** and *Tpbpa* **(F)**. Magnified images of the junctional zone in (A) – (F) are shown in (G) – (L), respectively. Black scale bars=500 μm. Yellow scale bars= 50 μm.

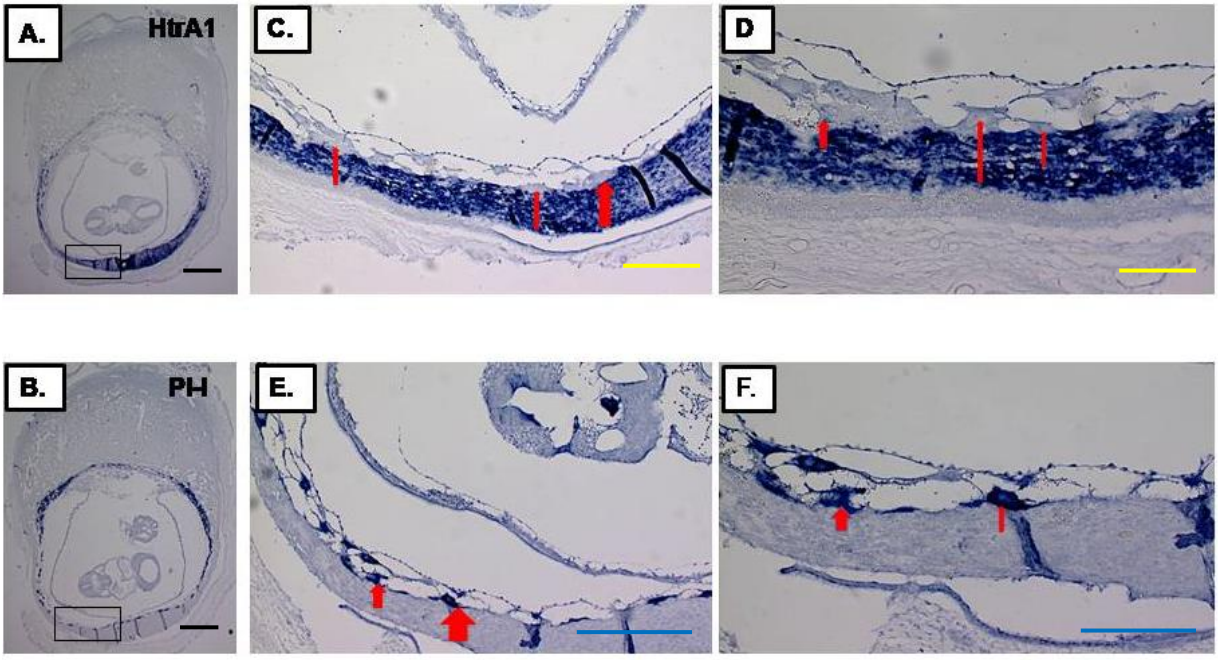

Figure 13. Trophoblast giant cells did not express *HtrA1*. Serial sections from an E 9.5 placenta were analyzed by in situ hybridization. **A)** In situ hybridization with the *HtrA1* probe. **B)** In situ hybridization with the *Pl-I* probe. **C), D)** Magnified images of the boxed area in (A). **E), F)** Magnified images of the boxed area in (B). *HtrA1* was not expressed by TGC. Red arrows show TGC, which express *Pl-I* but not *HtrA1*. Black scale bars=500 μm. Yellow scale bars= 100 μm. Blue scale bars= 50 μm.

3-5 Absence of *HtrA1* and *HtrA3* leads to reduction of *Tpbpa* positive cells in the junctional zone but their increase in the labyrinth

In section 3.3, I have shown that *HtrA1*$^{-/-}$, HtrA3$^{-/-}$ and *HtrA1/3*$^{-/-}$ placentas showed a drastic decrease in SpT and GlyT in the labyrinth. SpT and GlyT originate from the same precursors present in the ectoplacental cone where *Tpbpa* is expressed. *Tpbpa* is also a marker for SpT and GlyT. In fact, the cells expressing *Tpbpa* later differentiate into SpT and GlyT around E9.5. Since *HtrA1* expressing cells were positive for *Tpbpa*, I next examined whether the absence of *HtrA1* and *HtrA3* affected *Tpbpa* positive cell lineage. The *Tpbpa* expressing cells were clearly reduced in E10.5 placentas of all three types of the KO mice (Fig 14 B, C and D), as compared with the placenta of

the wild type mouse (Fig. 14 A).

The reduction in *Tpbpa* positive cells were also observed in a later stage. Placentas from all the KO mice showed decrease in *Tpbpa* positive cells at E12.5 (Fig. 15).

These results strongly suggest that the defects in *Tpbpa* positive precursor cells results in the reduction of SpT and GlyT observed in the junctional zone.

All the data obtained from conventional staining such as HE and PAS, and from the histomorphomteric analysis indicated abnormalities in trophoblasts differentiation and invasion. Hence I conducted in situ hybridization with *Tpbpa* to see whether those PAS positive glycogen cells are originated from *Tpbpa* positive precursors or not. The data revealed that islets like structure remained in the labyrinth at E14.5 are positive for *Tpbpa* (Fig 16 B, C and D).

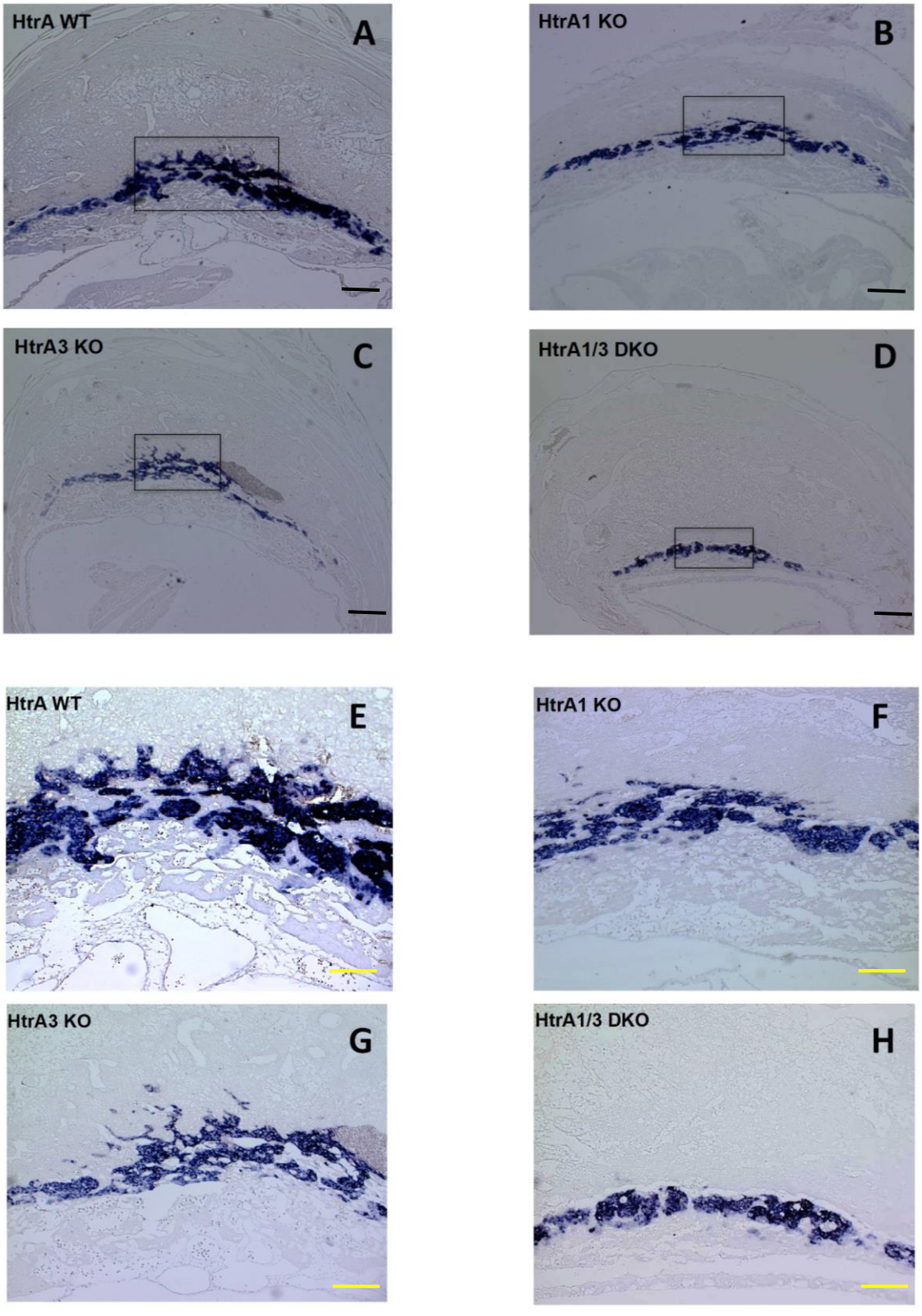
HtrA WT
A
HtrA1 KO
B
HtrA3 KO
C
HtrA1/3 DKO
D
HtrA WT
E
HtrA1 KO
F
HtrA3 KO
G
HtrA1/3 DKO
H

Figure 14. The expression of spongiotrophoblasts marker *Tpbpa* in E10.5 placenta was reduced in the absence of *HtrA1* and *HtrA3*. Placentas were harvested from *HtrA*+/+ **(A)**, *HtrA1*$^{-/-}$ **(B)**, *HtrA3*$^{-/-}$ **(C)** and *HtrA1/3*$^{-/-}$ **(D)** mice at E10.5 and analyzed by in situ hybridization with the *Tpbpa* probe (a marker for spongiotrophoblasts). **E), F), G) and H)** Magnified images of boxed areas in (A), (B), (C) and (D), respectively. Black scale bars=250 μm. Yellow scale bars= 100 μm.

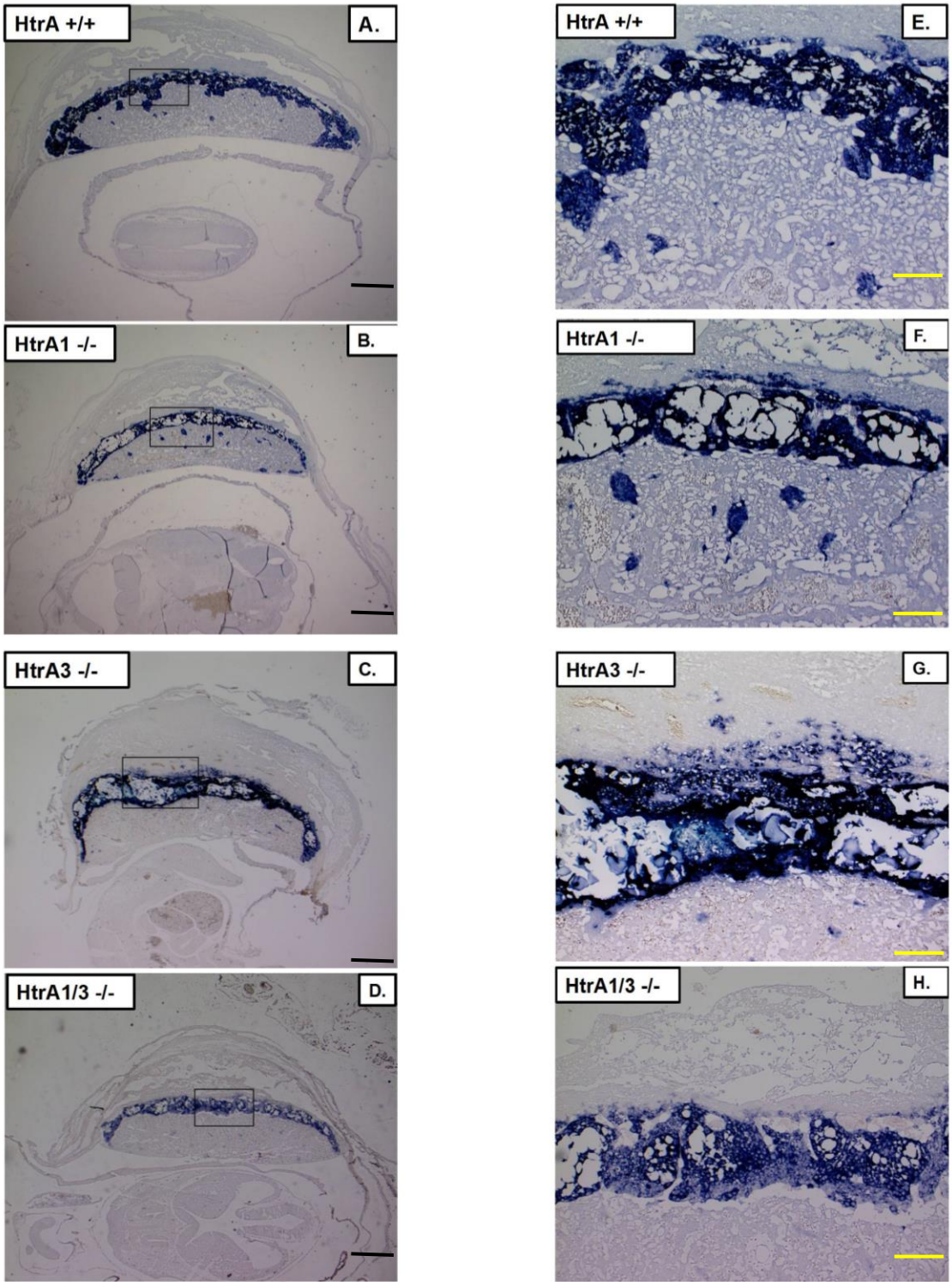
HtrA +/+
A.
HtrA1 -/-
B.
HtrA3 -/-
C.
HtrA1/3 -/-
D.
HtrA +/+
E.
HtrA1 -/-
F.
HtrA3 -/-
G.
HtrA1/3 -/-
H.

Figure 15. Decrease in *Tpbpa* positive cells in E12.5 placentas of *HtrA1* and *HtrA3* deficient mice. Placentas were harvested from *HtrA*+/+ **(A)**, *HtrA1*$^{-/-}$ **(B)**, *HtrA3*$^{-/-}$ **(C)** and *HtrA1/3* $^{-/-}$ **(D)** at E12.5 and analyzed by in situ hybridization using the *Tpbpa* probe. **E), F), G) and H)** Magnified images of the boxed areas in **(**A), (B), (C) and (D), respectively. Black scale bars=500 μm. Yellow scale bars= 100 μm.

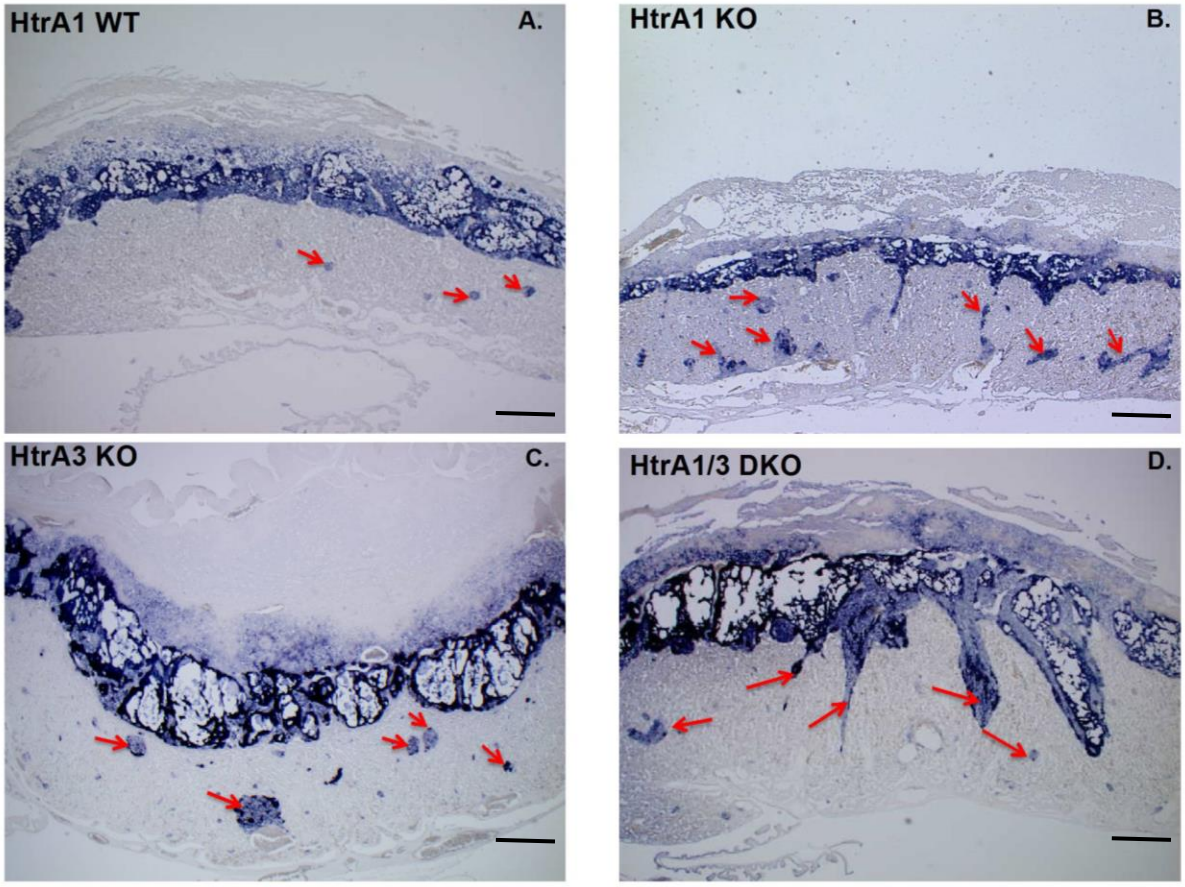

Figure 16. PAS positive islands in the labyrinth were positive for *Tpbpa* expression. Sections from placentas at E 14.5 were analyzed by in situ hybridization with the *Tpbpa* probe. **A)** *HtrA*+/+ placenta. **B)** *HtrA1*$^{-/-}$ placenta. **C)** *HtrA3*$^{-/-}$ placenta. **D)** *HtrA1/3*$^{-/-}$ placenta. PAS positive cells were also positive for *Tpbpa* (red arrows). Black scale bars=500 μm.

3-6 Spiral artery-associated trophoblasts are decreased and the maternal artery remodeling is compromised in the absence of *HtrA* and *HtrA3*

In order to reveal which trophoblast subtypes were affected by deletion of *HtrA1* and *HtrA3* genes, I examined E9.5 placentas from *HtrA* $^{-/-}$ and *HtrA1/3*$^{-/-}$ KO mice by in situ hybridization with *Pl-f*, *Pl-II*, and *Pl-I* probes, which are commonly used for trophoblast subtype identification.

Pl-f is expressed by parietal trophoblast giant cells (P-TGCs) and spiral artery associated trophoblast giant cells (SpA-TGCs). SpA-TGCs invade he decidual tissues and associate with maternal arteries. In E9.5 *HtrA1*$^{-/-}$ and *HtrA1/3*$^{-/-}$ placentas, fewer *Pl-f* positive cells invaded the decidua (Fig. 17 E and H, F and I) as compared with the wild type placenta (Fig. 17 D and G). The decrease is clearly shown in Fig. 20A which depicts the counting of *Pl-f* positive cells inside the decidua of the two KO mice and wild type mice. *Pl-f* positive cells were frequently associated with maternal arteries in wild type mice, but such association was reduced in both *HtrA1*$^{-/-}$ and *HtrA1/3*$^{-/-}$ placentas (Fig. 17 E and F). The association of SpA-TGCs with maternal arteries induces remodeling of arteries, which results in enlargement of arterial cavity to increase the blood flow to the fetal placenta (Adamson et al., 2002). I measured the luminal diameter of arteries, which were associated with *Pl-f* positive cells (Fig. 20 B). The data showed that, even though some SpA-TGCs attached to maternal arteries in *HtrA1*$^{-/-}$ and *HtrA1/3*$^{-/-}$ placentas, the association was not enough to induce enlargement of the cavity.

SpA-TGCs express *Tpbpa* as well. To confirm the results with *Pl-f*, I did in situ hybridization with the *Tpbpa* probe. Fewer *Tpbpa* positive cells invaded the decidua and associated with maternal arteries in *HtrA1*$^{-/-}$ and *HtrA1/3*$^{-/-}$ placentas at E9.5 as compared with the wild type placenta (Fig. 18).

These defects in invasion and arterial association were also observed in the decidua of E12.5 KO placenta (Fig. 19).

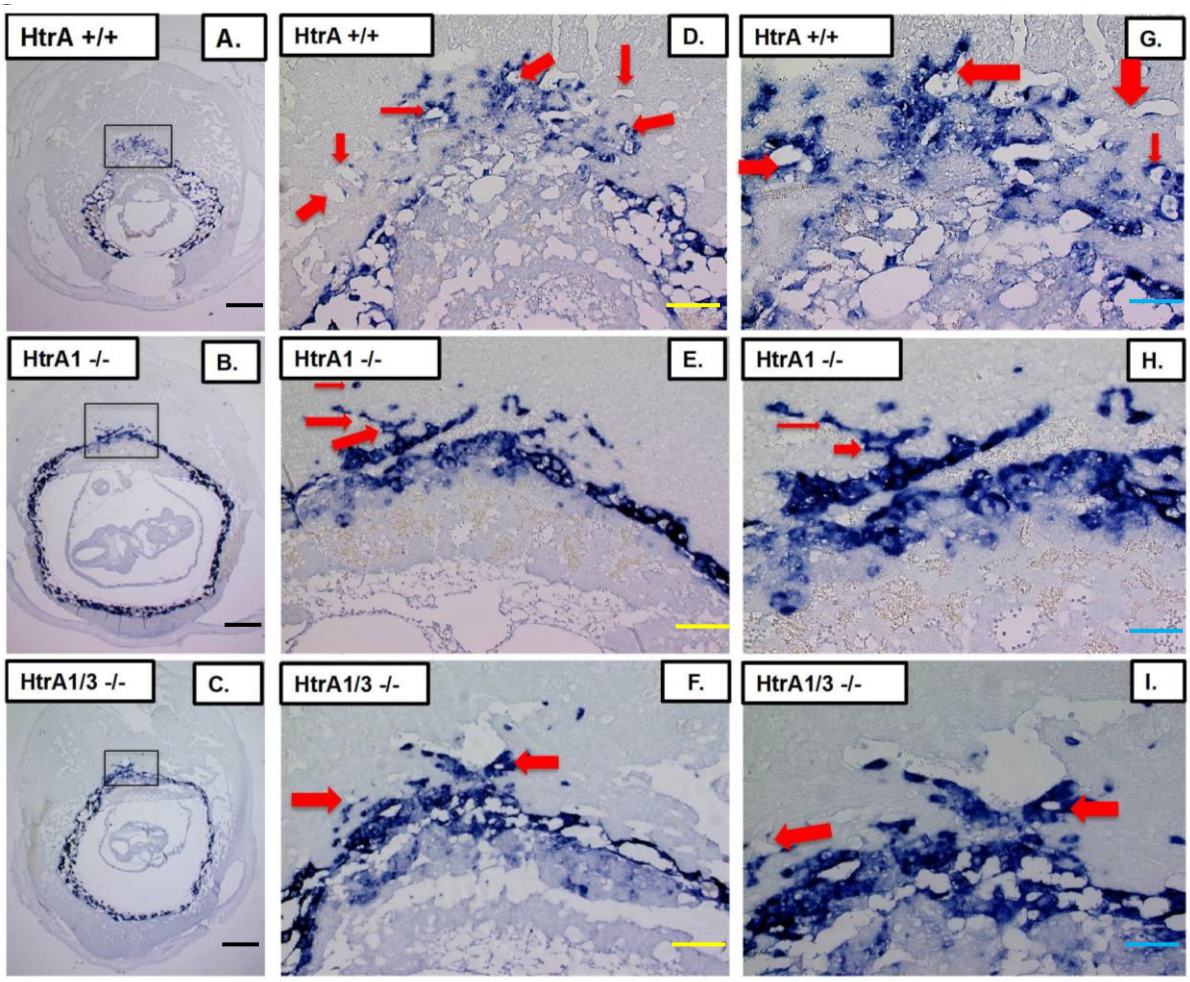

Figure 17. Fewer spiral artery related trophoblasts invaded the decidua at E 9.5. In situ hybridization with the *Pl-f* probe was carried out using sections from *HtrA*+/+ placenta **(A)**, *HtrA1*$^{-/-}$ placenta **(B)**, and *HtrA1/3* $^{-/-}$ placenta **(C)**. **(D)** and **(G)** are magnified images of the boxed are of (A), **(E)** and **(H)** are those of (B), and **(F)** and **(I)** are those of (C). Red arrows show SpA-TGCs. Black scale bars=500 μm. Yellow scale bars= 100 μm. Blue scale bars= 50 μm.

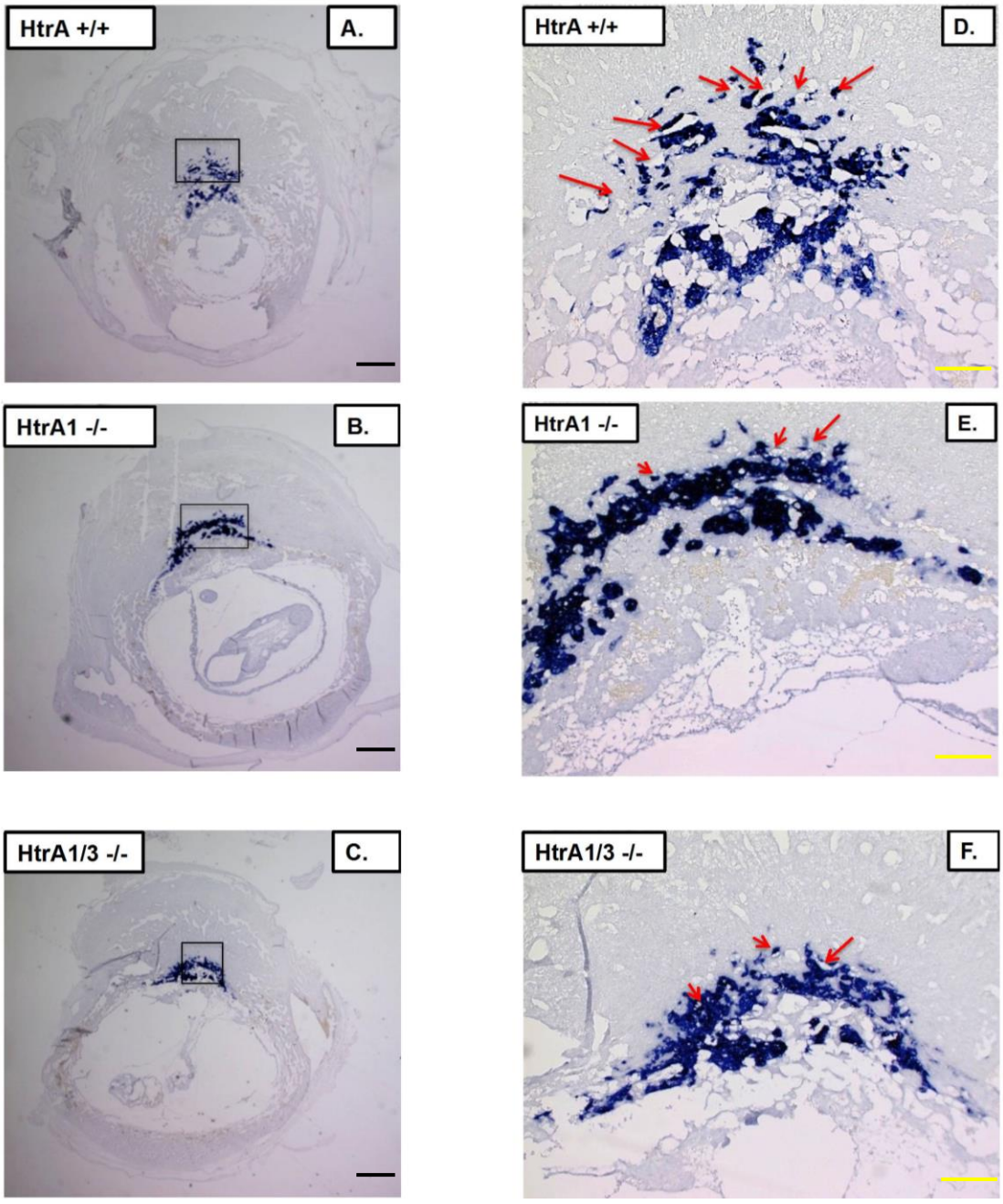

Figure 18. Fewer SpA-TGC invaded the decidua at E 9.5. In situ hybridization with the *Tpbpa* probe was carried out using sections from *HtrA*+/+ placenta **(A)**, *HtrA1*$^{-/-}$ placenta **(B)**, and *HtrA1/3* $^{-/-}$ placenta **(C)**. **(D)**, **(E)** and **(F)** are magnified images of the boxed are of (A), (B), and (C), respectively. Red arrows show SpA-TGCs. Black scale bars=500 μm. Yellow scale bars= 100 μm.

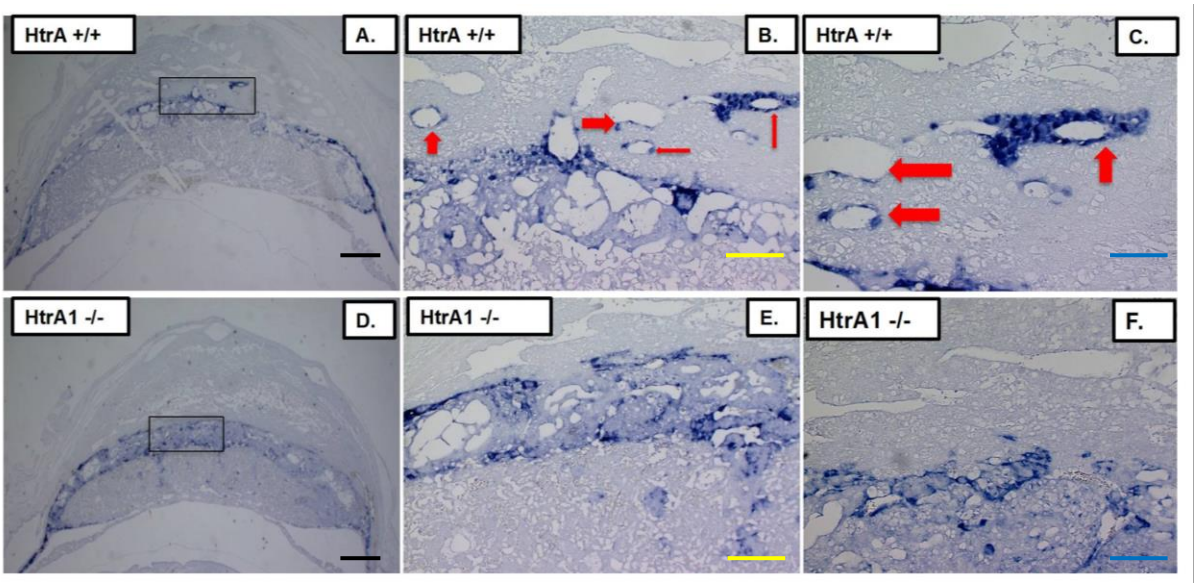

Figure 19. SpA-TGC was reduced in number in the decidua of *HtrA1*$^{-/-}$ placenta at E12.5. In situ hybridization with the *Pl-f* probe was carried out using sections from *HtrA*$^{+/+}$ placenta **(A)** and *HtrA1*$^{-/-}$ placenta **(D)**. **(B)** and **(C)** are the magnified images of the boxed are of (A), and **(E)** and **(F)** are those of (D). Red arrows indicate SpA-TGC. Black scale bars=500 μm. Yellow scale bars= 100 μm. Blue scale bars= 50 μm.

A

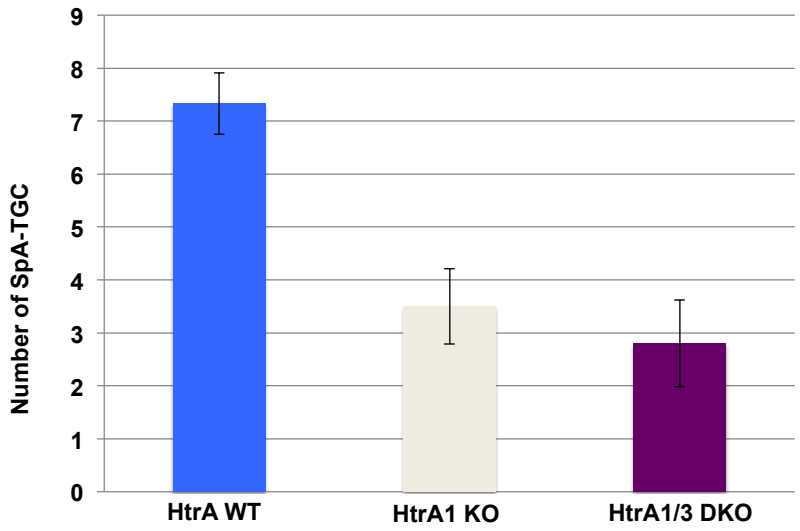

B

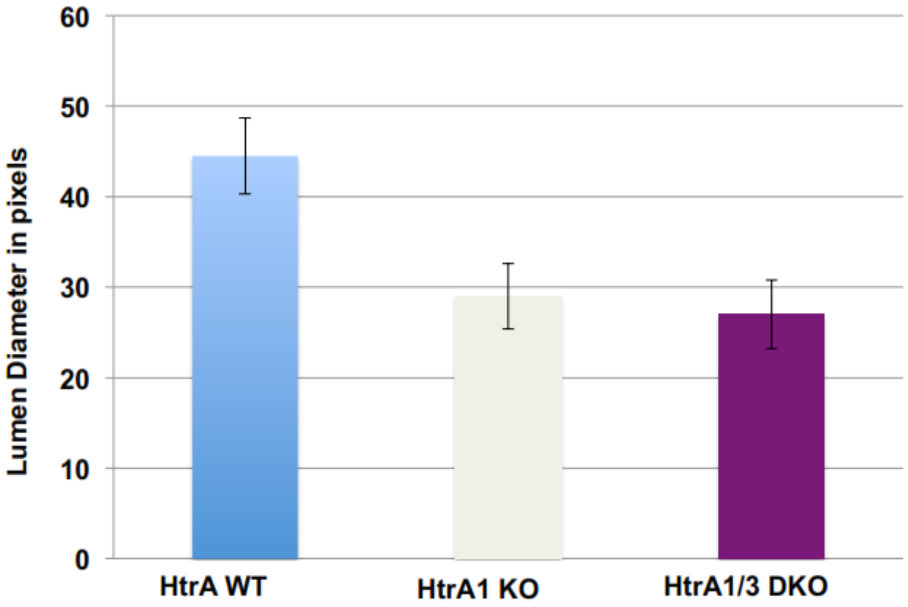

Figure 20. Reduction in the number of SpA-TGC that invaded the decidua of *HtrA1*$^{-/-}$ and *HtrA1/3*$^{-/-}$ placentas at E 9.5. (A) The number of *Pl-f*-positive SpA-TGC invading the decidua of *HtrA*+/+, *HtrA1*$^{-/-}$ and *HtrA1/3*$^{-/-}$ placentas at E9.5 (see Fig. 15) was counted. One section which had most *Pl-f* positive cells and five placentas for each genotype were analyzed. **(B)** Lumen diameter of the SpA-TGC-associated arteries was measured. More than five arteries for one placenta and three placentas for each genotype were measured.

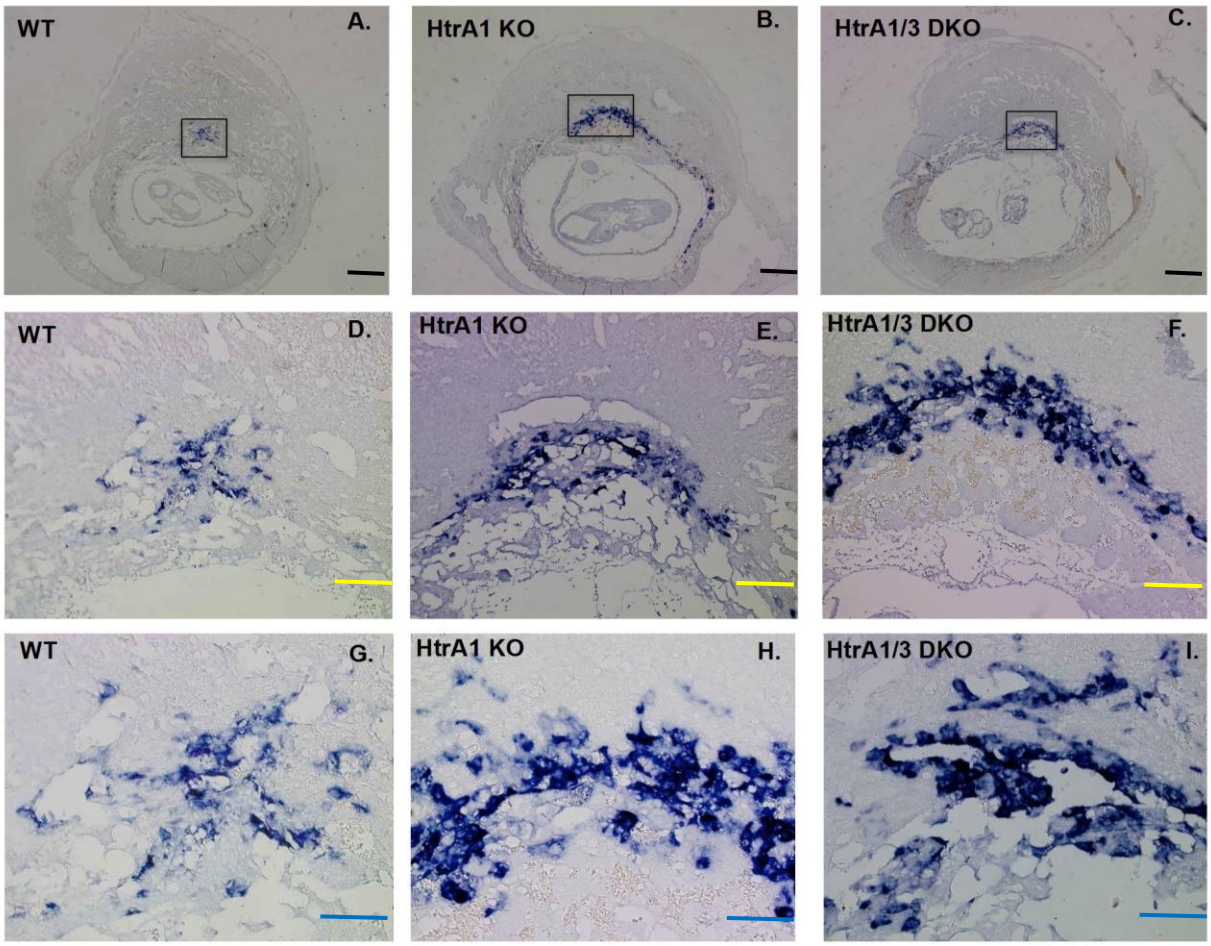

Figure 21. *Pl-II* expressing cells increased in *HtrA1*$^{-/-}$ and *HtrA1/3*$^{-/-}$ mouse placentas at E9.5. Sections from *HtrA*+/+ **(A)**, *HtrA1*$^{-/-}$ **(B)** and *HtrA1/3*$^{-/-}$ **(C)** mouse placentas at E9.5 were analyzed by in situ hybridization using the *Pl-II* probe. **(D)** and **(G)** are magnified images of the boxed area of (A); **(E)** and **(H)** are those of (B); **(F)** and **(I)** are those of (C). Black scale bars=500 μm. Yellow scale bars= 100 μm. Blue scale bars= 50 μm.

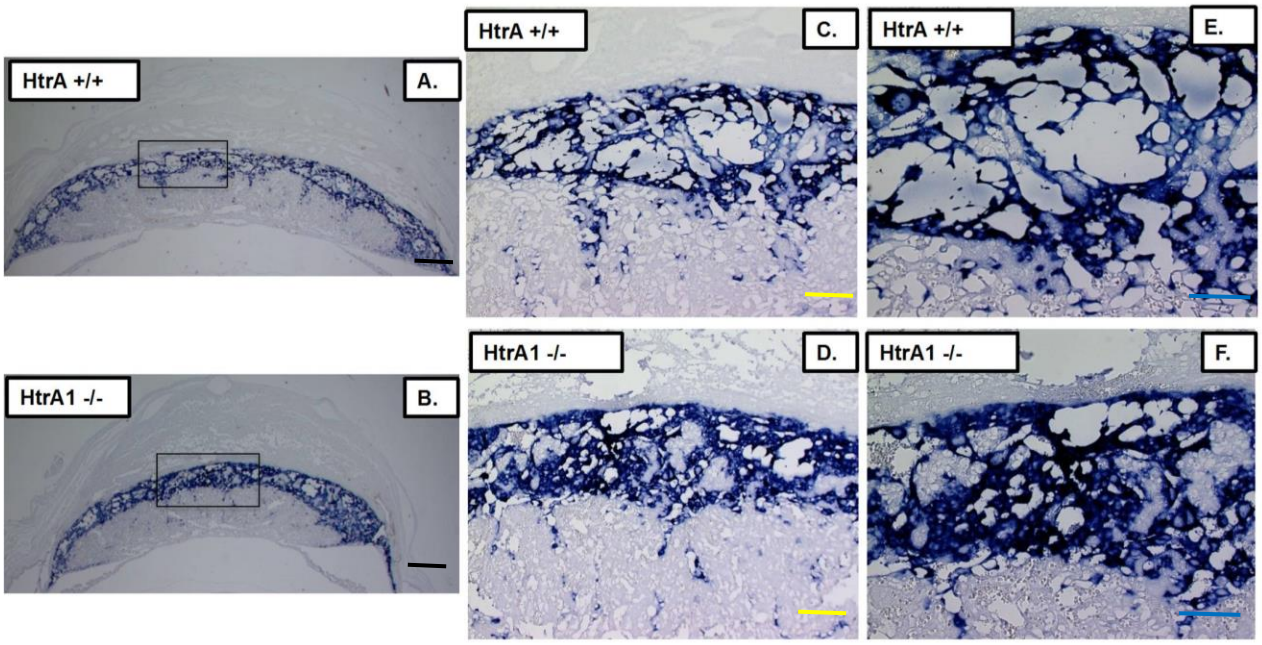

Figure 22. *Pl-II* expressing cells increased in *HtrA1*$^{-/-}$ mouse placentas at E 12.5. Sections from *HtrA*+/+ **(A)** and *HtrA1*$^{-/-}$ **(B)** mouse placentas at E12.5 were analyzed by in situ hybridization using the *Pl-II* probe. **(C)** and **(E)** are magnified images of the boxed area of (A); **(D)** and **(F)** are those of (B). Black scale bars=500 μm. Yellow scale bars= 100 μm. Blue scale bars= 50 μm.

3-7 Canal trophoblast giant cells are increased in the absence of *HtrA1* and *HtrA3*.

Pl-II is expressed by canal-associated trophoblast giant cells (C-TGC) in the junctional zone, sinusoidal TGCs (S-TGC) in the labyrinth, and parietal TGC (P-TGC). As I mentioned above, *Pl-II* positive cells increased markedly in the junctional zone of *HtrA1*$^{-/-}$ and *HtrA1/3*$^{-/-}$ mouse placentas at E 9.5 (Fig. 21) as well as at E12.5 (Fig. 22). In contrast, the number of *Pl-II* positive cells in the labyrinth, which may be S-TGCs, did not differ between KO and wild type mice (Fig. 22 C and D).

3-8 *Tpbpa* positive cell lineages are preferentially affected in the absence of *HtrA1* and *HtrA3*.

So far I have described abnormal trophoblast populations in the *HtrA1* and *HtrA3* KO mice, which include decrease in spongiotrophoblasts (SpTs) and glycogen trophoblasts (GlyTs) (those are *Tpbpa* positive) in the junctional zone, defects in migration of GlyT toward the decidua (Section 3.5), defects in invasion and arterial association of *Pl-f/Tpbpa*-positive SpA-TGC (Section 3.6), and increase in *Pl-II*-positive trophoblasts in the junctional zone (section 3.7). A common feature of those trophoblast cell lineages is that they originate from *Tpbpa*-positive precursor (Simmons et al., 2007).

To examine whether only *Tpbpa*-positive precursor-derived cells were affected in *HtrA1*$^{-/-}$ and *HtrA1/3*$^{-/-}$ placentas, I carried out in situ hybridization with the *Pl-I* probe. *Pl-I* is a marker for parietal trophoblast giant cells (P-TGC), which originate from both *Tpbpa*-negative and positive precursors. In situ hybridization of E 9.5 (Fig 23) and E 10.5 (Fig 24) placentas showed that the number and distribution of *Pl-I* positive cells were similar among *HtrA1*$^{+/+}$, *HtrA1*$^{-/-}$ and *HtrA1/3*$^{-/-}$ mouse placentas. This result suggests that *Tpbpa* positive cell lineages are preferentially affected by the loss of *HtrA1* and *HtrA3*.

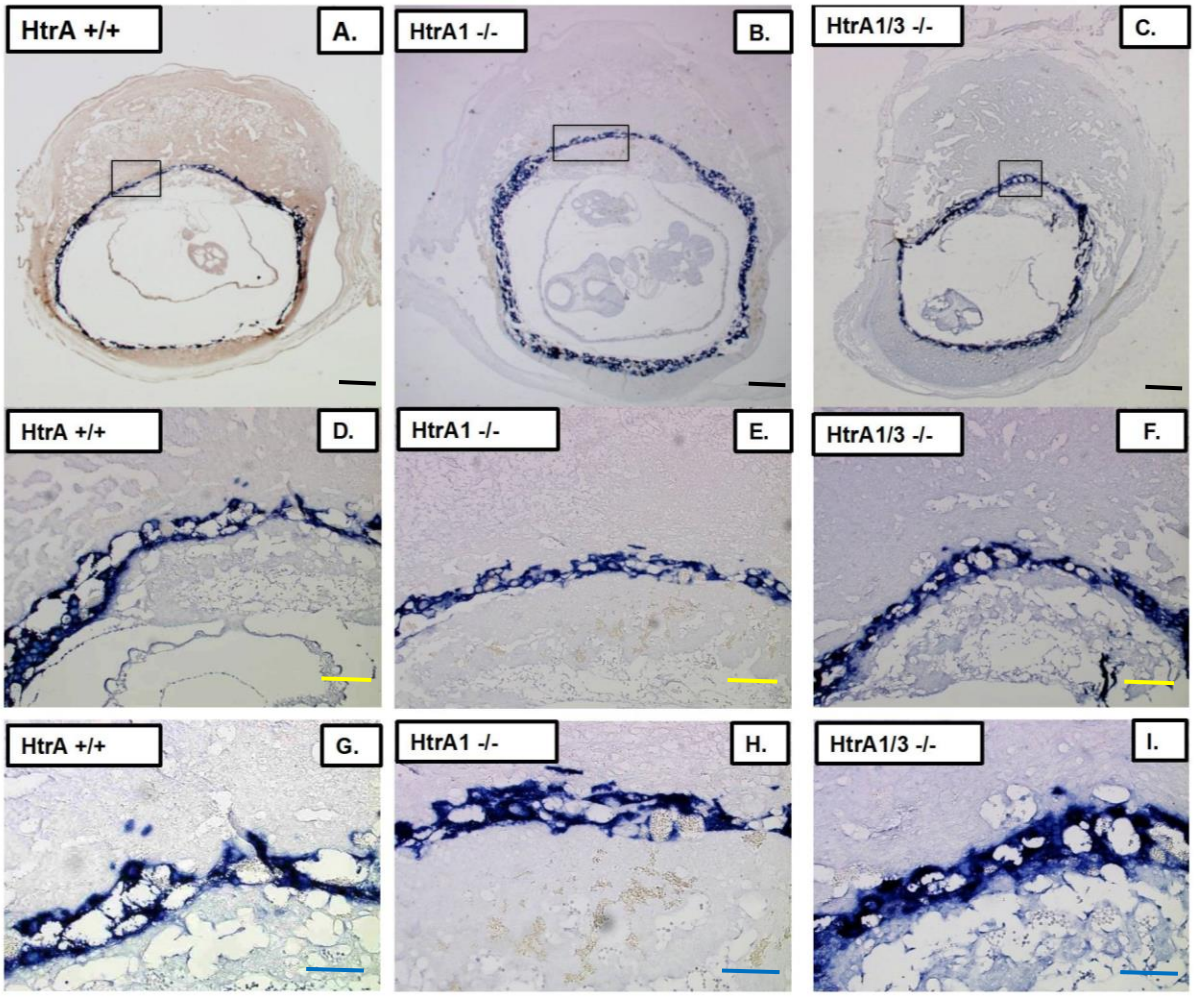

Figure 23. Expression of a primary TGC marker, *PL-I*, was similar among *HtrA*+/+, *HtrA1*$^{-/-}$ and *HtrA1/3*$^{-/-}$ mouse placentas at E9.5. Sections from *HtrA1*+/+ **(A)**, *HtrA1*$^{-/-}$ **(B)** and *HtrA1/3*$^{-/-}$ **(C)** mouse placentas at E9.5 were subjected to in situ hybridization using the *Pl-I* probe, a marker for primary trophoblast giant cells. **(D)** and **(G)** are magnified images of the junctional zone (boxed area) in (A); **(E)** and **(H)** are those in (B); **(F)** and **(I)** are those in (C). Black scale bars=500 μm. Yellow scale bars= 100 μm. Blue scale bars= 50 μm.

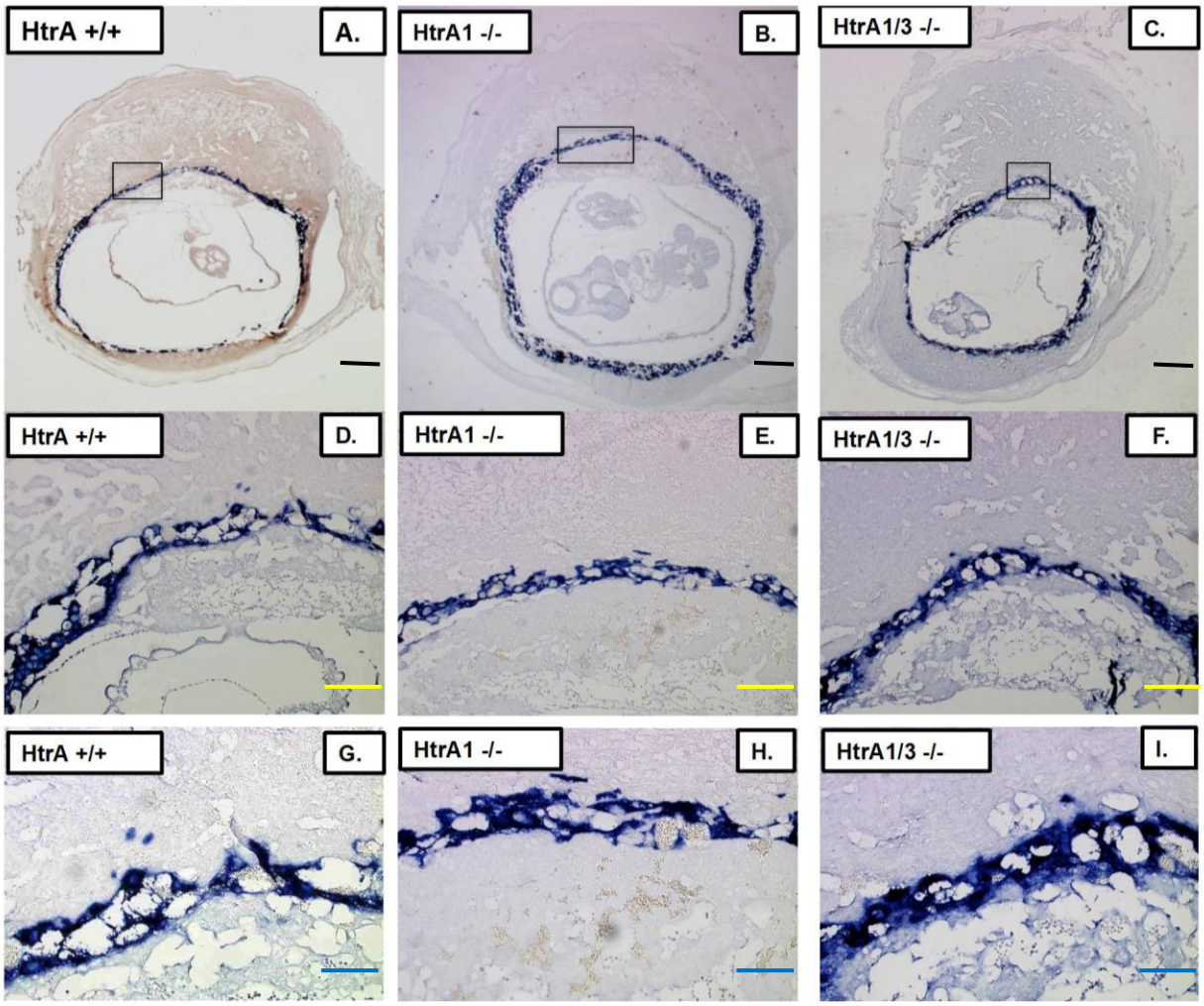

Figure 24. Expression of a primary TGC marker, *PL-I*, was similar among *HtrA*+/+, *HtrA1*$^{-/-}$ and *HtrA1/3*$^{-/-}$ mouse placentas at E10.5. Sections from *HtrA1*+/+ **(A)**, *HtrA1*$^{-/-}$ **(B)** and *HtrA1/3*$^{-/-}$ **(C)** mouse placentas at E10.5 were subjected to in situ hybridization using the *Pl-I* probe, a marker for primary trophoblast giant cells. **(D)** and **(G)** are magnified images of the junctional zone (boxed area) in (A); **(E)** and **(H)** are those in (B); **(F)** and **(I)** are those in (C). Black scale bars=500 μm. Yellow scale bars= 100 μm. Blue scale bars= 50 μm.

3-9 *HtrA1/3*$^{-/-}$ mouse exhibits a rise in blood pressure during pregnancy

Poor remodeling of maternal spiral artery is a prerequisite of preeclampsia with elevated blood pressure. Blood pressure of *HtrA*+/+ mice and *HtrA1/3*$^{-/-}$ mice was measured. Mice from 129/B6 background were used for both *HtrA*+/+ and *HtrA 1/3*$^{-/-}$ genotypes. Upon confirmation of pregnancy, female mice were separated from male and both wild type and KO mice were kept individually under the same conditions. Blood pressure was measured from E10.5 throughout the gestational periods until two days after successful delivery. The systolic and diastolic blood pressure was elevated in *HtrA1/3*$^{-/-}$ mice compared to *HtrA*+/+ mice (Fig 24); the systolic and diastolic blood pressure in *HtrA1/3*$^{-/-}$ started to increase from E14.5 and showed tendency to decrease after giving birth.

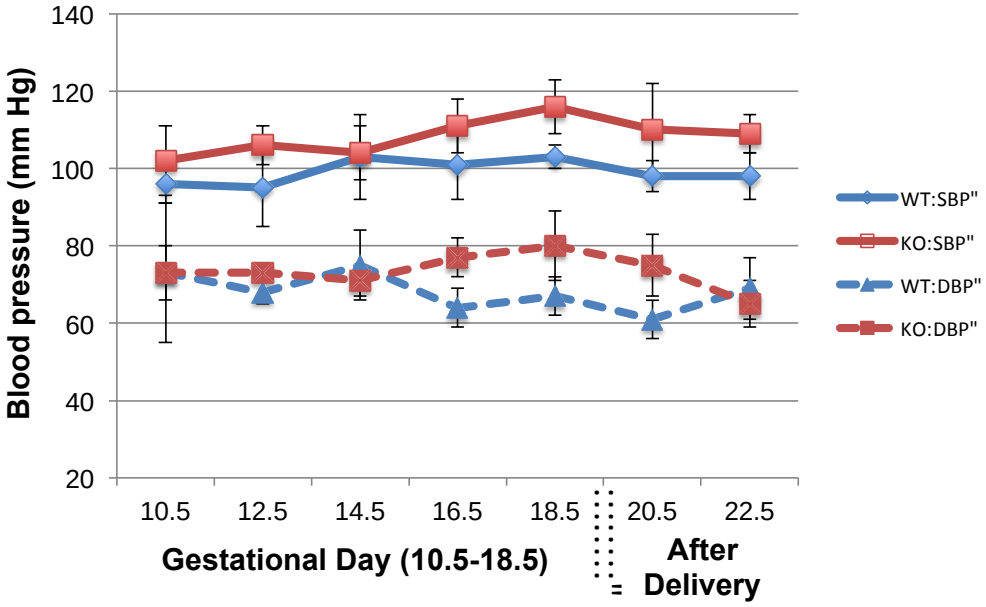

Figure 25. Systolic and diastolic blood pressure of *HtrA*+/+ and *HtrA1/3*$^{-/-}$ mice during pregnancy. Blood pressure of pregnant *HtrA*+/+ and *HtrA1/3*$^{-/-}$ mice were measured every two day from E10.5 to after delivery. Five pregnant mice from each genotype were used. Continuous lines show systolic pressure, and broken line diastolic pressure.

3-10 The level of phosphorylated Smad2 is increased in the placenta of *HtrA1*$^{-/-}$ mouse

HtrA1 is known to inhibit TGF-β signaling. The canonical TGF-β pathway transduces signals through phosphorylation of cytoplasmic receptor-associated Smad proteins. I examined if the absence of HtrA1 enhanced TGF-β signaling. The level of phosphorylated Smad2 was increased in the placentas from *HtrA1*$^{-/-}$ mice placenta at E 10.5 (Fig. 26), indicating that the TGF-β signaling was increased by the absence of *HtrA1*.

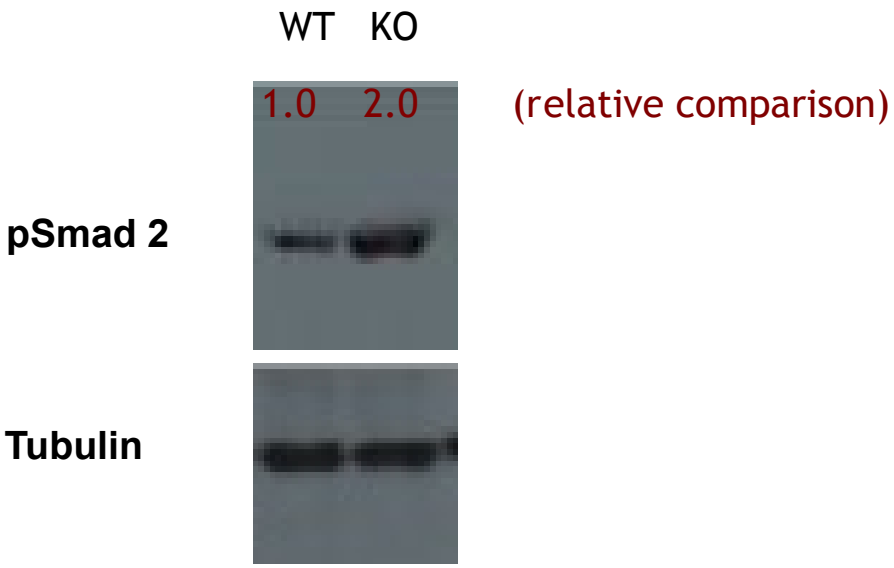

Figure 26. *HtrA1*$^{-/-}$ mouse placenta showed a higher level of phosphorylated Smad 2 protein. Extracts of placentas were prepared from *HtrA*+/+ and *HtrA1*$^{-/-}$ mice at E10.5. *HtrA1*$^{-/-}$ placenta shows 2-fold increase in the level of phosphorylated Smad2 compare to *HtrA*$^{+/+}$ placenta. Two placentas from each genotype were used for this experiment.

References

Adamson, S.L., Lu, Y., Whiteley, K.J., Holmyard, D., Hemberger, M., Pfarrer, C., and Cross, J.C. (2002).Interactions between trophoblast cells and the maternal and fetal circulation in the mouse placenta. Dev Biol 250: 358-373.

Adelman DM, Marina Gertsenstein, and EminMaltepe. (2000).Placental cell fates are regulated in vivo by HIF-mediated hypoxia responses. Genes Dev 14(24): 3191-3201.

Ajayi F, Douglas K. (2009). Low oxygen tension upregulates expression of HtrA1 in the RCHO-1 trophoblast cell line. American Journal of obstetrics and Gynecology. 201)6): 274.

Ajayi F, Kongoasa N, Gaffey T, et al. (2008) Elevated expression of serine protease HtrA1 in preeclampsia and its role in trophoblast cell migration and invasion.Am J ObstetGynecol199:557.e1-557.e10.

Alba BM, Gross CA. (2004) Regulation of the *Escherichia Coli* sigma-dependent envelope stress response. Mol. Microbiol. 52:613–619.

Alba BM., Leeds JA et al. (2002). DegS and YaeL participate sequentially in the cleavage of RseA to activate the sigma(E)-dependent extracytoplasmic stress response. Genes Dev, 16(16): 2156-68.

Baldi, A., A. De Luca, et al. (2002). The HtrA1 serine protease is down-regulated during human melanoma progression and represses growth of metastatic melanoma cells. Oncogene, 21(43): 6684.

Bevilacqua, E.M., and Abrahamsohn, P.A. (1989).Trophoblast invasion during implantation of the mouse embryo.Archivos de biologia y medicinaexperimentales, 22: 107-118.

Bogaerts V, Theuns J, van Broeckhoven C. (2008). Genetic findings in Parkinson's disease and translation into treatment: a leading role for mitochondria?Genes Brain Behav.7(2):129-51.

Brown MA, Hague WM, Higgins J, et al. (2000). The detection, investigation and management of hypertension in pregnancy: full consensus statement. Aust N Z J ObstetGynaecol, 40:139–55.

Candeloro L and Zorn Telma MT. (2007).Distribution and Spatiotemporal Relationship of Activin A and Follistatin in Mouse Decidual and Placental Tissue. AJRI, 58: 415-424.

Chien, J., J. Staub, et al. (2004). A candidate tumor suppressor HtrA1 is downregulated in ovarian cancer. Oncogene, 23(8): 1636-44.

Clausen, T., C. Southan, et al. (2002).The HtrA family of proteases: implications for protein composition and cell fate.Mol Cell, 10(3): 443-55.

De Luca, A., M. De Falco, et al. (2004). The serine protease HtrA1 is upregulated in the human placenta during pregnancy. J HistochemCytochem, 52(7): 885-92.

Dewan, A., M. Liu, et al. (2006).HTRA1 promoter polymorphism in wet age-related macular degeneration. Science, 314(5801): 989-92.

Dokras A., Darren S. Hoffmann et al. (2006). Severe Feto-Placental Abnormalities Precede the Onset of Hypertension and Proteinuria in a Mouse Model of Preeclampsia. Biolreprod, 75: 899-907.

Dong Hu and James Cross (2011). Ablation of Tpbpa-positive trophoblast precursors leads to defects in maternal spiral artery remodeling in the mouse placenta. Developmental Biology, 358: 231-239.

Dunwoodie, S. L. 2009. The role of hypoxia in development of the Mammalian embryo.Dev Cell, 17**,** 755-73.

Dupressoir, A., Vernochet, C., Bawa, O., Harper, F., Pierron, G., Opolon, P. &Heidmann, T. 2009.Syncytin-A knockout mice demonstrate the critical role in placentation of a fusogenic, endogenous retrovirus-derived, envelope gene. ProcNatlAcadSci,106**,** 12127-32.

El-Hashash AH, Esbrit P, Kimber SJ (2005). PTHrP promotes murine secondary trophoblast giant cell differentiation through induction of endocycle, upregulation of giant-cell-promoting transcription factors and suppression of other trophoblast cell types. Differentiation, 73: 154–174.

Erlebacher A, Price KA, Glimcher LH. (2004). Maintenance of mouse trophoblast stem cell proliferation by TGF-beta/activin**.**Dev. Biol., 275 : 158–169.

Esposito V, Campioni M, De Luca A, Spugnini EP, Baldi F, Cassandro R, ManciniA, Vincenzi B, Groeger A, Caputi M,Baldi A. (2006). Analysis of HtrA1 serineprotease expression in human lung cancer.Anticancer Res, 26:3455–3459.

Grau, S., P. J. Richards, et al. (2006)."The role of human HtrA1 in arthritic disease." J BiolChem, 281(10): 6124-9.

Graham CH and Lala PK (1992) Mechanisms of placental invasion of the uterus and their control.Biochem Cell Biol. 70: 867–874.

Guillemot, F., Nagy, A., Auerbach, A., Rossant, J., and Joyner, A.L. (1994).Essential role of Mash-2 in extraembryonic development. Nature, 371, 333-336.

Gupta, S., R. Singh, et al. (2004).The C-terminal tail of presenilin regulates Omi/HtrA2 protease activity. J BiolChem, 279(44): 45844-54.

Hara, K., A. Shiga, et al. (2009). Association of HTRA1 mutations and familial ischemic cerebral small- vessel disease. N Engl J Med 360(17): 1729-39.

Harris LK, Smith SD, Keogh RJ, Jones RL, Baker PN, Knofler M, Cartwright JE, Whitley GS, Aplin JD. (2010). Trophoblast- and vascular smooth muscle cell-derived

MMP-12 mediates elastolysis during uterine spiral artery remodeling.Am. J. Pathol. 177: 2103–2115

Harris LK, Aplin JD. (2007). Vascular remodeling and extracellular matrix breakdown in the uterine spiral arteries during pregnancy.Reprod. Sci.14: 28–34.

Hasselblatt, H., R. Kurzbauer, et al. (2007). Regulation of the sigmaE stress response by DegS: how the PDZ domain keeps the protease inactive in the resting state and allows integration of different OMP-derived stress signals upon folding stress. Genes Dev, 21(20): 2659-70.

Hemberger, M. (2008).IFPA award in placentology lecture - characteristics and significance of trophoblast giant cells.Placenta, 29 Suppl A, S4-9.

Hou S, Maccarana M, MinTH ,Strate I, Pera EM. (2007).The secreted serine protease xHtrA1 stimulates long-range FGF signaling in the early xenopus embryo.Dev. Cell, 13: 226–241.

Hung TH, Skepper JN, Charnock-Jones DS, Burton GJ. (2002). Hypoxia-reoxygenation: a potent inducer of apoptotic changes in the human placenta and possible etiological factor in preeclampsia. Circ. Res.90:1274–1281.

Inagaki A, Nishizawa H, Ota S, Suzuki M, Inuzuka H, Miyamura H, Sekiya T,Kurahashi H, Udagawa Y. (2012).Upregulation of HtrA4 in the placentas ofpatients with severe pre-eclampsia. Placenta, 33:919 – 926.

Jones A, Sandeep Kumar, Ning Zhang, Zongzhong Tong, Jia-Hui Yang, Carl Watt, James Anderson, Amrita, Heather Fillerup, Manabu McCloskey, Ling Luo, Zhenglin Yang, Balamurali Ambati, Robert Marc, Chio Oka, Kang Zhang and Yingbin Fu. (2011). Increased expression of multifunctional serine protease, HTRA1, in retinal pigment epithelium induces polypoidal choroidal vasculopathy in mice. PNAS. 108:14578-14583.

Jones RL, Stoikos C, Findlay JK &Salamonsen LA (2006).TGF- β superfamilyexpression and actions in the endometrium and placenta. Reproduction, 132: 217–232.

Kim, D. Y. and K. K. Kim (2005).Structure and function of HtrA family proteins, the key players in protein quality control. J BiochemMolBiol, 38(3): 266-74.

Knofler M. (2010).Critical growth factors and signalling pathways controllinghuman trophoblast invasion.International Journal of Developmental Biology. 54269–280

Kolmar, H., P. R. Waller, et al. (1996). The DegP and DegQperiplasmicendoproteases of Escherichia coli: specificity for cleavage sites and substrate conformation. J Bacteriol, 178(20): 5925-9.

Lipinska B, Fayet O, Baird L, Georgopoulos C. (1989). Identification, characterization, and mapping of the Escherichia coli htrAgene, whose product is essential for bacterial growth only at elevated temperatures.J Bacteriol.171:1574-84

Li Y, Puryer M, Lin E, Hale K, Salamonsen LA, et al. (2011) Placental HtrA3 is regulated by oxygen tension and serum levels are altered during early pregnancy in women destined to develop preeclampsia. J ClinEndocrinolMetab 96: 403– 411.

Lorenzi T, Marzioni D, Giannubilo S, Quaranta A, Crescimanno C, De Luca A, et al (2009). Expression patterns of two serine protease HtrA1 forms in human placentas complicated by preeclampsia with and without intrauterine growth restriction. Placenta, 30:35-40.

Martins, L. M., A. Morrison, et al. (2004).Neuroprotective role of the Reaper-related serine protease HtrA2/Omi revealed by targeted deletion in mice.Mol Cell Biol, 24(22): 9848-62.

Natale David RC, MyriamHemberger , Martha Hughes, James C. Cross (2009). Activin promotes differentiation of cultured mouse trophoblast stem cells towards a labyrinth cell fate. Developmental Biology 335: 120–131

Nie, G. Y., Y. Li, et al. (2003). A novel serine protease of the mammalian HtrA family is up-regulated in mouse uterus coinciding with placentation.Mol Hum Reprod, 9(5): 279-90.

Nie, G., K. Hale, et al. (2006). Distinct expression and localization of serine protease HtrA1 in human endometrium and first-trimester placenta. Dev Dyn, 235(12): 3448-55.

Nie, G., Y. Li, et al. (2005). Serine protease HtrA1 is developmentally regulated in trophoblast and uterine decidual cells during placental formation in the mouse. Dev Dyn, 233(3): 1102-9.

Nowak RA, Haimovici F, Biggers JD, Erbach GT. (1999). Transforming growth factor-beta stimulates mouse blastocyst outgrowth through a mechanism involving parathyroid hormone-related protein.Biol. Reprod., 60: 85–93

Oka. C., R. Tsujimoto, et al. (2004). HtrA1 serine protease inhibits signaling mediated by TGF- β family proteins. Development, 131(5): 1041-53.

Park, H. J., S. S. Kim, et al. (2006). Beta-amyloid precursor protein is a direct cleavage target of HtrA2 serine protease. Implications for the physiological function of HtrA2 in the mitochondria. J BiolChem, 281(45): 34277-87.

Plaks V., Rinkenberger J., Dai J., Flannery M., Sund M., Kanasaki K., Ni W., Kalluri R., Werb Z. (2013). Matrix metalloproteinase-9 deficiency phenocopies features of preeclampsia and intrauterine growth restriction. PNAS, 110(27): 11109-14.

Redman, C. W., and I. L. Sargent, 2005 Latest advances in understanding preeclampsia. Science, 308: 1592-1594.

Rodriguez TA, Sparrow DB, Scott AN, Withington SL, Preis JI, Michalicek J, Clements M, Tsang TE, Shioda T, Beddington RS, Dunwoodie SL. (2004). Cited1 is required in trophoblasts for placental development and for embryo growth and survival.Mol Cell Biol. 24(1): 228-44.

Rossant, J., and Cross, J.C. (2001). Placental development: lessons from mouse mutants. Nat Rev Genet 2, 538-548.

Rossant.J and Ofer I. (1977). Properties of extra-embryonic ectoderm isolated from post-implantation mouse embryos. J.Embryol.exp.Morph. 48: 239-247

Scifres CM and Nelson DM. (2009).Intreuterine growth restriction, human placental development and trophoblast cell death. J Physiol, 587, 3453-3458.

Sibley CP, Turner MA, Cetin I, Ayuk P, Boyd CA, D'Souza SW, Glazier JD, Greenwood SL, Jansson T, Powell T. (2005). Placental phenotypes of intrauterine growth.Pediatr Res, 58(5): 827-32.

Simmons, D.G., Fortier, A.L., and Cross, J.C. (2007).Diverse subtypes and developmental origins of trophoblast giant cells in the mouse placenta. Dev Biol, 304, 567-578.

Simmons, D.G., Natale, D.R., Begay, V., Hughes, M., Leutz, A., and Cross, J.C. (2008a). Early patterning of the chorion leads to the trilaminar trophoblast cell structure in the placental labyrinth. Development, 135, 2083-2091.

Simmons, D.G., Rawn, S., Davies, A., Hughes, M., and Cross, J.C. (2008b). Spatial and temporal expression of the 23 murine Prolactin/Placental Lactogen-related genes is not associated with their position in the locus. BMC Genomics, 9, 352.

Spiess, C., A. Beil, et al. (1999). A temperature-dependent switch from chaperone to protease in a widely conserved heat shock protein. Cell, 97(3): 339-47.

Strauss, K. M., L. M. Martins, et al. (2005). Loss of function mutations in the gene encoding Omi/HtrA2 in Parkinson's disease. Hum Mol Genet, 14(15): 2099-111.

Supanji, Shimomachi M, Hasan MZ, Kawaichi M, Oka C. (2013).HtrA1 is induced by oxidative stress and enhances cell senescence through p38 MAPK pathway.Exp. Eye Res.112: 79–92.

Suzuki Y., Imai Y., Nakayama H., Takahashi K., Takio K., Takahashi R (2001). A serine protease, HtrA2 is released from the mitochondria and interacts with XIAP, inducing cell death. Mol Cell, 2001 Sep; 8(3): 613-21.

Takahashi, Y., Carpino, N., Cross, J.C., Torres, M., Parganas, E., and Ihle, J.N. (2003). SOCS3: an essential regulator of LIF receptor signaling in trophoblast giant cell

differentiation. Embo J, 22, 372-384.

Tamai Y, Tomo-o Ishikawa, Michael R. Bösl, Masahiko Mori, Masami Nozaki, HeléneBaribault,i Robert G. Oshima,i and Makoto M. Taketo. (2000). Cytokeratins 8 and 19 in the mouse placental development. JCB, 151(3): 563.

Tanaka, M., Gertsenstein, M., Rossant, J., and Nagy, A. (1997). Mash2 acts cell autonomously in mouse spongiotrophoblast development. Dev Biol. 190: 55-65.

Tanaka, S., Kunath, T., Hadjantonakis, A.K., Nagy, A., and Rossant, J. (1998).Promotion of trophoblast stem cell proliferation by FGF4. Science, 282, 2072-2075.

Tocharus, J., A. Tsuchiya, et al. (2004). Developmentally regulated expression of mouse HtrA3 and its role as an inhibitor of TGF- β signaling. Dev Growth Differ, 46(3): 257-74.

Tsuchiya A, Yano M, Tocharus J, Kojima H, Fukumoto M, Kawaichi M, Oka C. (2005). Expression of mouse HtrA1 serine protease in normal bone and cartilage and its upregulation in joint cartilage damaged by experimental arthritis.Bone. 37: 323–336.

VandeWalle L., Lamkanfi M., Vandenabeele P. (2008) The mitochondrial serine protease HtrA2/Omi: an overview. Cell Death Differ. 15, 453–460

Vierkotten S, Muether PS, Fauser S (2011) Overexpression of HTRA1 Leads to Ultrastructural Changes in the Elastic Layer of Bruch's Membrane via Cleavage of Extracellular Matrix Components. PLoS ONE, 6(8): e22959.

Waller, P. R. and R. T. Sauer (1996).Characterization of degQ and degS, Escherichia coli genes encoding homologs of the DegP protease. J Bacteriol, 178(4): 1146-53.

Wang A, Rana S, Karumanchi SA. (2009).Preeclampsia: The role of angiogenic factors in its pathogenesis. Physiology. 24(3): 147-158.

Wang, H., Xie, H., Sun, X., Tranguch, S., Zhang, H., Jia, X., Wang, D., Das, S.K., Desvergne, B., Wahli, W., et al. (2007). Stage-specific integration of maternal and

embryonic peroxisome proliferator-activated receptor delta signaling is critical to pregnancy success. J BiolChem, 282, 37770-37782.

Wang LJ, Cheong ML, et al. (2012). High-temperature requirement protein A4 (HtrA4) suppresses the fusogenic activity of Syncytin-1 and promotes trophoblast invasion. Molecular and Cellular Biology. 32: 3707-3717.

Watson ED and Cross C. (2005). Development of structures and transport functions in the mouse placenta.Physiology.20:180-93.

Whitley G.S., Cartwright J.E.(2010). Cellular and molecular regulation of spiral artery remodelling: lessons from the cardiovascular field. Placenta, 31:465–474.

Y Cui., Wei Wang, et al. (2012).Role of corin in trophoblast invasion and uterine spiral artery remodelling in pregnancy. Nature, 484, 246-250

Yan J, Tanaka S, Oda M, Makino T,Ohgane J, Shiota K. (2001). Retinoic acid promotes differentiation of trophoblast stem cells to a giant cell fate. Dev. Biol., 235: 422–432.

Yang.Z., N. J. Camp, et al. (2006).A variant of the HTRA1 gene increases susceptibility to age-related macular degeneration. Science, 314(5801): 992-3.

Zhou Y, Fisher SJ, Janatpour M, Genbacev O, Dejana E, Wheelock M, Damsky CH. (1997). Human cytotrophoblasts adopt a vascular phenotype as they differentiate. A strategy for successful endovascular invasion? J. Clin. Invest.99:2139–2151.

Zumbrunn, J. and B. Trueb (1996). Primary structure of a putative serine protease specific for IGF- binding proteins. FEBS Lett, 398(2-3): 187-92.

Zurawa-Janicka D, Kobiela J, Stefaniak T, Wozniak A, Narkiewicz J, Wozniak M, Limon J, Lipinska B. (2008). Changes in expression of serine proteases HtrA1 and HtrA2 during estrogen-induced oxidative stress and nephro carcinogenesis in male Syrian hamster. ActaBiochim. Pol., 55: 9–19.